Modeling the unphysical pseudomode model with physical ensembles: Simulation, mitigation, and restructuring of non-Markovian quantum noise

Mauro Cirio [1,*] Si Luo [1] Pengfei Liang [1,†] Franco Nori [2,3,4] and Neill Lambert [2,‡]

[1]*Graduate School of China Academy of Engineering Physics, Haidian District, Beijing, 100193, China*
[2]*Theoretical Physics Laboratory, Cluster for Pioneering Research, RIKEN, Wakoshi, Saitama 351-0198, Japan*
[3]*Quantum Computing Center, RIKEN, Wakoshi, Saitama, 351-0198, Japan*
[4]*Physics Department, University of Michigan, Ann Arbor, Michigan 48109-1040, USA*

(Received 4 January 2024; revised 16 May 2024; accepted 11 June 2024; published 17 July 2024)

The influence of a Gaussian environment on a quantum system can be described by effectively replacing the continuum with a discrete set of ancillary quantum and classical degrees of freedom. This defines a pseudomode model which can be used to classically simulate the reduced system dynamics. Here we consider an alternative point of view and analyze the potential benefits of an analog or digital quantum simulation of the pseudomode model itself. Superficially, such a direct experimental implementation is, in general, impossible due to the unphysical properties of the effective degrees of freedom involved. However, we show that the effects of the unphysical pseudomode model can still be reproduced using measurement results over an ensemble of physical systems involving ancillary harmonic modes and an optional stochastic driving field. This is done by introducing an extrapolation technique whose efficiency is limited by stability against imprecision in the measurement data. We examine how such a simulation would allow us to (i) perform a quantum simulation of the effects of complex nonperturbative and non-Markovian environments in regimes that are challenging for classical simulation; (ii) conversely, mitigate potential unwanted non-Markovian noise present in quantum devices; and (iii) restructure some of the properties of a given physical bath, such as its temperature.

DOI: 10.1103/PhysRevResearch.6.033083

I. INTRODUCTION

The definition of a physical system requires a distinction between *internal* and *external* degrees of freedom. The interaction between these constituents causes the internal, or *closed*, system dynamics to become *open*, i.e., affected by the external environment. For example, information stored in the system can propagate towards a measurement device or it can simply be lost, or *dissipated*, in the continuum of a thermal bath. Interestingly, this distinction between internal and external degrees of freedom becomes more ambiguous as the coupling between the system and the environment increases. In this case, information can be coherently exchanged between the system and the bath before the dynamics eventually stabilizes into a state characterizing *hybridization* properties of the whole system environment.

As a consequence, a mathematical model for these so-called non-Markovian regimes [1,2], must also include a characterization of the external continuum alongside the system. This can be achieved by selecting the most. relevant physical environmental degrees of freedom engaging in the interaction using, for example, the polaron transformation [3–18], chain mappings [19–22], tensor networks [23–27], or the reaction coordinate model [21,28–32]. In parallel, it is also possible to follow an *effective* philosophy, i.e., to focus on the *influence* of the environment on the system rather than on the full system-bath dynamics. This leads to effective master equations for the system dynamics which can include deterministic [33,34] and stochastic [35–38] *memory kernels* or use the path-integral [39–47] or the canonical formalism [1,48–51] to derive time-local differential equations involving additional ancillary degrees of freedom in Liouville space [52–63] or within the hierarchical equation of motion formalism (HEOM) [64–79]. Among this last category of methods is the pseudomode model [25,26,80–94], which encodes all nonperturbative effects of a Gaussian environment (such as bosonic and fermionic baths initially at thermal equilibrium) using ancillary harmonic modes and, possibly, classical stochastic processes [95].

An interesting characteristic of the pseudomode model (PM) is that, while its ancillary degrees of freedom superficially resemble simple physical harmonic modes and driving fields, in reality they can take on unphysical features and exhibit unphysical dynamics. Here the word unphysical specifically means that both the Hamiltonian and the density matrix of the full model can be non-Hermitian. This combination of superficial simplicity and unintuitive unphysicality is a consequence of the *effective* nature of the model which

*Contact author: cirio.mauro@gmail.com
†Contact author: pfliang@gscaep.ac.cn
‡Contact author: nwlambert@gmail.com

focuses on *reproducing the reduced system dynamics after averaging over the ancillary degrees of freedom*. This point of view can be more formally described as a map $E \mapsto \mathrm{PM}_{\mathrm{can}}$ between a *physical environment* E and its corresponding *canonical pseudomode model* $\mathrm{PM}_{\mathrm{can}}$, whose unphysical parameters allow us to reduce the number of pseudomodes, and hence computational resources, needed to represent a given environment. In other words, the collection of these models directly correspond to real physical environments. In this context, pseudomodes have primarily been seen as a numerical tool that allows us to simulate non-Markovian and nonperturbative environments [96,97] in a transparent and simple way. *Here we enlarge the domain of applicability of the method by considering how pseudomodes can be used as ancilla degrees of freedom in experiments as a means to simulate, mitigate, or restructure physical environments.*

To develop a framework encompassing all these applications, it is useful to consider PMs with fully *unconstrained* parameters, i.e., corresponding to a map $E_{\mathrm{PM}} \mapsto \mathrm{PM}$ which generalizes the canonical case, $\mathrm{PM}_{\mathrm{can}}$, to simulate a potential unphysical *pseudoenvironment* E_{PM}.

To give meaning to this analysis, it is necessary to analyze what applications would be made available given the possibility to engineer these generalized environments in experiments (either via analog or digital techniques).

As an intuitive example, it is useful to consider what happens when such environments are coupled to the system alongside some originally present environmental bath E. We can then restrict the analysis to the situation in which the resulting "total," target environment E_{target} is physical, i.e.,

$$\begin{array}{ccccc} E_{\mathrm{PM}} & + & E & = & E_{\mathrm{target}} \\ \downarrow & & \downarrow & & \downarrow \\ \text{pseudomode bath} & & \text{original bath} & & \text{"restructured"} \\ \text{(unphysical)} & & \text{(physical)} & & \text{(physical)} \end{array} \tag{1}$$

as exemplified in Fig. 1. This simple setting can be used to show different benefits of a possible simulation of the unphysical pseudomode environment E_{PM} (henceforth dubbed *pseudoenvironment*). Specifically, we will analyze three different applications.

(i) *Quantum simulation.* First, we note that, by imposing $E = 0$ in the equation above, we recover the canonical pseudomode model $\mathrm{PM}_{\mathrm{can}}$ in which the pseudoenvironment directly correspond to a physical one. As a consequence, a protocol able to engineer the canonical pseudoenvironment would correspond to performing a *quantum simulation of non-Markovian quantum noise* by using physical analogs or digital simulations [98–114].

(ii) *Mitigation of non-Markovian noise.* Second, by imposing $E_{\mathrm{target}} = 0$, the equation above tells us that the pseudoenvironment E_{PM} is the one which exactly counteracts all the effects of the original E, resulting in the possibility to *mitigate the effects non-Markovian noise* generated by the physical environment E. As a consequence, in this case the simulation of such a pseudoenvironment can be interpreted as an extrapolation or error-mitigation procedure on the lines of Refs. [115–128]. The generality of these mitigation techniques usually rely on an underlying error model. For example, in Ref. [120], non-Markovian noise is analyzed in terms of Lindblad equations with negative rates, whose explicit derivation can be involved unless perturbative assumptions are made. In this context, the technique presented here can be interpreted as a non-Markovian mitigation protocol whose underlying error model is defined by the pseudomode mapping. On the one hand, this has the advantage of being an explicit nonperturbative model but its applicability is, on the other hand, limited to noise originating from Gaussian bosonic baths.

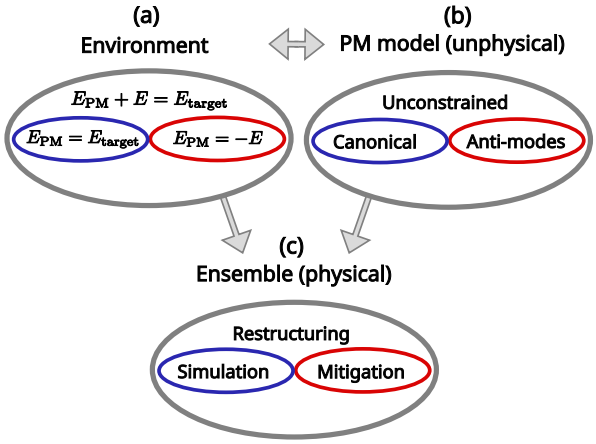

FIG. 1. Logical structure of the presented framework. The parameters of a pseudomode model PM can be extended to describe physical target environments E_{target} once their corresponding bath E_{PM} is coupled to a system alongside another physical environment E as in (a). In the most general case, this pseudoenvironment E_{PM} corresponds to an abstract unconstrained pseudomode model (b) which can be realized with a physical ensemble leading to a "restructuring" of the original bath E (c). More specific applications are found (blue ellipses) by imposing $E = 0$ (a) which leads to a simulation of the environment E_{target} (b) through the canonical pseudomode model (c). Similarly (red ellipses), imposing $E_{\mathrm{target}} = 0$ (a) corresponds to a mitigation of the effects of the bath E (c) on the system, through what we call "antimodes" (b).

(iii) *General bath restructuring.* Third, more generally, when E_{target} is a modified version of E, the formalism can be interpreted as a way to *restructure* some environmental properties without assuming them to be experimentally accessible. As an example, E_{target} could specify a new bath having the very same properties as the original E apart from a different temperature. This restructuring can be realized when the pseudoenvironment defined by Eq. (1) is coupled to the system alongside the original bath E.

To achieve these goals (the simulation, mitigation, or reshaping of the properties of non-Markovian noise), we need a means to physically implement the pseudomode model experimentally, either with digital or analog simulation. At first glance, this seems challenging, because of the previously mentioned innate unphysicality of the pseudomodes formulation which we use. For example, as we will show later, this unphysicality can appear in the form of complex non-Hermitian couplings between system and pseudomodes, which may also have complex temperatures or complex frequencies, as well as imaginary-valued classical stochastic fields acting on the system. *In this article we describe a solution to this problem in the form of general protocol to enable*

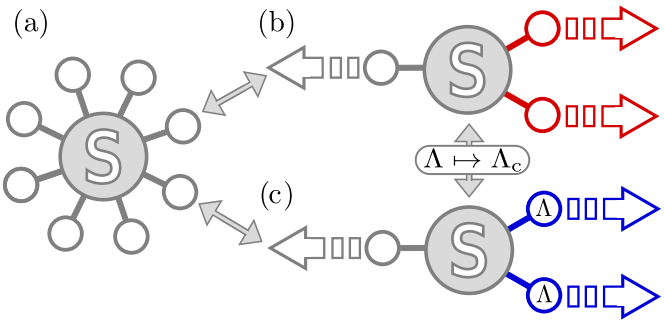

FIG. 2. Graphical representation of the protocol to simulate unphysical pseudoenvironments. In (a), a system S interacts with a continuum of bosonic degrees of freedom. In (b), the reduced dynamics of the system is approximated by the one in which the system interacts with a discrete set of pseudomodes or stochastic fields, see Eq. (10). Some of these modes or fields can be unphysical (represented by the color red). In (c), an ensemble of *physical* pseudomodes or fields (represented by the color blue) leads to the same reduced system dynamics as the original pseudomode model in (b) and the original open quantum system in (a) once the parameter Λ parametrizing the ensemble is analytically continued to the critical value Λ_c. This prescription for the physical implementation of unconstrained pseudomode model opens an avenue to the applications presented in Fig. 1.

the experimental realization of such unphysical pseudomode models.

This is achieved by analytical continuation of measurement results over an ensemble of physical systems [129], see Fig. 2. By using bounds provided by the theory of polynomial approximation and extrapolation, we describe the limitations of this technique in terms of an interplay between bias and stability errors. Mainly, while the order of the extrapolating polynomial allows one to increase the predictive power of the method under perfect conditions (reducing its bias), it also increases the sensitivity to imprecision in the initial data (observable outcomes over a physical ensemble). This leads to a limitation in the complexity of the effects of the environment on the system which can be recovered using this method.

This article is organized as follows. In Sec. II we start by reviewing open quantum systems to introduce the pseudomode model in Sec. III. In Sec. IV, we describe the main result of this article, i.e., a protocol to simulate the pseudomode model using an ensemble of physical systems. In Sec. V, we present an overview of the possible use of these results to simulate, mitigate, and restructure non-Markovian noise. In Sec. VI, we provide specific numerical examples for each of these use cases for an environment described by an underdamped Brownian spectral density. In Sec. VII, we further provide an error analysis of the algorithm. We finish presenting our conclusions in Sec. VIII.

II. OPEN QUANTUM SYSTEMS

In this article, we focus on Gaussian bosonic environments, whose effects on a system can be fully characterized by the correlation of the operator through which they couple to the system. In this section, tildes are used over some of the parameters to explicitly distinguish them from conceptually related ones used to describe the effective baths introduced in the next sections.

We consider a system S interacting with a physical bosonic environment E with a total Hamiltonian ($\hbar = 1$),

$$H = H_S + \hat{s}X + H_E, \tag{2}$$

where H_S is the Hamiltonian of the system and $H_E = \sum_{\tilde{k}} \omega_{\tilde{k}} \tilde{a}^\dagger_{\tilde{k}} \tilde{a}_{\tilde{k}}$ is the free Hamiltonian of the environment with $\tilde{a}_{\tilde{k}}$ the annihilation operator for the environmental mode $\tilde{k}$ with frequency $\omega_{\tilde{k}}$. The interaction term is a function of a generic system operator $\hat{s}$ and it has a linear dependency on the environment, i.e.,

$$X = \sum_{\tilde{k}} \tilde{\lambda}_{\tilde{k}} (\tilde{a}_{\tilde{k}} + \tilde{a}^\dagger_{\tilde{k}}), \tag{3}$$

where we introduced the coupling strengths $\tilde{\lambda}_{\tilde{k}} \in \mathbb{R}$. We explicitly note that nonlinear environmental couplings are outside the scope of the pseudomode model and, as a consequence, of the method presented here. The reduced dynamics of the system is

$$\tilde{\rho}_S(t) = \mathrm{Tr}_E[\rho_{S+E}(t)], \tag{4}$$

where ρ_{S+E} is the density matrix of the full system+environment. In general, the reduced dynamics of the system depends on all the n-point free correlation functions involving the interaction operator $X(t)$ (where the time dependence indicates the Heisenberg picture). However, for Gaussian environments, all this information is encoded, through Wick's theorem, in the two-point correlation function,

$$C_E(t_2, t_1) = \mathrm{Tr}_E\left[X(t_2)X(t_1)\rho_E^{\mathrm{eq}}\right], \tag{5}$$

where the average is taken over the equilibrium distribution ρ_E^{eq} of the environment. When the environment is initially in a thermal equilibrium at inverse temperature β, the correlation function is translational invariant and takes the form $C_E(t_2, t_1) = C_E(t_2 - t_1)$, where

$$C_E(t) = \int_0^\infty d\omega \frac{J(\omega)}{\pi}\left[\coth\left(\frac{\beta\omega}{2}\right)\cos(\omega t) - i\sin(\omega t)\right], \tag{6}$$

in terms of the spectral density function,

$$J(\omega) = \pi \sum_{\tilde{k}} \tilde{\lambda}^2_{\tilde{k}} \delta(\omega - \omega_{\tilde{k}}). \tag{7}$$

In the next section, we introduce the pseudomode model as a map between the reduced dynamics for the open quantum system described here and the one computed by averaging over the effects of a discrete set of ancillary harmonic quantum modes and classical stochastic fields.

III. PSEUDOMODE MODEL

The pseudomode method consists in replacing the original continuum of environmental modes with a discrete set of dissipative harmonic modes and stochastic driving fields. The main purpose of these ancillary degrees of freedom is to reproduce the correlation function characterizing the original Gaussian environment and, ultimately, to reproduce the original reduced system dynamics in Eq. (4). We refer to Refs. [89,90,95] and to Appendixes A and B for more details.

PM will be used to indicate a possibly stochastic operator $\mathcal{M}$ acting linearly on the density matrix $\rho_{S\text{-PM}}$ in a space composed by the system and N_{PM} ancillary Fock spaces. The influence of $\mathcal{M}$ can thereby be interpreted as the effect of an artificial environment made of N_{PM} dissipative harmonic modes (pseudomodes) and an optional stochastic driving field acting on the system. Perhaps the most important feature of the model is the existence of a nonperturbative relation between these "*pseudoenvironments*" and physical, Gaussian bosonic environments as described in Sec. II. This "*pseudomode mapping*" defines the dependency of $\mathcal{M}$ on a set of parameters G_{PM} which directly depend on the spectral density in Eq. (7) and hence on the properties of the physical bath. This mapping is defined by matching the coupling statistics of the pseudomode model and the original bath [encoded in the correlation in Eq. (6)].

These definitions take a practical form in specifying the dynamics of the density matrix $\rho_{S\text{-PM}}$ of the pseudomode model as

$$\dot{\rho}_{S\text{-PM}}(t;G_{\text{PM}}) = \mathcal{M}(G_{\text{PM}})[\rho_{S\text{-PM}}(t;G_{\text{PM}})]. \tag{8}$$

The parameters in G_{PM} are optimized so that the reduced system dynamics,

$$\rho_S(t;G_{\text{PM}}) = \mathbb{E}[\rho_{S\text{-PM}}(t;G_{\text{PM}})], \tag{9}$$

is equivalent to the one in the original open quantum system, i.e., that

$$\tilde{\rho}_S(t) = \rho_S(t;G_{\text{PM}}). \tag{10}$$

Here $\mathbb{E}$ indicates the expected value over the optional stochastic properties of $\mathcal{M}$.

It is useful to stop for a moment in order to introduce a few examples describing how to qualitatively different environmental effects can be modeled using the formalism above.

A. Reproducing environmental effects

The pseudomode model is designed to exactly reproduce all the effects of a Gaussian bosonic bath linearly coupled to a system. For concreteness, here we analyze how to model specific effects. Since the aim of this section is to highlight the generality of the pseudomode model in characterizing qualitatively different environmental properties, the specific dependence of the model parameters on the original environment is not explicitly described. We refer to Refs. [89,90,95] and Appendix B for more details.

1. Markovian effects

Markovian effects arise as a consequence of memory-less contributions $C_\delta(t) = \Gamma\delta(t)$ to the correlation in Eq. (6), so that Γ can be interpreted as a decay rate. In this limit, the operator $\mathcal{M}$ takes a Lindblad form, i.e., it can be written as the sum of dissipators,

$$\mathcal{M} \mapsto \mathcal{M}_\delta(\{\Gamma\}) = \Gamma D_{\hat{s}}, \tag{11}$$

where $D_{\hat{s}}[\cdot] = 2\hat{s}\cdot\hat{s}^\dagger - \hat{s}^\dagger\hat{s}\cdot - \cdot\hat{s}^\dagger\hat{s}$, for a system operator $\hat{s}$.

2. Classical effects

This case, which includes the previous one, amounts in modeling effects which can be ascribed to a symmetric contribution $C_{\text{class}}(t) = C_{\text{class}}(|t|)$ to the correlation in Eq. (6). The corresponding model can be written in terms of a stochastic drive,

$$\mathcal{M} \mapsto \mathcal{M}_{\text{class}}(\{c_n\}) = -i\xi(t)[\hat{s},\cdot], \tag{12}$$

where the coefficients $\{c_n\}$, $n = 1,\ldots,N_{\text{stoch}}$, define the spectral representation of a Gaussian field with zero mean and correlation matching $C_{\text{class}}(t)$, i.e.,

$$C_{\text{class}}(t) = c_0 + 2\sum_{n=1}^{N_{\text{stoch}}} c_n \cos[n\pi t/T], \tag{13}$$

which can always be achieved by increasing the cut-off parameter N_{stoch}.

3. Quantum effects

This case, which includes both previous ones, amounts in modeling general effects related to a nonclassical contribution $C_Q(t)$ to the correlation in Eq. (6). The corresponding model can be written in terms of a sum of terms taking the form

$$\begin{aligned}\mathcal{M} &\mapsto \mathcal{M}_Q(\{\Omega,\lambda,\Gamma,n\})\\ &= -i[\Omega a^\dagger a + \lambda\hat{s}(a+a^\dagger),\cdot] + \Gamma(n+1)D_a + \Gamma n D_{a^\dagger},\end{aligned} \tag{14}$$

written in terms of a pseudomode operator a and dependent on its frequency Ω, the coupling strength λ, the decay rate Γ, and the distribution n. This form implies the effects due to N_{PM} pseudomodes to be encoded in a correlation contribution written as

$$C_Q(t) = \sum_{j=1}^{N_{\text{PM}}} C_Q^j(t), \tag{15}$$

where

$$C_Q^j(t) = \lambda_j^2[(n_j+1)e^{-i\Omega_j t} + n_j e^{i\Omega_j t}]\exp[-\Gamma_j|t|]. \tag{16}$$

The pseudomode mapping consists in finding the optimal value for these parameters such that, in general,

$$C_E(t) = C_\delta + C_{\text{class}} + C_Q(t). \tag{17}$$

By considering all these different effects together, the canonical pseudomode model associated with the environment E is determined by the collection

$$G_{\text{PM}} = \{\Omega_k, \lambda_k^2, \Gamma_k, n_k, c_n\}, \tag{18}$$

where $k = 1,\ldots,N_{\text{PM}}$, $n = 0,\ldots,N_{\text{stoch}}$, characterizing the environmental correlation in Eq. (17) in terms of pseudomodes and fields (where we omitted the Markovian component as its effects can always be included in the other degrees of freedom).

In Ref. [90], it was shown that the correlation of environments characterized by a Brownian spectral density in the underdamped regime can be well approximated by a sum of purely quantum contributions, even in the zero-temperature case. In this case, some of the modes were shown to require imaginary couplings λ to the system. In Ref. [95], it was further shown that such an environment can always be modeled by a single, physical, quantum contribution with $n = 0$ alongside a classical one representing a single, imaginary, stochastic field for any temperature of the original bath. These

results imply that, in order to correctly reproduce the reduced system dynamics, the artificial environment representing the pseudomode model might require to have "unphysical" parameters.

While preventing a direct physical interpretation, this enlarged parameter domain also implies the possibility for a more optimized description of the original environment. At the same time, it is worthwhile to explicitly point out that, since the form of the dynamical equation *does not* depend on the physicality of the parameters, its unphysical solutions can be interpreted as the *analytical continuation of the physical solutions* (considered as functions of the variables in the set $G_{\rm PM}$). For example, non-Hermitian contributions to the unitary dynamics are not compensated by taking the Hermitian conjugate on the Hamiltonian when acting on the right of the density matrix [90]. This makes the procedure qualitatively different than the orthodox concept of non-Hermitian quantum mechanics [130,131].

In order to give a more formal terminology, we define a parameter $\eta \in G_{\rm PM}$ as *physical* if $\eta \in \mathbb{R}^+$ and *unphysical* otherwise. This language sets the basis for the generalizations which we are going to analyze in this article.

B. Beyond the canonical pseudomode model

The pseudomodel described above is labeled "*canonical*" because, despite its possible unphysicality, all the parameters are constrained to mimic the effects of *physical environments* on the system through Eq. (10). Here we are interested in a more general case whose parameters are *unconstrained* to lie outside the canonical model, thereby corresponding to *unphysical environments*. Given a set of parameters $G_{\rm PM}$ of an unconstrained pseudomode model, we define $E_{G_{\rm PM}}$ as its corresponding pseudoenvironment,

$$E_{G_{\rm PM}} \leftrightarrow G_{\rm PM}, \tag{19}$$

which is composed of the (potentially unphysical) modes and fields characterized by the parameters in $G_{\rm PM}$, through Eq. (18). We will show that, while unphysical, these environments can be used to effectively change, or "restructure," the properties of a physical bath.

Given this general setting, our goal is *to describe how to reproduce the effects of such an unconstrained pseudomode model from measurement results over physical ensembles*. We will achieve this by defining an analytical continuation protocol on the unphysical parameters to allow observable outcomes in a physical ensemble to reproduce the effects of any general unphysical pseudomode model. In turn, this will lead to a physical representation of models associated to physical environments (thereby defining a tool for their simulation) and models corresponding to more general effects, such as noise mitigation or the restructuring of some environmental properties such as temperature.

IV. UNPHYSICAL PSEUDOMODES WITH PHYSICAL ENSEMBLES

In this section, we analyze a physical characterization of the unconstrained pseudomode model. The possibility to do so stems from the fact that the analytical continuation considered here can intuitively be interpreted as a Wick's rotation (used to map time to an imaginary temperature-like quantity akin to the methods used in the context of quantum Monte Carlo [132–150]) on a parameter Λ. In this context, we follow the specific theoretical protocol presented in Ref. [129] (see also Ref. [151]) where observable results over an ensemble of quantum systems are used to perform a Wick rotation to relate classical statistical systems to quantum measurements and vice versa.

Here we implement a similar strategy to analytically continue observables extracted from a physical pseudomode model into observables of the corresponding unphysical pseudomode model. To start, we denote the unphysical or physical parameters as $\eta_j^{\rm unphys}/\eta_k^{\rm phys}$, where $k = 1, \ldots, N^{\rm phys}$ and $j = 1, \ldots, N^{\rm unphys}$, specifying their total number. These definitions can be used to write the set $G_{\rm PM}$ characterizing the model as

$$G_{\rm PM} \equiv \left\{\eta_j^{\rm unphys}, \eta_k^{\rm phys}\right\}. \tag{20}$$

The physical intuition behind this definition is directly related to the parameters of the model defined in Eq. (18), whose positivity constitutes a sufficient condition to obtain a fully physical effective Hamiltonian. For example, a negative coefficient c_n would give rise to a non-Hermitian contribution to the Hamiltonian through the square roots defining the stochastic drive in Eq. (A13). Similarly, we further require that the frequency, squared coupling strength, decay rate, and Bose-Einstein distribution associated to each pseudomode to all be positive in order for the model to be considered physical. We now consider a set of $N^{\rm unphys}$ functions $\Xi_j : \mathbb{C} \to \mathbb{C}$ such that

$$\begin{aligned} &\Xi_j(\Lambda) \in \mathbb{R}^+ \quad \text{for} \quad \Lambda \in D_{\rm phys}, \\ &\Xi_j(\Lambda_{\rm c}) = \eta_j^{\rm unphys} \quad \text{for} \quad \Lambda_{\rm c} \in \mathbb{C},\ \Lambda_{\rm c} \notin D_{\rm phys}. \end{aligned} \tag{21}$$

Here the first set of conditions allows us to interpret the values $\Xi_j(\Lambda)$ as physical parameters on the domain $D_{\rm phys}$ which, here, is arbitrarily set to be

$$D_{\rm phys} = [-1, 1]. \tag{22}$$

This specific choice is motivated by its compatibility with the domain of the Chebyshev polynomials which are a convenient tool for extrapolation. The second condition requires that the unphysical parameters $\eta_j^{\rm unphys}$ can be recovered by analytical continuation of the functions $\Xi_j(\Lambda)$ for $\Lambda \mapsto \Lambda_{\rm c} \in \mathbb{C}$. While not necessary, it is convenient to further impose

$$\Xi_j(-1) = 0, \quad \Xi_j(1) = 1, \tag{23}$$

to reflect bounds on accessible physical regimes. The parameter Λ is the one we will eventually analytically continue. We now define a "physical regularization" of the set $G_{\rm PM}$ as

$$G_{\rm PM}^{\rm phys}(\Lambda) \equiv \left\{\eta_j^{\rm unphys} \mapsto \eta_j(\Lambda) = \Xi\big(\Lambda; \eta_j^{\rm unphys}\big), \eta_k^{\rm phys}\right\}, \tag{24}$$

which uses Λ to parametrize an ensemble of pseudomodes models which are physical in the domain $\Lambda \in [-1, 1]$. Using the second condition in Eq. (21), it is possible to directly verify that

$$G_{\rm PM}^{\rm phys}(\Lambda_{\rm c}) = G_{\rm PM}. \tag{25}$$

This shows that, indeed, *the analytical continuation of the physically regularized model recovers the unconstrained pseudomode model.* For concreteness, it is possible to define the function $\tilde{\Xi}(\Lambda)$ as

$$\tilde{\Xi}(\Lambda) = (1+\Lambda)/2, \tag{26}$$

which, together with

$$\Lambda_c = -1 + 2i, \tag{27}$$

fulfills the constraints in Eq. (21) and Eq. (23) through the definition

$$\Xi\big(\Lambda; \eta_j^{\text{unphys}}\big) \equiv F_\Lambda\big(\eta_j^{\mathcal{R}}\big) + \tilde{\Xi}(\Lambda) F_\Lambda\big(\eta_j^{\mathcal{I}}\big), \tag{28}$$

where $\eta_j^{\mathcal{R}} \equiv \text{Re}[\eta_j^{\text{unphys}}]$, $\eta_j^{\mathcal{I}} \equiv \text{Im}[\eta_j^{\text{unphys}}]$, and where

$$\begin{aligned} F_\Lambda(x) &\equiv \theta(x)x + \tilde{\Xi}^2(\Lambda)\theta(-x)|x| \\ &= [\theta(x) - \tilde{\Xi}^2(\Lambda)\theta(-x)]x, \end{aligned} \tag{29}$$

is defined in terms of the step function $\theta(x) = 1$ for $x \geqslant 1$ and zero otherwise. While other choices are possible, this will be the default one used throughout this article. The function defined in Eq. (29) satisfies

$$0 \leqslant F_{\Lambda \in D_{\text{phys}}}(x) \leqslant |x|, \ \forall x, \tag{30}$$

where the physical domain D^{phys} is defined in Eq. (22). In turn, using Eq. (28), this implies the following corresponding properties for the function $\eta_j(\Lambda) = \Xi(\Lambda; \eta_j^{\text{unphys}})$ in Eq. (24) as

$$0 \leqslant \eta_j(\Lambda \in D_{\text{phys}}) \leqslant \big|\text{Re}\big[\eta_j^{\text{unphys}}\big]\big| + \big|\text{Im}\big[\eta_j^{\text{unphys}}\big]\big|. \tag{31}$$

This equation directly provides the range of parameters defining the physical ensemble required by the protocol. We can see this explicitly by recalling that each η_j^{unphys} characterizes a parameter in the full unphysical model through Eq. (18). In other words, for each unphysical parameter η_j^{unphys} present in the model through Eq. (18), we assume it is possible to physically tune its physical version [i.e., $\eta_j(\Lambda) = \Xi(\Lambda; \eta_j^{\text{unphys}})$ for $\Lambda \in D_{\text{phys}}$ as defined in Eq. (24)] for all the values between zero and the upper bound in Eq. (31).

In order to provide an example to these formal definitions, we can consider the case of an imaginary coupling $\lambda^{\text{unphys}} = i\bar{\lambda}$ (in terms of a physical energy scale $\bar{\lambda}$) between a pseudomode and the system. This is a relevant case as the corresponding correlation for such a pseudomode is going to be negative even at zero time, consistently with the "Matsubara contribution" analyzed in Ref. [90]. While the imaginary coupling above does not immediately allow a physical realization, we can nonetheless interpret it as the result of an analytical continuation procedure. To do this, we can follow Eq. (24), Eq. (28), and Eq. (26) to write

$$\lambda^{\text{unphys}} \mapsto \lambda(\Lambda) = \Xi(\Lambda; \lambda^{\text{unphys}}) = \tilde{\Xi}(\Lambda)\bar{\lambda} = \bar{\lambda}(1+\Lambda)/2. \tag{32}$$

We can now explicitly check that this physical version of the unphysical coupling ranges from zero to $\bar{\lambda}$ (for $\Lambda \in D_{\text{phys}} = [-1, 1]$), thereby satisfying the general bound given in Eq. (31). Furthermore, for $\Lambda \to \Lambda_c$ we also recover the unphysical version of the coupling by construction.

In summary, we formally defined physical versions of the pseudomodes parametrized by a *single* parameter Λ whose analytical continuation to $\Lambda \mapsto \Lambda_c$ reproduces the unphysical pseudomodes model as shown in Eq. (25). Our attention now shifts towards the implementation of this analytical continuation using measurement results over the physical ensemble $G_{\text{PM}}^{\text{phys}}(\Lambda)$ corresponding to sweeping over different values of Λ.

A. Analytical continuation

In the previous sections we showed that, given a pseudomode model defined by a set $G_{\text{PM}}(\Lambda)$ of unconstrained parameters, there exists a regularized version $G_{\text{PM}}^{\text{phys}}(\Lambda)$ whose parameters are physical for $\Lambda \in D^{\text{phys}}$. This implies that the corresponding models $\mathcal{M}_{\text{PM}}^{\text{phys}}(\Lambda)$ can be interpreted as a physical ensemble parametrized by $\Lambda \in D^{\text{phys}}$. Here the word "physical" takes an operative meaning [152], as each of these models can, in principle, be experimentally realized by coupling the system to a set of ancillary resonators and by driving it with a classical stochastic field. This means that, for such Λs, and for a given time t, we can always perform a sequence of measurements to reconstruct the density matrix,

$$\rho_S(t; \Lambda) \equiv \rho_S\big(t; \big\{\eta_j^{\text{unphys}} \mapsto \Xi_j(\Lambda), \eta_k^{\text{phys}}\big\}\big), \tag{33}$$

which simply corresponds to the dynamics of the model as in Eq. (8). The density matrix, interpreted as a function of the parameter Λ, can be analytically continued to the value Λ_c to finally achieve our goal, i.e., the simulation of the unphysical pseudomdode model corresponding to the density matrix,

$$\rho_S(t; \Lambda_c) \equiv \rho_S\big(t; \big\{\eta_j^{\text{unphys}} \mapsto \Xi_j(\Lambda_c), \eta_k^{\text{phys}}\big\}\big). \tag{34}$$

This result can also be rephrased in terms of equivalent pseudoenvironments. In fact, generalizing Eq. (19), we can define $E_{\text{PM}}^{\text{phys}}(\Lambda)$ as the physical pseudoenvironment corresponding to the regularized set $G_{\text{PM}}^{\text{phys}}(\Lambda)$, i.e.,

$$E_{G_{\text{PM}}}^{\text{phys}}(\Lambda) \leftrightarrow G_{\text{PM}}^{\text{phys}}. \tag{35}$$

In this way, Eq. (34) can be interpreted as an analytical continuation of the corresponding pseudoenvironments, i.e.,

$$E_{\text{PM}}^{\text{phys}}(\Lambda_c) = E_{\text{PM}}. \tag{36}$$

While this can be considered just as an equivalent way to interpret Eq. (34), it also allows us to grasp its meaning from a different point of view. In fact, Eq. (36) can be intuitively interpreted as manifesting the *possibility to define a parametrization for physical environments such that, on analytical continuation, the effects on the system are equivalent to those generated by a generalized, unphysical pseudomode model*. This different prospective paves the way for the applications which will be analyzed in Sec. V.

Here it is worth remembering that the correlation for the full environment affecting the dynamics of $\rho_S(t; \Lambda)$ is made by both the original open system and the Λ-parametrized pseudomode model. This means that the overall correlation for this composite environment can be written as

$$C(t; \Lambda) = C_E(t) + C_{\text{PM}}(t; \Lambda). \tag{37}$$

If we now denote the correlation of the target environment E_{target} as $C_{E_{\text{target}}}(t)$, then the general expression in Eq. (1)

translates into the following correspondence for correlations:

$$C(t;\Lambda_c) = C_{E_{\text{target}}}(t) + \Delta C(t). \tag{38}$$

Here $\Delta C(t)$ quantifies the discrepancy between the correlations of the analytical continued model and the target one so that Eq. (38) could also be interpreted as its definition. In practice, we can only assume the physical ensemble $E^{\text{phys}}_{\text{PM}}(\Lambda)$ to be realized for a discrete grid of points, which is the case we are going to analyze in the next section.

B. Polynomial extrapolation

In this section, we analyze the analytical continuation of the expectation values of a system observable,

$$f^t_n \equiv \langle \hat{O}_S \rangle(t;\Lambda_n) \equiv \text{Tr}_S[\hat{O}_S \rho_S(t;\Lambda_n)], \tag{39}$$

over the physical ensemble described by a set of N_{cont} points $\Lambda_n \in \Lambda$ for $n = 1, \ldots, N_{\text{cont}}$. We note that this is a weaker version of the case considered in the previous section. In fact, the analytical continuation of the full density matrix can be considered as the limiting, and more resource-consuming, task where we analytically continue not just one but a complete set of observables.

We now introduce the following practical procedure for analytical continuation. We first define the function $p_M(t;\Lambda)$ as the order M polynomial which minimizes the distance,

$$d^2 = \sum_{n=0}^{N_{\text{cont}}} \left| p_M(t;\Lambda_n) - f^t_n \right|^2. \tag{40}$$

This least-squares fitting can be used to reconstruct the observable as

$$\langle \hat{O}_S \rangle(t;\Lambda_c) \equiv p_M(\Lambda_c). \tag{41}$$

The ability to reconstruct the full pseudomode model from an ensemble of pseudomodes constrained to physical dynamics opens up the possibility of several interesting applications that would be otherwise physically inaccessible. In the next section, we analyze these applications, in terms of simulation, restructuring, and mitigation of non-Markovian quantum noise. We explicitly note that this analytical continuation procedure does not allow us to infer the expectation values of observables which are independent from the ones measured.

V. APPLICATIONS

In this section we describe different possible applications of our protocol. Mainly, we show that, by driving a system with classical noise and by coupling it to ancillary harmonic modes, it is possible to analogically simulate, mitigate, or restructure the effects of a Gaussian bosonic environment.

A. Simulation

We start by defining a procedure to simulate a physical environment E', which we assume to be well described by a pseudomode model characterized by a parameter set G'_{PM}. We note that this corresponds to imposing $E = 0$ in Eq. (1), which then translates to

$$E_{\text{PM}} = E_{\text{target}}. \tag{42}$$

In other words, a simulation of the open quantum system $S + E_{\text{target}}$ can be achieved by coupling the (closed) system to the pseudoenvironment E_{PM} corresponding to the pseudomode model with parameters G'_{PM}. As noted in our previous discussion, the pseudoenvironment E_{PM} is, in general, not directly physically realizable. To circumvent this problem, we follow the analysis in Sec. IV and define a set of regularized parameters $G^{\text{phys}}_{\text{PM}}(\Lambda)$ corresponding to a collection of *physical* pseudoenvironments $E^{\text{phys}}_{\text{PM}}(\Lambda)$. By measuring observables in this ensemble, it is then possible to proceed with the analytical continuation protocol illustrated in Sec. IV, i.e.,

$$G^{\text{phys}}_{\text{PM}}(\Lambda_c) = G_{\text{PM}}, \quad E^{\text{phys}}_{\text{PM}}(\Lambda_c) = E_{\text{PM}}, \tag{43}$$

which corresponds to simulating the effects of the original environment E' on the system.

B. Mitigation

Another interesting application is the use of the pseudomode model to mitigate the effects of a non-Markovian environment E, which we assume to be well described by a pseudomode model characterized by a parameter set $G_{\text{PM}} = \{\Omega_k, g_k^2, \Gamma_k, n_k, c_n\}$. The mitigation procedure corresponds to imposing $E_{\text{target}} = 0$ in Eq. (1), which brings it to the form

$$E + E_{\overline{\text{PM}}} = 0. \tag{44}$$

This equation describes the (unphysical) pseudoenvironment $E_{\overline{\text{PM}}}$ which, once coupled to the system, completely cancels all effects of the environment E. Since we assume the knowledge of the pseudomode model describing E, the parameters defining this "antimode" environment $E_{\overline{\text{PM}}}$ can be explicitly written as

$$G_{\overline{\text{PM}}} = \left\{\Omega_k, -g_k^2, \Gamma_k, n_k, -c_n\right\}. \tag{45}$$

To derive this equation we simply noted that if the original set G_{PM} describes a correlation $C_E(t)$, then the set $G_{\overline{\text{PM}}}$ must correspond to

$$C_{\overline{\text{PM}}}(t) = -C_{\text{PM}}(t), \tag{46}$$

since Eq. (A12) and Eq. (14) are linear in c_n and g_k^2, respectively. In other words, the compound effect of the pseudomode model and its "antimode" version does not have any influence on the system since the two correlations sum up to zero: A system simultaneously in contact with a Gaussian environment and its unphysical "mirror" or antienvironment should evolve as if no environment were present at all, i.e., noise free. Because of its effective noise-cancelling action, the antimode environment is necessarily unphysical. However, following Sec. IV, we can regularize its parameters to define the corresponding physical ensemble $E^{\text{phys}}_{\overline{\text{PM}}}(\Lambda)$ parametrized by Λ, from which gathering all the information needed for the analytical continuation

$$E^{\text{phys}}_{\overline{\text{PM}}}(\Lambda_c) = E_{\overline{\text{PM}}} = -E, \tag{47}$$

to achieve mitigation using measurements on a physical ensemble.

C. Restructuring

In its most general form, Eq. (1) reads

$$E_{\rm PM}^{\rm restructuring} + E = E_{\rm target}, \tag{48}$$

and can, for example, be interpreted as a "restructuring" of a given physical environment E (which we assume associated to a pseudoenvironment $E_{\rm PM} = E_{\rm phys}$) into a version $E_{\rm target}$ (associated to the pseudoenvironment $E_{\rm PM'} = E_{\rm target}$) characterized by different physical properties (such as temperature or system-bath coupling). This is achieved by coupling the system to a pseudoenvironment $E_{\rm PM}^{\rm restructuring}$ whose parameters must be a function of those in $E_{\rm PM}$ and $E_{\rm PM'}$ encoding the specific "changes" to be imposed on the bath. For the most interesting cases, the resulting environment is going to be unphysical so that, as done in the previous cases, we will need to resort to the analytical continuation procedure outlined in Sec. IV for the physical implementation of its effects.

Here we note that, while more optimized versions might be possible (as shown in the example in Sec. VI B), in the worst case, the restructuring can always be defined by using both the simulation and mitigation techniques presented in the previous sections. In fact, thanks to our assumptions and the definition in Eq. (44) we can directly check that

$$E_{\rm PM}^{\rm restructuring} = E_{\rm PM'} + E_{\overline{\rm PM}}, \tag{49}$$

satisfies Eq. (48). In other words, in order to restructure a bath $E_{\rm phys}$ into $E'_{\rm phys}$ it is always possible to couple the system to both the antienvironment relative to $E_{\rm phys}$ and an additional one simulating $E'_{\rm phys}$. As mentioned, this worst-case scenario can be optimized depending on the specific requirements of the restructuring as we will show in the example in Sec. VI B.

In the following, we are going to present explicit numerical examples for each of these applications.

VI. NUMERICAL EXAMPLES

To show a practical numerical implementation [153–156] of the applications presented in the previous section, here we present three examples: the mitigation and simulation of the effects of an environment characterized by an underdamped Brownian spectral density at zero and finite temperature and the "restructuring" of the finite-temperature case into the zero-temperature one. We note that, for exposition clarity, the order in which these examples are presented is different with respect to the previously reported one.

For concreteness, we will focus on a Gaussian bosonic environment characterized by the spectral density function

$$J^B(\omega) = \frac{\gamma\lambda^2\omega}{\left(\omega^2 - \omega_0^2\right)^2 + \gamma^2\omega^2}, \tag{50}$$

written in terms of a resonance frequency ω_0, a frequency width γ, and a (frequency)$^{3/2}$ strength λ. It describes a Ohmic behavior at low frequency, i.e.,

$$J^B(\omega) \sim \alpha\omega \quad \text{for} \quad \omega \ll \omega_0, \tag{51}$$

and it has a polynomial cutoff at high-frequencies, i.e.,

$$J^B(\omega) \sim \alpha\omega_0^4/\omega^3 \quad \text{for} \quad \omega \gg \omega_0, \tag{52}$$

in terms of the adimensional scale $\alpha = \lambda^2\gamma/\omega_0^4$. We further restrict ourselves to the underdamped regime which requires

$$\omega_0^2 - \gamma^2/4 > 0. \tag{53}$$

By inserting the spectral density $J_B(t)$ in Eq. (6) the correlation function can be computed as [95]

$$C^B(t;\beta) = C^B_{\rm class}(t;\beta) + C^B_Q(t), \tag{54}$$

where

$$\begin{aligned} C^B_{\rm class}(t;\beta) = {} & \frac{\lambda^2}{4\Omega}\coth\left[\beta(\Omega + i\Gamma)/2\right]e^{i\Omega|t|}e^{-\Gamma|t|} \\ & - \frac{\lambda^2}{4\Omega}\coth\left[\beta(-\Omega + i\Gamma)/2\right]e^{-i\Omega|t|}e^{-\Gamma|t|} \\ & - \frac{\lambda^2}{4\Omega}(e^{-i\Omega t} + e^{i\Omega t})e^{-\Gamma|t|} \\ & + \frac{2i}{\beta}\sum_{k>0} J\left(\omega_k^M\right)e^{-|\omega_k^M||t|}. \end{aligned} \tag{55}$$

This expression, written in terms of the Matsubara frequencies $\omega_k^M = 2\pi k i/\beta$ $(k = 1, \ldots, \infty)$, is the symmetric, or "classical" contribution which contains all temperature effects which can, thereby, be modeled within the statistics of a single temperature-dependent, classical field $\xi_\beta(t)$, defined explicitly in Appendix A, such that

$$C^B_{\rm class}(t;\beta) = \mathbb{E}[\xi_\beta(t_2)\xi_\beta(t_1)], \tag{56}$$

where $t = t_2 - t_1$. We can label the remaining contribution,

$$C^B_Q(t) = \frac{\lambda^2}{2\Omega}\exp\left[-i\Omega t - \Gamma|t|\right], \tag{57}$$

as "quantum," since it does not have specific symmetries, but it has the form of Eq. (A10), i.e., it can be reproduced using a single harmonic mode initially at zero temperature.

To be specific, we will consider the open system to be composed of a two-level system coupled to the Brownian environment B described above. Specifically, given a full density matrix $\rho_{S+B}(t)$ in the system+environment space whose dynamics is described by a full Hamiltonian H_{S+B} as

$$\dot\rho_{S+B}(t) = -i[H_{S+B}, \rho_{S+B}(t)], \tag{58}$$

we want to compute the reduced dynamics encoded in

$$\rho_S(t) = {\rm Tr}_B[\rho_{S+B}(t)]. \tag{59}$$

By defining the system Hamiltonian as

$$H_S = \frac{\omega_s}{2}\sigma_z + \frac{\Delta}{2}\sigma_x, \tag{60}$$

and assuming that the operator $\hat s = \sigma_x$ mediates the interaction to the environment, the reduced dynamics can be computed by using the pseudomode model, i.e., by computing

$$\rho_S(t) = {\rm Tr}_B[\rho_{S+{\rm PM}}(t)], \tag{61}$$

which requires us to solve the differential equation

$$\dot\rho_{S+{\rm PM}} = -i[H_S + \xi_\beta(t)\hat s, \rho_{S+{\rm PM}}] + L_{a_{\rm res}}[\lambda_{\rm res}; \rho_{S+{\rm PM}}]. \tag{62}$$

Here $\rho_{S+{\rm PM}}$ is the density matrix in the system+pseudomode space. This dynamics is driven by a single field $\xi_\beta(t)$ whose statistics depends on the inverse temperature β to reproduce

the Matsubara contribution to the correlation in Eq. (70) and a single pseudomode $a_{\rm res}$ to describe the resonant properties of the spectral density in Eq. (50). Following the standard pseudomode mapping [89,90,95], we have

$$L_{a_{\rm res}}[\lambda_{\rm res};\cdot] = -i[H_{\rm res}(\lambda_{\rm res}),\cdot] + \Gamma_{\rm res} D^{T=0}_{a_{\rm res}}[\cdot] \tag{63}$$

in terms of the Hamiltonian

$$H_{\rm res}(\lambda_{\rm res}) = \Omega_{\rm res} a^\dagger_{\rm res} a_{\rm res} + \lambda_{\rm res}\hat{s}(a_{\rm res} + a^\dagger_{\rm res}), \tag{64}$$

the zero-temperature dissipator

$$D^{T=0}_a[\rho] = 2a\rho a^\dagger + a^\dagger a\rho + \rho a^\dagger a, \tag{65}$$

written for a generic operator a, and the coefficients

$$\lambda_{\rm res} = \sqrt{\lambda^2/2\Omega}, \quad \Omega^2_{\rm res} = \omega_0^2 - \Gamma^2_{\rm res}, \quad \Gamma_{\rm res} = \gamma/2. \tag{66}$$

The initial state is $\rho_{S+\rm PM}(0) = \rho_S(0) \otimes |0\rangle\langle 0|$ in terms of the vacuum $|0\rangle$ annihilated by the harmonic mode a.

An interesting feature of this hybrid model associated to the spectral density in Eq. (50) is that [95]

(i) all the parameters associated with the resonant mode $a_{\rm res}$ are physical, i.e., $\lambda_{\rm res}$, $\Omega_{\rm res}$, and $\Gamma_{\rm res}$ are real and positive.

(ii) all temperature effects are encoded in the statistics of the field $\xi_\beta(t)$; i.e., in its autocorrelation function.

Given this specific environment, we are now going to analyze three specific applications in terms of mitigation, restructuring, and analog simulation.

A. Noise mitigation

In this section, we are going to analyze the mitigation of the effects of the environment specified by the spectral density in Eq. (50) both at zero and finite temperature to ultimately compute observables corresponding to the noise-free dynamics,

$$\dot{\rho}_{\rm free} = -i[H_S, \rho_{\rm free}]. \tag{67}$$

To do this, we add stochastic driving and coupling to ancillary quantum modes to the original $S+B$ open quantum system such that, after analytical continuation of a single parameter, their correlation is exactly the opposite of the original one $C^B(t)$. We can achieve this using the formalism described in Sec. V B.

First, we want to define the unphysical "antimode" model $\overline{\rm PM}$ whose correlation satisfies

$$C_{\overline{\rm PM}} = -C^B(t). \tag{68}$$

Using Eq. (45) this can be done by introducing a resonant "antimode" $\bar{a}_{\rm res}$ and an "antifield" $\bar{\xi}_\beta$, whose parameters are the same as those associated with $a_{\rm res}$ and ξ_β in Eq. (62), except for an additional complex rotation in the interaction to the system. Specifically,

$$\bar{\lambda}_{\rm res} \equiv i\lambda_{\rm res}, \quad \bar{\xi}_\beta \equiv i\xi_\beta \ (\text{or}\ \bar{c}_n = -c_n), \tag{69}$$

where the field coefficients c_n are explicitly defined in Eq. (A14).

To continue, we need to define a physical ensemble whose effects are the same as the antimode model after analytical continuation. Before doing this, it is worth differentiating between the zero- and finite-temperature cases.

1. Zero temperature

In the zero-temperature limit, it is interesting to note that a simplification occurs in the classical expression for the correlation function as [90,95]:

$$C^B_{\rm class}(t;\beta=\infty) = \frac{i}{\pi}\int_0^\infty dx J^B(ix) e^{-x|t|}. \tag{70}$$

This zero-temperature "Matsubara" contribution is negative at zero time, hinting that imaginary fields are necessary to ensure that the correct sign is reproduced in Eq. (56). This is, in fact, the case, and the field $\xi_{\beta=\infty}(t)$ is purely imaginary, which, using Eq. (69), corresponds to a real antifield $\bar{\xi}_{\beta=\infty}(t)$. Therefore, the stochastic part of the model does not require introducing any additional analytical continuation procedure [see Eq. (28)]. Thus, the analytical continuation needs only to be performed on a single unphysical parameter (the coupling $\overline{\lambda}_{\rm res}$ between the system and the resonant mode).

Given this construction of the antimode model, we can now define its physically regularized version, i.e., we want to couple the system to a physical ensemble which can be analytically continued to the antimode model above. Specifically, given the Hamiltonian H_{S+B} in the original system+bath space, we couple the system to a physical regularized-antimode $\bar{a}^{\rm phys}_{\rm res}$ and drive it by a physical field $\bar{\xi}^{\rm phys}_{\beta=\infty}(t)$, such that the dynamics is described by

$$\dot{\rho}_{S+B} = -i\big[H_{S+B} + \bar{\xi}^{\rm phys}_{\beta=\infty}\hat{s}, \rho_{S+B}\big] + L_{\bar{a}^{\rm phys}_{\rm res}}[\Xi(\Lambda)\lambda_{\rm res};\rho_{S+B}]. \tag{71}$$

Here the physicality of the field $\bar{\xi}^{\rm phys}_{\beta=\infty}(t) = \bar{\xi}^{\mathcal{I}}_{\beta=\infty}(t)$ explicitly corresponds to having an autocorrelation function of the form

$$\begin{aligned}\mathbb{E}\big[\bar{\xi}^{\rm phys}_{\beta=\infty}(t_2)\bar{\xi}^{\rm phys}_{\beta=\infty}(t_1)\big] &= -\frac{i}{\pi}\int_0^\infty dx J^B(ix)e^{-x|t|} \\ &= -C^B_{\rm class}(t;\beta=\infty) > 0 \ \forall t.\end{aligned} \tag{72}$$

In parallel, the parameters characterizing the physically regularized antimode $\bar{a}^{\rm phys}_{\rm res}$ are the same as those for the antimode $\bar{a}_{\rm res}$ in Eq. (62), except for the presence of the additional parameter Λ [introduced through the function Ξ defined in Eq. (26)], renormalizing the coupling to the system into the physical domain. We assume such a coupling to be constrained in the range $[0, \lambda_{\rm res}]$, corresponding to $\Lambda \in [-1, 1]$. The correlation function of this mode is then given by

$$\bar{C}^B_{\rm res}(t) = \Xi^2(\Lambda) C^B_{\rm res}(t), \tag{73}$$

which, by construction, gives rise to a minus sign for $\Lambda = \Lambda_{\rm c} = -1 + 2i$ using Eq. (26). In this way, Eq. (72) and Eq. (73) fulfill the identity in Eq. (68) defining the antimode model. In other words, by performing the analytical continuation $\Lambda \mapsto \Lambda_{\rm c}$, the model in Eq. (71) adds a correlation $-C^B_{\rm res}(t)$ to the open quantum system in the $(S+B)$ space in Eq. (58), i.e., it completely counteracts, in principle, all environmental noise ultimately leading to the free dynamics in Eq. (67).

We give a graphical exemplification of this procedure in Fig. 3. It is important to note that, in order to compute the dynamics plotted in this figure, we did not solve the differential equation in Eq. (71) which involves the original environmental continuum. Instead, the physically regularized antimode model is introduced on top of the deterministic pseudomode

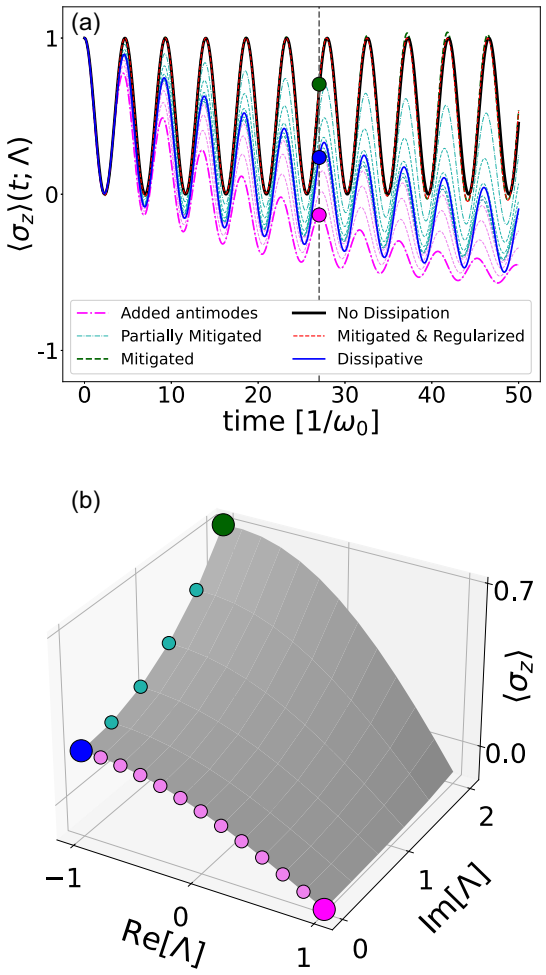

FIG. 3. Mitigation of an underdamped Brownian environment at zero temperature. (a) Dynamics of the observable σ_z. In blue, the original dissipative dynamics, solving Eq. (62). A physical version of the antimode model is added to generate the different violet curves corresponding to different $\Lambda \in [-1, 1]$ in Eq. (74). In green, partial and full mitigation as an analytical continuation on the function $\sigma_z(t;\Lambda)$ for $\Lambda \in [-1, -1-2i]$. In red, a regularization is applied to the analytically continuation of the full density matrix. (b) Analytical continuation at the specific time described by the gray line in (a). Violet points corresponds to the measured observables for different real Λ. The green points correspond to the partially and fully implemented analytical continuation. In blue, the original value in the sole presence of the bath B. The overall gray surface is the polynomial $p_M(t;\Lambda)$ used to define the analytical continuation as an extrapolation. The specific parameters used are $\alpha = 0.02$, $\Gamma = 0.3\omega_0$, $\omega_s = \Delta = \omega_0$, $M = 10$, $N_{\text{cont}} = 12$, and $N_{\text{stoch}} = 100$.

model characterizing such a continuum. In other words, we are going to model the original continuum with a pseudomode model which only includes three "deterministic" quantum degrees of freedom. On the other hand, we are going to use the "stochastic" version of the pseudomode model (involving one quantum mode and a driving noise) to simulate the environment used to mitigate the original one. In this way, the full master equation reads

$$\dot{\rho}_{S+\text{PM}+\overline{\text{PM}}} = -i[H_S + H_{\text{PM}} + \overline{\xi}_{\beta=\infty}\hat{s}, \rho_{S+\text{PM}+\overline{\text{PM}}}] + \sum_{j=1}^{3} L_{a_j}[\lambda_j; \rho_{S+\text{PM}+\overline{\text{PM}}}] + L_{\bar{a}_{\text{res}}^{\text{reg}}}[\Xi(\Lambda)\lambda_{\text{res}}; \rho_{S+\text{PM}+\overline{\text{PM}}}], \tag{74}$$

which corresponds to using the antimode model alongside the deterministic pseudomode model in Ref. [90] [used to describe the continuum B in Eq. (71)]. We refer to Appendix B 3 for a brief overview. The solutions of this differential equation for different values of Λ in $\Lambda_n \in [-1, 1]$ are used to compute the observable $\langle\hat{O}_S\rangle^{\text{phys}}(t;\Lambda)$. This is done by interpolating the values $\langle\hat{O}_S\rangle^{\text{phys}}(t;\Lambda_n)$ with an order M polynomial $p_M(t;\Lambda)$ which is then analytically continued to $\Lambda \mapsto \Lambda_c$ to compute $\langle\hat{O}_S\rangle(\Lambda_c;t) = \langle\hat{O}_S\rangle^{\text{free}}(t)$ corresponding to Eq. (67). To improve the accuracy of the reconstruction, we also perform a regularization procedure by analytically continuing a complete set of observables (in this case, the three Pauli matrices) and imposing physicality on the extrapolated result. Specifically, the regularization we considered here corresponds to writing

$$\rho_S^{\text{reg}}(t) = \frac{1}{2}\left(1 + \sum_{i=x,y,z} \frac{\text{Re}[\langle\sigma_i\rangle(t;\Lambda_c)]}{Z}\right), \tag{75}$$

where

$$Z = \max\left[1, \sum_{i=x,y,z} \{\text{Re}[\langle\sigma_i\rangle(t;\Lambda_c)]\}^2\right]. \tag{76}$$

In Fig. 3(a) we show the original dissipative dynamics alongside the ones determined by coupling additional noise (i.e., the regularized antimode environment) to the system. The values of these observables are then used to recover the noise-free dynamics. In Fig. 3(b) the underlying analytical continuation procedure is shown explicitly in the complex plane for a specific time of the dynamics. As shown in Fig. 3(a), the effect of the further regularization in Eq. (75) helps in reproducing the correct values for the noise-free dynamics. We note that, while this feature offers a potential regularization for unwanted unphysicalities that can emerge from the analytical continuation procedure, it also comes at the cost of performing a full tomography on the system state. Furthermore, the benefits of a regularization involving the full density matrix are not expected to scale over extended systems, since they rely on only a single extra condition. For this reason, this work mainly focuses on the analytical continuation of the expectation values of single observables, instead.

We present a further exemplification in Fig. 4, where we plot the fidelity of a simple single-qubit gate, consisting of a $\pi/2$ rotation around the y axis in the Bloch sphere. The qubit is in contact with a zero-temperature bath which lowers the quality of the gate as the gate time is increased. We show that the effects of the bath on this single-qubit operation can be mitigated through analytical continuation.

2. *Finite temperature*

As mentioned in the introduction to this section, the effects of a bath with spectral density given by Eq. (50) in the underdamped regime can be modeled using a single resonant

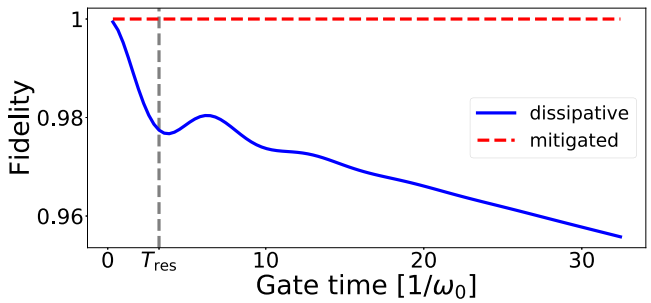

FIG. 4. Gate fidelity against gate time for a noisy $\theta = \pi$ rotation around the z axis on a two-level system before and after analytical continuation. Here noise is modeled through the coupling to an underdamped Brownian environment at zero temperature. The dashed gray vertical line represents the time $T_{\rm res}$ where the two-level system is on resonance with the environment, i.e., when $\omega_s = \theta/T_{\rm res} = \Omega$. The specific parameters used are $\lambda = 0.2\omega_0^{3/2}$, $\Gamma = 0.5\omega_0$, $\omega_s = \Delta = 0$, $M = 7$, $N_{\rm cont} = 12$, and $N_{\rm stoch} = 100$.

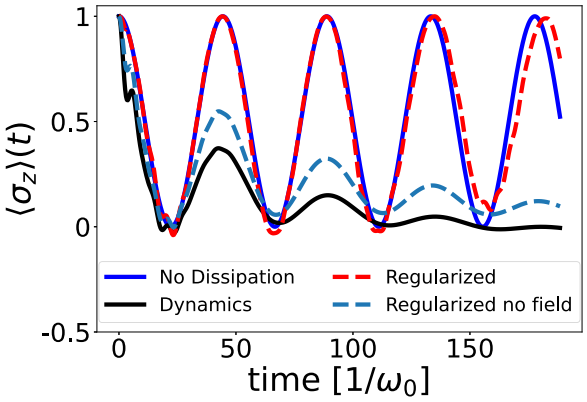

FIG. 5. Mitigation of an underdamped Brownian environment at finite temperature. The black or blue curves show the dissipative or free dynamics. The dashed red or blue curves show the mitigation with or without a stochastic field. The original system bath is here modeled with the hierarchical equations of motion. The specific parameters used here are $\alpha = 8 \times 10^{-3}$, $\Gamma = 0.1\omega_0$, $\omega_s = \Delta = 0.1\omega_0$, $M = 10$, $N_{\rm cont} = 12$, $N_{\rm stoch} = 5000$, and $\beta = 1/\omega_0$.

harmonic mode and a classical stochastic field even at finite temperature. In fact, *all temperature effects of the bath are encoded in the statistics of this driving field*. As a consequence, in order to mitigate temperature effects, we only need to update the way we handle this classical stochastic process with respect to the (zero-temperature) analysis in the previous section. Such a case was, in fact, rather special as the stochastic driving field in the antimode model was real, thereby not requiring regularization and analytical continuation. This is no longer the case at finite temperature where, in order to satisfy its defining Eq. (56), the field $\xi_\beta(t)$ is no longer restricted to imaginary values but must, in general, be written as

$$\xi_\beta(t) = \bar{\xi}_\beta^{\mathcal{I}}(t) - i\bar{\xi}_\beta^{\mathcal{R}}(t), \tag{77}$$

in terms of real and imaginary parts. Here the notation simply follows from using the definition $\bar{\xi}_\beta(t) = \bar{\xi}_\beta^{\mathcal{R}}(t) + i\bar{\xi}_\beta^{\mathcal{I}}(t)$ for the antifield in Eq. (69). The mitigation of the imaginary part follows the same procedure as in the zero-temperature case, i.e., it only requires the introduction of a corresponding real antifield. However, the mitigation of the real part now requires to be regularized and analytically continued, similarly to what was done before for the system-pseudomode coupling. In turn, this leads to the following modification to the regularized antimode model in Eq. (71) as:

$$\begin{aligned}\dot{\rho}_{S+B} = &-i\big[H_{S+B} + \bar{\xi}_\beta^{\rm reg}(t;\Lambda)\hat{s}(t),\, \rho_{S+B}\big] \\ &+ L_{\bar{a}_{\rm res}^{\rm reg}}[\Xi(\Lambda)\lambda_{\rm res};\, \rho_{S+B}],\end{aligned} \tag{78}$$

in terms of the physically regularized version of the antifield which, following Eq. (28), reads

$$\bar{\xi}_\beta^{\rm reg}(t;\Lambda) = \bar{\xi}_\beta^{\mathcal{R}} + \Xi(\Lambda)\bar{\xi}_\beta^{\mathcal{I}}. \tag{79}$$

These equations define the ensemble whose physical observables can be used to mitigate the noise of the environment B at finite temperature. In Fig. 5, we analyze a specific example to highlight this model.

B. Restructuring the environment

In this section, we consider a scenario in which one might wish to modify, i.e., *restructure*, some properties of an environment without assuming them to be directly accessible. We specifically focus on the case in which the temperature of an environment is algorithmically reduced by using the analytical continuation procedure presented in the previous sections.

Interestingly, in the underdamped Brownian bath considered here, the modeling of this situation does not require the introduction of any additional *quantum* degree of freedom. Indeed, it is possible to algorithmically modify the temperature of the original bath by simply performing analytical continuation over the intensity of a classical stochastic drive. In fact, we can explicitly write the finite-temperature stochastic pseudomode model as

$$\dot{\rho}_{S+{\rm PM}}^{\beta} = -i\big[H_S + \xi_\beta(t)\hat{s},\, \rho_{S+{\rm PM}}^{\beta}\big] + L_{a_{\rm res}}\big[\lambda_{\rm res};\, \rho_{S+{\rm PM}}^{\beta}\big], \tag{80}$$

whose field satisfies Eq. (56). Therefore, the differential equation for a pseudomode model at a different temperature β' can be obtained by simply adding an extra field $\xi_{\Delta\beta}(t)$ to the previous equation with

$$\mathbb{E}[\xi_{\Delta\beta}(t)\xi_{\Delta\beta}(0)] = C_{\rm class}^{B}(t;\beta') - C_{\rm class}^{B}(t;\beta). \tag{81}$$

Given these considerations, the temperature β of a bath B acting on a system S can be algorithmically modified to a new temperature β' by driving the system with a regularized stochastic field

$$\xi_{\Delta\beta}(t;\Lambda) = \xi_{\Delta\beta}^{\mathcal{R}}(t) + \Xi(\Lambda)\xi_{\Delta\beta}^{\mathcal{I}}(t). \tag{82}$$

To be more explicit, the dynamics in the full $(S+B)$ space becomes

$$\dot{\rho}_{S+B} = -i[H_{S+B} + \xi_{\Delta\beta}(t;\Lambda)\hat{s},\, \rho_{S+B}], \tag{83}$$

so that, assuming the original dynamics to be well described by the model in Eq. (80), the analytical continuation to $\Lambda_{\rm c}$ effectively changes the classical correlation function to $C_{\rm class}^{B}(t;\beta')$; thereby achieving the mentioned algorithmic

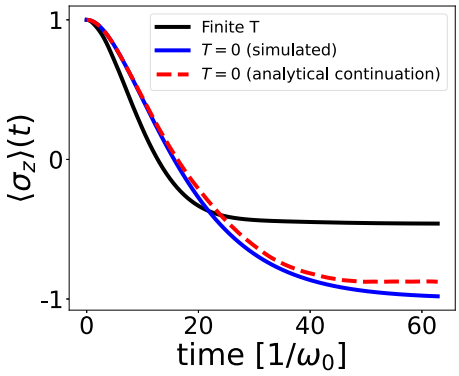

FIG. 6. Restructuring of a finite-temperature environment into a zero-temperature one. The black and blue curves correspond to the dissipative dynamics when the system is in contact with a finite- and zero-temperature environment. For the dashed red curve, a stochastic field is added to effectively approximate the zero-temperature dynamics after analytical continuation. The specific parameters used here are $\omega_z = \omega_0$, $\Delta = 0$, $\lambda = 0.1\omega_0^{3/2}$, $\gamma = 0.3\omega_0$, and $\beta = 1/\omega_0$.

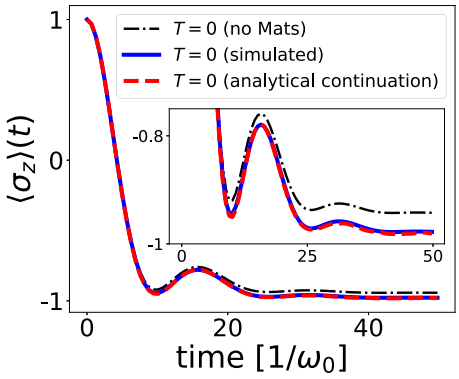

FIG. 7. Analog simulation of a zero-temperature environment. The blue curve shows the true dissipative dynamics and in dashed red the simulated one obtained by coupling the system to a harmonic mode and by analytically continuing a classical stochastic drive. The dashed black curve shows the simulation done without the additional field, which is necessary to predict the correct hybridization to the environment, when the system is in contact with a zero-temperature environment. The dashed red curve shows the dynamics after analytical continuation is performed on an additional stochastic field. In the inset, a restricted scale of the main plot is shown to better highlight the effects of the simulation. The specific parameters used here are $\omega_s = \omega_0$, $\Delta = 0$, $\lambda = 0.3\omega_0^{3/2}$, $\gamma = 0.3\omega_0$, $N_{\text{cont}} = 12$, and $N_{\text{stoch}} = 10^3$.

change in temperature. We give an example of this procedure in Fig. 6.

C. Simulation

Perhaps the most immediate application of the formalism presented here is in the analog simulation of the non-Markovian effects of an environment. This can be implemented in a rather direct way since the resonant pseudomode is physical. Given a closed system with Hamiltonian H_S, the effects of a Brownian environment at inverse temperature β can be reconstructed from the physical ensemble obtained from Eq. (80) with the replacement

$$\xi_\beta(t) \mapsto \xi_\beta^{\mathcal{R}}(t) + \Xi(\Lambda)\xi_\beta^{\mathcal{I}}(t). \tag{84}$$

It is interesting to note that this expression is the "dual" of Eq. (79). In fact, while Eq. (79) is used to *mitigate* the classical effects of the environment, Eq. (84) is used to *simulate* them. We present a specific example of this analog procedure in Fig. 7, where we simulate the effects of a zero-temperature environment. As mentioned above, the only obstacle preventing from a direct simulation of an environment is the imaginary component of the field $\xi(t)$. It is then worth asking whether there are regimes where such component is negligible. To do this, we can recall that the stochastic fields depend on the square-root of the parameters c_n defining the spectral decomposition of the classical contribution to the bath correlation function, see Eq. (A13). Assuming the time dynamics to be the largest timescale in the model, these coefficients become

$$c_n \to S_{\text{class}}[\omega]\, d\omega, \tag{85}$$

which can be interpreted as a continuum version of Eq. (A14) and written in terms of the "classical" spectrum of the bath,

$$S_{\text{class}}[\omega] = \frac{1}{2\pi}\int_{-\infty}^{\infty} d\tau\; C_{\text{class}}(\tau)e^{i\omega\tau}. \tag{86}$$

In the limit, the question about the possibility to simulate a bath using physical fields then becomes equivalent to check whether this quantity is positive, i.e., $S_{\text{class}}[\omega] \in \mathbb{R}_+$ for all ω. For the Brownian spectral density considered here, the expression for the classical contribution to the correlation is given explicit in Eq. (B58) in terms of a sum of decaying exponentials, corresponding to a spectrum represented as an infinite sum of Lorentzians functions. In Fig. 8, we plot the spectrum for a specific set of parameters. From this figure we can recover the previously analyzed case: At low temperatures, the classical correlation is determined by the Matsubara

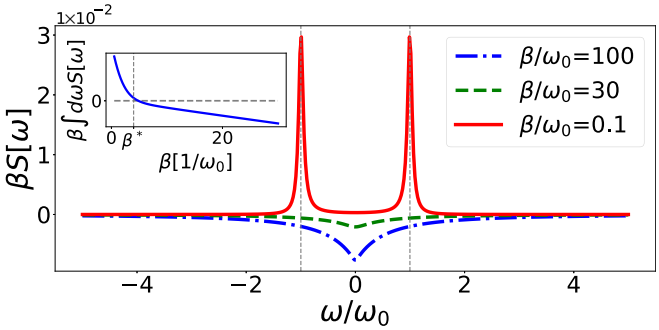

FIG. 8. Classical spectrum corresponding to an underdamped Brownian spectral density as a function of frequency. At low temperatures, the correlation is characterized by the Matsubara contribution leading to a negative spectrum. In this regime, imaginary fields are required for the simulation of this environment. At higher temperatures, resonant terms (vertical lines highlight $\omega = \pm\omega_0$) dominate, leading to a positive spectrum. In this regime, the classical contribution to the correlation can be simulated using physical (real) fields. In the inset, we show, in arbitrary units, the integral of the spectrum as a function of inverse temperature β to highlight the crossover (as the curve intersects zero) between the two regimes. Other parameters used here are $\gamma = 0.1\omega_0$ and $\lambda = 0.1/\sqrt{2\pi}\omega_0^{3/2}$.

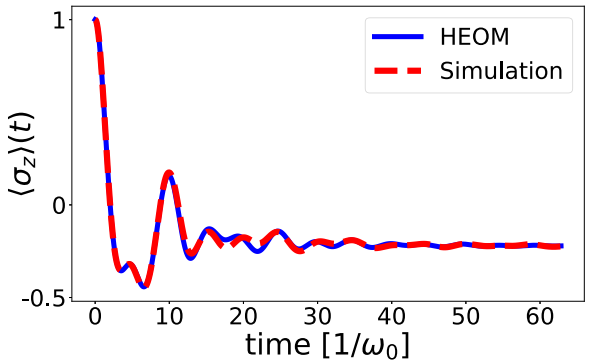

FIG. 9. Dynamics of a two-level system corresponding to a model for excitonic energy transfer dynamics in a molecular dimer system [160] at room temperature. The blue curve shows the results simulated by the HEOM and the dashed red curve shows the ones arising from a quantum simulation protocol in which the system is coupled to a single harmonic mode at zero temperature and a classical field. The high-temperature regime allows this field to be physical, thereby not requiring any analytical continuation procedure. The parameters were chosen to be on the same order as the ones used in Fig. 5 in Ref. [160] and they explicitly are $\omega_0 = 220\ \mathrm{cm}^{-1}$, $\omega_s = 100\ \mathrm{cm}^{-1}$, $\Delta = 100\ \mathrm{cm}^{-1}$, $\gamma = 20\ \mathrm{cm}^{-1}$, $\alpha = 2\lambda^2/\omega_0^2 = 80\ \mathrm{cm}^{-1}$, and $T = 300$ K [corresponding to $1/\beta = k_B T = (k_B T)\lambda_0/(2\pi\hbar c)\hbar\omega_0 = 0.94\hbar\omega_0$, in terms of the Boltzmann constant k_B, the speed of light c, the wavelength $\lambda_0 = (1/220)$ cm] in units such that $\hbar = 2\pi c = 1$. For consistency, in this simulation, the coupling operator to the environment is set to $\hat{s} = \sigma_z$.

contribution to the correlation which is negative, corresponding to imaginary fields. However, at higher temperatures, resonant terms in the correlation become dominant leading to a positive spectrum. This argument can be used (see Appendix B 3) to derive an estimate for the inverse temperature locating the crossover between the two regimes as

$$\beta^*\omega_0 = 2\sqrt{4 - (\gamma/\omega_0)^2}. \tag{87}$$

For $\beta < \beta^*$, it is possible to produce a direct analogical simulation of non-Markovian effects at higher temperatures, such as in the case of the excitonic energy transfer in molecular dimer systems [69,157–160]. In Fig. 9, we simulate one of the environments analyzed in Ref. [160].

VII. ERROR ANALYSIS

The protocol analyzed here allows us to compute the analytical continuation of the expectation value of a system observable $\langle\hat{O}_S\rangle(t;\Lambda_c)$ at time t, see Eq. (41), using an extrapolation procedure based on the pseudomode model. By construction, this protocol estimates the expectation $\langle\hat{O}_S\rangle_{\mathrm{target}}(t)$ that the observable had if the system was coupled to the target environment we are interested in simulating; see Eq. (1). Here we analyze the expected uncertainty inherent to this estimate. To do this, we distinguish between two qualitatively different sources of errors, i.e., the ones (labeled as $\mathrm{Err}_{\mathrm{cont}}$) originating from the analytical continuation and the ones (labeled as as $\mathrm{Err}_{\Delta C}$) originating from a possible discrepancy $\Delta C(t)$ between the correlation of the pseudomode model and the target environment, as described in Eq. (38). This distinction allows us to write

$$\langle\hat{O}_S\rangle_{\mathrm{target}}(t) = \langle\hat{O}_S\rangle(t;\Lambda_c) + \mathrm{Err}_{\mathrm{cont}} + \mathrm{Err}_{\Delta C}, \tag{88}$$

which simply corresponds to the fact that these two sources of errors are completely independent. For an intuitive representation of the logic behind this equation, we further refer to the diagram in Fig. 11. An estimate for an upper bound on $\mathrm{Err}_{\Delta C}$ has been derived in [87,95] as

$$\frac{\mathrm{Err}_{\Delta C}}{||\hat{O}_S||_\infty} \leqslant \exp\left[4||\hat{s}||_\infty \int_0^t dt_2 \int_0^{t_2} dt_1 |\Delta C(t_2 - t_1)|\right] - 1, \tag{89}$$

in terms of the infinity norm of system operators. The remaining contribution $\mathrm{Err}_{\mathrm{cont}}$ to the overall error is due to the analytical continuation procedure and it has been elegantly analyzed in Ref. [161], using the properties of Chebyshev polynomials (see also Appendix C). Specifically, it depends on the interplay between uncertainties in the experimental data and the degree M of the extrapolating polynomial, i.e., it can be further decomposed as

$$\mathrm{Err}_{\mathrm{cont}} = \mathrm{Err}_{\mathrm{bias}} + \mathrm{Err}_{\mathrm{stability}}, \tag{90}$$

in terms of two contributions characterizing the bias and the stability of the algorithm. We are now going to describe the overall scaling of these quantities whose explicit expressions are summarized in Appendix C 3 b and explicitly derived in Appendixes D and E.

Intuitively, the bias error $\mathrm{Err}_{\mathrm{bias}}$ characterizes how precisely the function $\langle\hat{O}_S\rangle(t;\Lambda)$ can be reproduced by an order M polynomial. More precisely, it estimates the distance between the polynomial extrapolation value $p_M(t;\Lambda_c)$ and the target value $\langle\hat{O}_S\rangle(t;\Lambda_c)$ in the absence of experimental errors. This distance "bias" originates from (i) a lack of knowledge about the function $\langle\hat{O}_S\rangle(t;\Lambda)$ and quantified by the number N_{cont} of data points $\langle\hat{O}_S\rangle(t;\Lambda_n)$, for $\Lambda_n \in D_{\mathrm{phys}}$, constituting the input for the algorithm, and (ii) a bound on the order M of the extrapolating polynomial $p_M(t;\Lambda)$.

Interestingly, as beautifully shown in Ref. [161] (see also Appendix C), this error depends on the functional form of $\langle\hat{O}_S\rangle(t;\Lambda)$ over the whole complex plane, i.e., not just the final extrapolation point Λ_c. This can be seen explicitly from the optimization domain in Eq. (C56) in Appendix C 3 b. Equally importantly, it also becomes exponentially small as we increase M.

The efficiency of this bias is balanced, or rather unbalanced in this case, by the remaining contribution in Eq. (90) characterizing the stability of the algorithm, i.e., its sensitivity to imperfections in the initial data $\langle\hat{O}_S\rangle(t;\Lambda_n)$ which, even in numerical simulations, cannot be assumed to be identically zero. Not surprisingly, this instability scales exponentially with the order of the extrapolating polynomial, see Eq. (C59). In other words, a large M corresponds to an overfitting of the original experimental data, ultimately implying a sensitivity to data imperfections which grows exponential in M. On the other hand, a small M corresponds to underfitting the original data, restoring stability against data errors at the cost of limiting the predictivity of the model, i.e., increase the bias. We can observe this interplay in Fig. 10, where we computed the error as a function of the degree of the interpolating polynomial showing the emergence of an optimal range for the degree M.

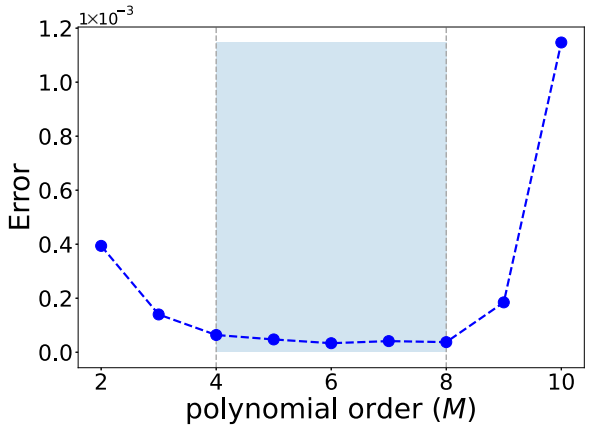

FIG. 10. Reconstruction error as a function of the order M of the interpolating polynomial. The error refers to the open quantum system analyzed in Fig. 3. More precisely, we defined $\mathrm{Err} = |\langle\sigma_z(t)\rangle^{\mathrm{free}} - \langle\sigma_z\rangle^{\mathrm{reg}}(\Lambda_c; t)|$ where the averages are taken with respect to $\rho^{\mathrm{free}}(t)$ and $\rho^{\mathrm{reg}}(t)$, respectively, and the time corresponds to the gray vertical line in Fig. 3. For small values of M the error is biased, i.e., the polynomial is not able to encode the complexity of the environmental effects we want to mitigate. For high values of M, the algorithm is unstable with respect to errors in the initial data. In this example, the artificially injected error is modeled as a normal variable with zero mean and standard deviation $\sigma = 10^{-5}$. As the variance of the error decreases, the optimal parameter range of the algorithm (shaded blue) extends towards the right, allowing us to model more subtle features.

Overall, the exponential dependence of the uncertainties of the protocol on both the order M of the extrapolating polynomial and the discrepancy $\Delta C(t)$ between the target and modeled correlation, is a direct consequence of the two main techniques, namely extrapolation and the pseudomode model, used to produce these results. In other words, the nonefficiency of the algorithm in the worst-case scenario is an unavoidable consequence of the complexity of the analyzed task, namely the simulation of the effects of rather general bosonic environments or the mitigation of general non-Markovian noise. However, both the pseudomode model and extrapolation techniques have been successfully used to, respectively, classically simulate open quantum systems [25,26,81–94] and for applications in error mitigation [115–128]. As further exemplified by the numerics provided in Sec. VI, this suggests that, while the general bounds in Eq. (89) and Eq. (90) can be used to gather intuition on the scaling of the efficiency of the algorithm in the worst case, reasonable performances can still be obtained when applying the method in practical, i.e., non-worst-case, scenarios.

We finish this section with an intuitive interpretation of a more specific analysis provided in Appendix E 1. There, we present a detailed estimate of the scaling of the error for the special case of an analytical continuation over the system-bath coupling of a single pseudomode. In the limit of large N_{cont}, the overall error has an upper bound which only depends on M and an adimensional variable α_{compl} which, intuitively, we can interpret as quantifying the "complexity" of the effects of the environment on the system which the method is trying to either mitigate or simulate. This meaning simply corresponds to the fact that the effects corresponding to a higher value for α_{compl} can be extrapolated only at the cost of a higher polynomial order M and, as a consequence, ultimately require a higher precision in collecting the experimental data. Explicitly, this quantity can be estimated as

$$\alpha_{\mathrm{compl}} \simeq t\bar{\lambda}^2 ||\hat{s}||_\infty/\Gamma, \tag{91}$$

in terms of the scale $\bar{\lambda}$ for the pseudomode-system coupling strength, the norm of the system interaction operator $\hat{s}$, the dissipation rate Γ, and the overall time t needed for the environmental effects to manifest in the system. As a possible example of the information which this parameter could provide, the applicability of the algorithm for larger systems would, intuitively, correspond to the requirement of stationarity of α_{compl} on the system size. Implicit in this consideration is (i) the explicit dependence of the pseudomode parameters on the original open system [an example of which is given in Eq. (66)] and (ii) a better characterization of the time t. This could be the focus of future analysis.

It is worth mentioning that further independent noise in the ancillary system could be, in principle, included in the model by updating the functional form of the correlation of the model. Interestingly, the presence of such intrinsic noise could, in certain cases, be used as a resource for optimization [128].

In order to more clearly highlight the different sources of uncertainty in the protocol, we now provide an outline which will serve both as a summary and as a way to track the different sources of imprecision analyzed above and in Appendixes C, D, and E.

A. Outline

Here we provide an outline of the analytical continuation protocol with special emphasis on the procedures which can potentially give rise to different sources of imprecision for the overall final estimate of system observables. We further exemplify this outline diagrammatically in Fig. 11.

The starting point is an open quantum system consisting of a quantum system S linearly coupled to a bosonic environment E. The properties of the environment are characterized by its correlation $C_E(t)$, while the interaction is characterized by a system coupling operator $\hat{s}$. We further assume the choice of a given system observable of interest $\hat{O}_S$. With this setup, we now proceed as follows:

(1) Choose a target environment E_{target} with correlation $C_{E_{\mathrm{target}}}(t)$. Our goal is to estimate the expectation of the observable $\hat{O}_S$ as if the system was interacting with E_{target} instead of the actual E. Possible choices of the target environment are the ones corresponding to a

(a) *Mitigation* of the effects of the original environment E, i.e., $E_{\mathrm{target}} = 0$.

(b) *Simulation* of an open quantum system. In this case, one can assume the original open system to be closed (i.e., $E \to 0$) and then choose, for example, E_{target} to be a zero-temperature environment for ground-state engineering; see Ref. [112].

(c) *Restructuring* of some of the properties of the original environment E as, for example, lower its temperature.

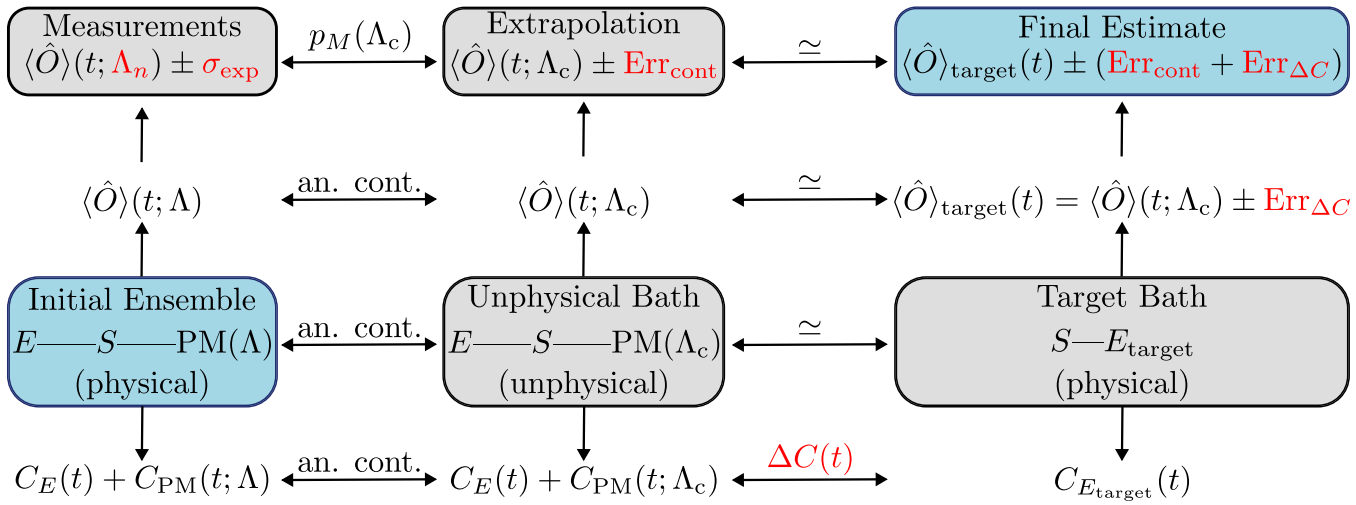

FIG. 11. Diagram highlighting the main ideas behind the algorithm and the different sources of potential imprecisions (in red). Given an open quantum system composed of a system S and a physical environment E, the goal is to simulate the target open quantum system characterized by the (physical) environment $E_{\rm target}$ (lower right box). This target environment can be approximated [with modeling error characterized by a correlation discrepancy $\Delta C(t)$] by coupling the original open system to an (unphysical) pseudomode model (lower middle box). In turn, this unphysical model can be interpreted as the analytical continuation of a physical open system (lower left box) whose parameters depend on the parameter Λ. To compute this continuation, it is possible to collect experimental values of a given observable for different values Λ_n of Λ which can be affected by an imprecision $\sigma_{\rm exp}$ (upper left box). These data can be used to define an order M extrapolating polynomial $p_M(\Lambda)$ which can be analytically continued to the value Λ_c (upper middle box). By considering both the errors originating from the analytical continuation procedure and the ones due to the imperfection in the modeling, a final estimate is obtained (upper right box). This estimate corresponds to an expectation value as if the system was coupled to the target environment $E_{\rm target}$ instead of the original E.

(2) Characterize a pseudomode model PM approximating the effects of a bath $E_{\rm PM}$ such that $E+E_{\rm PM}\simeq E_{\rm target}$. In other words, the pseudomode environment $E_{\rm PM}$ is such that, when coupled to the system alongside the original environment E, it effectively generates the target environment $E_{\rm target}$. The pseudomode model is defined by its correlation $C_{\rm PM}(t)=C_{E_{\rm target}}(t)-C_E+\Delta C(t)$, where $\Delta C(t)$ includes a potential error in the modeling. We note the following:

(a) The PM model is composed of a collection of quantum modes whose dissipation is described by a Lindblad equation.

(b) Optionally, the model can also include driving the system with a time-dependent stochastic noise $\xi(t)$.

(c) The PM model usually has unphysical parameters, consistently with the possibility of using it for tasks such as the mitigation of noise.

(3) Because of its unphysicalities, the pseudomodes defined above do not directly correspond to an environment which can be physically realized. However, it is possible to define a parametrized version PM(Λ) of the unphysical pseudomode model PM, such that

(a) PM(Λ_c) $\to$ PM, for a critical value Λ_c. In other words, the analytical continuation of the parametrized model PM(Λ) corresponds to the model PM we need to simulate.

(b) PM(Λ) is physical (i.e., its dynamics is a, physical, Lindblad equation) when $\Lambda\in D_{\rm phys}$, for $D_{\rm phys}\subset\mathbb{R}$. In other words, the set of physical models PM($\Lambda\in D_{\rm phys}$) constitutes a *physical pseudomodes ensemble*.

(4) We now want to collect data from this ensemble and then extrapolated them outside their physical domain. To do this, we choose a set of $N_{\rm cont}$ points $\Lambda_n\in D_{\rm phys}$. For each of these points, we proceed to

(a) Couple the system to the pseudomodes described in PM(Λ_n).

(b) Measure $\langle\hat{O}\rangle(t;\Lambda_n)\pm\sigma_{\rm exp}$, in terms of an experimental error bound $\sigma_{\rm exp}$. By the law of total expectation, this variance can be decomposed in terms of a "quantum" part (dependent on the overall density matrix) and a "classical" part (dependent on the, optional, stochastic driving ξ).

(5) After collecting the data $\langle\hat{O}\rangle(t;\Lambda_n)$ at the discrete points Λ_n as in the previous point, we can now define an order M polynomial $p_M(t;\Lambda)$ approximating the function $\langle\hat{O}(t;\Lambda)\rangle$ for $\Lambda\in D_{\rm phys}$.

(6) We can now use this polynomial to extrapolate the value $p_M(t;\Lambda_c)$. This simply means computing the approximating polynomial $p_M(t;\Lambda)$ at the critical value Λ_c. We can note the following:

(a) By construction, the value $p_M(t;\Lambda_c)$ corresponds to the expectation value of $\hat{O}$ for the model $S+E+{\rm PM}(\Lambda_c)$, i.e., $\langle\hat{O}(t;\Lambda_c)\rangle=p_M(t;\Lambda_c)\pm{\rm Err}_{\rm cont}$. Here ${\rm Err}_{\rm cont}$ takes into account the extrapolation errors which critically depend on M and $\sigma_{\rm exp}$.

(b) By 3(a), the value $p_M(t;\Lambda_c)$ also corresponds to the expectation of $\hat{O}$ for the model $S+E+{\rm PM}$ which, by point 2, has correlation $C_{E_{\rm target}}(t)+\Delta C(t)$, i.e., it approximates the effects of the target environment.

(c) Together, points (a) and (b) above imply that $\langle\hat{O}\rangle_{\rm target}(t)=p_M(t;\Lambda_c)\pm({\rm Err}_{\rm cont}+E_{\Delta C})$, where $E_{\Delta C}$ takes into account the effects of the modeling error.

This completes our step-by-step overview of the protocol analyzed in this article; see also Fig. 11 for a corresponding diagram.

VIII. CONCLUSIONS

We presented an extrapolation technique to mitigate, restructure, and simulate the effects of Gaussian non-Markovian environments on a quantum system. The method relies on the interaction of the system with ancillary leaky modes and a stochastic driving field to define a physical ensemble parameterized by a single parameter. Measurements results over this ensemble can be used to define an analytical continuation procedure, allowing us to use these ancilla modes to perform one of the following tasks:

(i) Simulating the effects of a non-Markovian environment.

(ii) Mitigating non-Markovian noise affecting the system.

(iii) Restructuring some of the properties of a given environment (already interacting with the system) without directly accessing it.

We presented the details and proof of the general formalism, as well as several numerical examples to showcase the flexibility of the algorithm to adapt to different environments (such as zero- and finite-temperature ones and a physically motivated example related to simulating excitonic energy transfer in a molecular dimer systems). These examples also demonstrated how the above range of applications can be used in practice (such as noise mitigation for the dynamics of quantum observables or quantum gate operations, simulation of zero-temperature environments, and restructuring of a finite-temperature bath to a zero-temperature one). The algorithm used in all these tasks is based on polynomial extrapolation and it is thereby ultimately limited by instability against imperfections in experimental data.

As an outlook, the protocol presented here could also be adapted to specify or optimize digital quantum algorithms for the mitigation of non-Markovian noise in quantum computing tasks or for the simulation of zero-temperature environments for ground-state engineering; see Ref. [112]. In this context, it would be relevant to relax any requirement on prior knowledge about the environment by preceding the presented protocols with noise characterization techniques such as in Ref. [128]. We further note that the regularization procedure used in here could be extended to bigger system sizes by analytically continuing a reconstructed version of the full state using classical shadow tomography [162–164]. In addition, the possibility of restructuring a given environment could, possibly, be helpful to push experimental setups past the limits imposed by the presence of physical baths elusive of direct manipulation.

ACKNOWLEDGMENTS

We thank Jhen-Dong Lin feedback on the manuscript. M.C. acknowledges support from NSFC (Grant No. 11935012) and NSAF (Grant No. U2330401). F.N. is supported in part by Nippon Telegraph and Telephone Corporation (NTT) Research, the Japan Science and Technology Agency (JST) [via the Quantum Leap Flagship Program (Q-LEAP), and the Moonshot R&D Grant No. JPMJMS2061], the Asian Office of Aerospace Research and Development (AOARD) (via Grant No. FA2386-20-1-4069), and the Office of Naval Research (ONR) Global (via Grant No. N62909-23-1-2074). N.L. is supported by the RIKEN Incentive Research Program and by MEXT KAKENHI Grants No. JP24H00816 and No. JP24H00820.

APPENDIX A: THE PSEUDOMODE MODEL: MAIN IDEAS

The pseudomode method consists in replacing the original continuum of environmental modes with a discrete set of dissipative harmonic modes and stochastic driving fields. The main purpose of these ancillary degrees of freedom is to reproduce the correlation function characterizing the original Gaussian environment and, ultimately, to reproduce the original reduced system dynamics in Eq. (4).

Explicitly, the pseudomode model consists in the following linear differential equation:

$$\dot{\rho}_{S\text{-PM-}\xi}(t) = L_{S\text{-PM}}[\rho_{S\text{-PM}}(t)], \tag{A1}$$

for a (possibly stochastic) density matrix $\rho_{S\text{-PM}}(t)$ whose Hilbert space includes the system and N_{PM} PM. The Lindblad superoperator in the full system+pseudomodes space is written as the sum of three parts,

$$L_{S\text{-PM-}\xi} = L_S + \sum_{k=1}^{N_{\mathrm{PM}}} L^k_{S\text{-PM}}[\cdot] + L^{\xi}_S, \tag{A2}$$

where $L_S = -i[H_S, \cdot]$ describes the free dynamics of the system and depends on its Hamiltonian H_S. The second term describes the dynamics of the quantum degrees of freedom as

$$L^k_{S\text{-PM}}[\cdot] = -i\big[H^k_{\mathrm{PM}}, \cdot\big] + D_k[\cdot]. \tag{A3}$$

Here $H^k_{\mathrm{PM}} = \Omega_k a^\dagger_k a_k + \hat{s} X^k_{\mathrm{PM}}$, in terms of the annihilation operator a_k associated with the kth pseudomode with frequency $\Omega_k \in \mathbb{C}$, $k = 1, \ldots, N_{\mathrm{PM}}$. The coupling to the system is described by the interaction operator

$$X^k_{\mathrm{PM}} = g_k(a_k + a^\dagger_k), \tag{A4}$$

where $g_k \in \mathbb{C}$ constitutes an important conceptual difference from (3), where the realness of the $\tilde{\lambda}_{\tilde{k}}$ couplings is required for Hermiticity. The dissipative properties of the kth pseudomode are independently characterized by the superoperator,

$$\begin{aligned} D_k[\cdot] = {} & (n_k + 1)\Gamma_k(2a_k[\cdot]a^\dagger_k - a^\dagger_k a_k[\cdot] - [\cdot]a^\dagger_k a_k) \\ & + n_k\Gamma_k(2a^\dagger_k[\cdot]a_k - a_k a^\dagger_k[\cdot] - [\cdot]a_k a^\dagger_k), \end{aligned} \tag{A5}$$

where $\Gamma_k, n_k \in \mathbb{C}$. We set the initial condition for Eq. (A1) to be $\rho_S(0) \otimes \rho_{\mathrm{PM}}(0)$, where

$$\rho_{\mathrm{PM}}(0) = \rho^{\mathrm{eq}}_{\mathrm{PM}} = \prod_{k=0}^{N_{\mathrm{PM}}} \exp\left[-\beta_k \Omega_k a^\dagger_k a_k\right]/Z_k, \tag{A6}$$

where Z_k are the coefficients needed to impose unity trace and where we assume the consistency condition $2n_k + 1 = \coth(\beta_k\Omega_k/2)$. The presence of dissipation in this pseudoenvironment does not break the Gaussianity of the model whose

effect on the system are fully characterized by the two-point correlation,

$$C_Q(t) = \mathrm{Tr}_{\mathrm{PM}}\big[X_{\mathrm{PM}}(t)X_{\mathrm{PM}}(0)\rho_{\mathrm{PM}}^{\mathrm{eq}}\big], \tag{A7}$$

with

$$X_{\mathrm{PM}}(t) = \exp\{L_{S\text{-PM}}^{\dagger}[\cdot]t\}X_{\mathrm{PM}}, \tag{A8}$$

in terms of $X_{\mathrm{PM}} = \sum_k X_{\mathrm{PM}}^j$ and $L_{S\text{-PM}}^{\dagger}$, the adjoint of $L_{S\text{-PM}} = \sum_{k=1}^{N_{\mathrm{PM}}} L_{\mathrm{S\text{-PM}}}^k$. Explicitly, each pseudomode independently contributes to the correlation function above as

$$C_Q(t) = \sum_{k=0}^{N_{\mathrm{PM}}} C_{\mathrm{PM}}^k(t), \tag{A9}$$

where

$$C_{\mathrm{PM}}^k(t) = g_k^2[(n_k+1)e^{-i\Omega_k t} + n_k e^{i\Omega_k t}]\exp[-\Gamma_k|t|] \tag{A10}$$

characterizes the effect of the kth pseudomode; see Refs. [89,90,95].

The last term in Eq. (A2) is optional and its nontrivial presence defines a stochastic hybrid [95] version of the fully deterministic pseudomode model above. In fact, this contribution can be interpreted as a stochastic driving of the system, i.e.,

$$L_S^{\xi} = -i\xi(t)[\hat{s},\cdot], \tag{A11}$$

where the field $\xi(t)$ is assumed to be a Gaussian stochastic process with zero mean. Furthermore, we assume its autocorrelation function,

$$C_{\mathrm{class}}(t) = \mathbb{E}[\xi(t)\xi(0)], \tag{A12}$$

to be stationary (invariant on translation of time) so that it can be used to model classical properties of the original environment. In the spirit of this method, this driving field is allowed to explore complex values, so that, in general, $\mathrm{Im}[\xi(t)] \neq 0$. As shown in Ref. [95], it is possible to write this field in terms of the following spectral decomposition:

$$\xi(t) = \sqrt{c_0}\xi_0 + \sum_{n=1}^{N_{\mathrm{stoch}}} \sqrt{2c_n}[\xi_n\cos(\omega_n t) + \xi_{-n}\sin(\omega_n t)], \tag{A13}$$

with $\omega_n = n\pi/T$ and where ξ_n, $n = 1,\ldots,N_{\mathrm{stoch}}$ ($N_{\mathrm{stoch}} \in \mathbb{N}$) are Gaussian random variables with zero mean and unit variance. The coefficients

$$c_n = \frac{1}{2T}\int_{-T}^{T} d\tau\,\cos(n\pi\tau/T)\,C_{\mathrm{class}}(\tau) \tag{A14}$$

define the spectral decomposition by ensuring that

$$C_{\mathrm{class}}(t) = c_0 + 2\sum_{n=1}^{N_{\mathrm{stoch}}} c_n\cos(\omega_n t). \tag{A15}$$

In the following, we will denote the average over the stochastic realization of the field $\xi(t)$ as $\mathbb{E}[\cdot]$.

It is important to stop for a moment and note that, within this formalism, the reduced density matrix,

$$\rho_S(t) = \mathbb{E}[\underset{\mathrm{PM}}{\mathrm{Tr}}[\rho_{\mathrm{S\text{-PM}}}(t)]], \tag{A16}$$

is as a function of the parameter set,

$$G_{\mathrm{PM}} \equiv \big\{\Omega_k, g_k^2, \Gamma_k, n_k, c_n\big\}, \tag{A17}$$

parametrizing the model. *The pseudomode model consists in the characterization of these parameters; i.e., it can be interpreted as a map from the original Gaussian open quantum system to* G_{PM}. For Gaussian environments, a sufficient condition for

$$\rho_S(t) = \tilde{\rho}_S(t), \tag{A18}$$

to hold is that

$$C_E(t) = C_{\mathrm{PM}}(t) \equiv C_Q(t) + C_{\mathrm{class}}(t), \tag{A19}$$

which can be interpreted as *the optimization equation defining the parameters of the pseudomode model in Eq. (A17).*

We note that the second term in Eq. (A19) is the autocorrelation function of the stochastic process $\xi(t)$ defined in Eq. (A12) which is symmetric, i.e., classical, by construction. For generic spectral densities, the correlation in Eq. (6) cannot be exactly reproduced by a finite number of psedudomodes, while this is possible, on average, within the stochastic hybrid approach [95]. At the same time, it is important to stress that, while adding stochastic resources to the model might lead to a more efficient simulation of the open quantum system, it is not necessary. In other words, by imposing $\xi(t) = 0$, the model above reduces to the fully deterministic pseudomode model. However, its inclusion leads to some advantages, like a reduction of the Hilbert space dimension and the possibility to include all temperature effects in the noise statistics. In practice, this allows us to initialize all the pseudomodes at zero temperature *for any temperature of the original bath*, i.e., to impose $\rho_{\mathrm{PM}}(0) = \prod_{k=0}^{N_{\mathrm{PM}}}|0\rangle\langle 0|$. This is going to be the preferred choice throughout this article.

APPENDIX B: PSEUDOMODE MODEL: ADDITIONAL DETAILS

In this section we present more details about the deterministic and hybrid pseudomode model based on the work done in Refs. [89,90,95].

1. The deterministic pseudomode model

We consider a Gaussian open quantum system $S+E$ composed of a system S and its environment E such that the interaction operator has the free correlation function $C_E(t)$ given in Eq. (6). Following the strategy developed in Refs. [89], we then proceed with the following steps:

(a) Introduce an open quantum system $S+E'$ in terms of an alternative environment E', such that the interaction operator with the system has a correlation given by $C_{E'}(t) = \sum_{k=0}^{N} C_{\mathrm{PM}}^k(t)$, with the $C_{\mathrm{PM}}^k(t)$ defined in Eq. (A10). The environment E' is made by $(N_{\mathrm{PM}}+1)$ pseudomodes and $(N+1)$ bosonic baths for each of them. The reduced system dynamics of this model is equivalent to that of the original one, provided $C_E(t) = C_{E'}(t)$.

(b) Show that reduced dynamics in the system+pseudomode space of the open quantum system $S+E'$ above is equivalent to the one originating from the Lindblad Eq. (A1).

(c) As a consistency check, we show that this Lindblad model has correlations given by Eq. (A9).

The next three sections, labeled a, b, and c, will prove the three points itemized above.

a. Pseudomodes as an open quantum system

Let us consider an open quantum system in which a subsystem of interest S interacts with an alternative environment E' composed of a set of $(N+1)$ pseudomodes a_k, each coupled to its own bosonic bath (whose modes are denoted as $b_{k\alpha}$) as

$$H = H_S + H_B + \hat{s}X_{\rm PM}, \tag{B1}$$

where the Hamiltonian of the environment H_B is

$$H_{\rm PM} = \sum_k H^k_{\rm PM}, \tag{B2}$$

with

$$H^k_{\rm PM} = \Omega_k a_k^\dagger a_k + \sum_\alpha \left[\frac{ig_{k\alpha}}{\sqrt{2\omega_\alpha}}(b^\dagger_{k\alpha}a_k - a_k^\dagger b_{k\alpha}) + \omega_{k\alpha}b^\dagger_{k\alpha}b_{k\alpha}\right]. \tag{B3}$$

We also defined the interaction operator

$$X_{\rm PM} = \sum_{k=0}^{N_{\rm PM}} X^k_{\rm PM} = \sum \lambda_k/\sqrt{2\Omega_k}(a_k + a_k^\dagger). \tag{B4}$$

We assume that the environment of each pseudomode is populated by modes with both positive and negative frequencies, i.e., $\omega_{k\alpha} \in (-\infty, +\infty)$. We further suppose that the spectral density associated with the bath of the kth pseudomode is constant, i.e.,

$$J_k(\omega) = \pi \sum_\alpha \frac{g^2_{k,\alpha}}{2\omega_{k,\alpha}}\delta(\omega - \omega_{k,\alpha}) = \Gamma_k, \tag{B5}$$

and that each of the pseudomodes a_k and the corresponding environmental modes $b_{k\alpha}$ are in an initial state $\rho^0_k = \exp[-\beta_k\Omega_k a_k^\dagger a_k]/Z_k$ and $\rho^0_{k\alpha} = \exp[-\beta_{k\alpha}\omega_{k\alpha}b^\dagger_{k\alpha}b_{k\alpha}]/Z_{k\alpha}$, respectively (with Z_k and $Z_{k\alpha}$ imposing unit trace), together with the consistency condition

$$\beta_{k\alpha}\omega_{k\alpha} = \beta_k\Omega_k, \tag{B6}$$

which, in the continuum limit, reads

$$\beta_k(\omega)\omega = \beta_k\Omega_k. \tag{B7}$$

We explicitly highlight the slight abuse in notation as $\beta_k(\omega)$ denotes the inverse temperature associated with environmental mode at frequency ω for the pseudomode k, while β_k denotes the inverse temperature associated with the pseudomode k). We note that these unorthodox conditions define a state for the full environment,

$$\rho_{E'} = \prod_k \rho^0_k \prod_{k,\alpha}\rho^0_{k,\alpha} = \exp[F_0]/Z_0, \tag{B8}$$

which is not a thermal state but it is the closest quantum idealization of classical white noise (see Ref. [2], p. 164). Here we defined

$$F_0 = \sum_k \beta_k\Omega_k a_k^\dagger a_k + \sum_{k\alpha}\beta_{k\alpha}\omega_{k\alpha}b^\dagger_{k\alpha}b_{k\alpha}, \tag{B9}$$

and Z_0 as a constant to impose unit trace. The free correlation function of the interaction operator can be obtained as

$$C_{\rm PM}(t_1,t_2) = {\rm Tr}_{E'}[X_{\rm PM}(t_2)X_{\rm PM}(t_1)\rho_{E'}], \tag{B10}$$

where $X_{\rm PM}(t) = e^{iH_Bt}X_{\rm PM}e^{-iH_Bt}$. The unorthodox definition of the equilibrium state of the bath is designed to allow (see Appendix B 1 d)

$$[H_B, F_0] = 0, \tag{B11}$$

which, in turn, makes the correlation translational invariant in time since

$$\begin{aligned} C_{\rm PM}(t_1,t_2) &= {\rm Tr}_{E'}\left[e^{iH_B(t_2-t_1)}X_{\rm PM}e^{-iH_B(t_2-t_1)}X_{\rm PM}\right. \\ &\quad \left.\times\, e^{-iH_Bt_1}\rho_{E'}e^{iH_Bt_1}\right] \\ &= {\rm Tr}_{E'}[X_{\rm PM}(t_2-t_1)X_{\rm PM}\rho_{E'}] \\ &\equiv C_{\rm PM}(t_2-t_1). \end{aligned} \tag{B12}$$

Note that this is nontrivial because the Hamiltonian H_B involves a Jaynes-Cummings interaction between the pseudomodes and the modes of their baths. Because of this, the previous relation does not hold in the presence of a true thermal equilibrium [2]. In order to make progress evaluating $C_{\rm PM}(t)$, we can first compute the formal solution for the Heisemberg equation of motion $\dot{b}_{k\alpha} = i[H_B, b_{k\alpha}]$ and use it in the Heisemberg equation of motion for the pseudomodes $\dot{a}_k = i[H_B, a_k]$. This leads to the following result for the Laplace transforms $\bar{x}_k$, $\bar{p}_k$ of the quadratures $x_k = a_k^\dagger + a_k$ and $p_k = i(a_k^\dagger - a_k)$:

$$\begin{aligned} s\bar{x}_k &= x_k(0) + \left[\Omega_k - \int_{-\infty}^{\infty} d\omega \frac{J_k(\omega)\omega}{\pi(s^2+\omega^2)}\right]\bar{p}_k \\ &\quad -s\int_{-\infty}^{\infty} d\omega \frac{J_k(\omega)}{\pi(s^2+\omega^2)}\bar{x}_k - x^{\rm in}_k \\ s\bar{p}_k &= p_k(0) + \left[\Omega_k - \int_{-\infty}^{\infty} d\omega \frac{J_k(\omega)\omega}{\pi(s^2+\omega^2)}\right]\bar{x}_k \\ &\quad -s\int_{-\infty}^{\infty} d\omega \frac{J_k(\omega)}{\pi(s^2+\omega^2)}\bar{p}_k - p^{\rm in}_k, \end{aligned} \tag{B13}$$

where

$$\begin{aligned} x^{\rm in}_k &= \sum_{k,\alpha}\frac{g_{k,\alpha}}{\sqrt{2\omega_{k,\alpha}}}\left[\frac{b^\dagger_{k,\alpha}(0)}{s-i\omega_{k,\alpha}} + \frac{b_{k,\alpha}(0)}{s+i\omega_{k,\alpha}}\right] \\ p^{\rm in}_k &= i\sum_{k,\alpha}\frac{g_{k,\alpha}}{\sqrt{2\omega_{k,\alpha}}}\left[\frac{b^\dagger_{k,\alpha}(0)}{s-i\omega_{k,\alpha}} - \frac{b_{k,\alpha}(0)}{s+i\omega_{k,\alpha}}\right]. \end{aligned} \tag{B14}$$

Now, using the expression for the spectral density in Eq. (B5), we find

$$\begin{aligned} s\bar{x}_k &= x_k(0) + \Omega_k\bar{p}_k - \Gamma_k\bar{x}_k - x^{\rm in}_k \\ s\bar{p}_k &= p_k(0) - \Omega_k\bar{x}_k - \Gamma_k\bar{p}_k - p^{\rm in}_k, \end{aligned} \tag{B15}$$

which leads to

$$\big[(s+\Gamma_k)^2+\Omega_k^2\big]\bar{x}_k = (s+\Gamma_k)[x_k(0)-x^{\rm in}] + \Omega_k\big[p_k(0)-p_k^{\rm in}\big]. \tag{B16}$$

We can now use this result in the expression for the stationary correlation in Eq. (B12) to obtain

$$\begin{aligned} C(t) &= \sum_k \frac{\lambda_k^2}{2\Omega_k}\mathcal{L}_t^{-1}\{{\rm Tr}_{E'}[\bar{x}_k x_k(0)\rho]\} \\ &= \sum_k \frac{\lambda_k^2}{2\Omega_k}\frac{1}{2\pi i}\int ds\, e^{st}\left\{\frac{[s+\Gamma_k]\langle x_k(0)x_k(0)\rangle}{\big(s+\Gamma_k^2\big)+\Omega_k^2}\right. \\ &\quad \left. + \frac{\Omega_k\langle p_k(0)x_k(0)\rangle}{\big(s+\Gamma_k^2\big)^2+\Omega_k^2}\right\}, \end{aligned} \tag{B17}$$

where we defined $\langle\cdot\rangle \equiv {\rm Tr}_{\rm PM}(\cdot\prod_k \rho_k)$, the trace being over the pseudomodes space. We note that, in the above derivation, translational invariance in time [derived thanks to the condition in Eq. (B6)] was essential as it allowed a great simplification through the identity $\langle x^{\rm in}x(0)\rangle = 0$. Using $\langle x_k(0)x_k(0)\rangle = 2n_k+1$ [with $2n_k+1 = \coth(\beta_k\Omega_k/2)$], and $\langle p_k(0)x_k(0)\rangle = -i$, we obtain

$$C_{\rm PM}(t) = \sum_{k=0}^{N_{\rm PM}} \frac{\lambda_k^2}{2\Omega_k}[n_k e^{i\Omega_k t} + (1+n_k)e^{-i\Omega_k t}]e^{-\Gamma_k t}, \tag{B18}$$

as in Eq. (A10) in the main text on the definition $g_k = \lambda_k^2/2\Omega_k$. Since, by hypothesis, this is a Gaussian open quantum system, the reduced dynamics of the system is fully determined by the functional form of $C_{\rm PM}(t)$ through Dyson equation. As a consequence, this model reproduces the same dynamics as the original model as long as $C_E(t) = C_{\rm PM}(t)$.

b. Dissipative pseudomodes

The dynamics in the system+pseudomodes space can be explicitly written in terms of the following influence functional expression:

$$\rho_{\text{S-PM}} = \hat{T}\exp\{\hat{F}_t[\cdot]\}\rho_{\text{S-PM}}(0), \tag{B19}$$

where $\hat{T}$ is the time-ordering operator and where the influence superoperator is

$$\hat{F}_t[\cdot] = -\int_0^t dt_2\int_0^{t_2} dt_1 G(t_1,t_2)[\cdot], \tag{B20}$$

where (using the shorthand $G \equiv G(t_1,t_2)[\cdot]$)

$$\begin{aligned} G = &\sum_k \langle B_k^\dagger(t_2)B_k(t_1)\rangle[a_k(t_2)a_k^\dagger(t_1)[\cdot] - a_k^\dagger(t_1)[\cdot]a_k(t_2)] \\ &\times \sum_k \langle B_k(t_2)B_k^\dagger(t_1)\rangle[a_k^\dagger(t_2)a_k(t_1)[\cdot] - a_k(t_2)[\cdot]a_k^\dagger(t_1)] \\ &\times \sum_k \langle B_k(t_1)B_k^\dagger(t_2)\rangle[[\cdot]a_k^\dagger(t_1)a_k(t_2) - a_k(t_2)[\cdot]a_k^\dagger(t_1)] \\ &\times \sum_k \langle B_k^\dagger(t_1)B_k(t_2)\rangle[[\cdot]a_k(t_1)a_k^\dagger(t_2) - a_k^\dagger(t_2)[\cdot]a_k(t_1)], \end{aligned} \tag{B21}$$

where we defined

$$B_k(t_i) = \sum_\alpha g_{k,\alpha}/\sqrt{2\omega_{k,\alpha}}b_{k,\alpha}(t_i), \tag{B22}$$

for $i = 1, 2$ to characterize the interaction operator between the pseudomodes and their environment [see Eq. (B2)]. Notice that the interaction picture used in the previous expression implies a change of frame defined by $U = \exp[i(H_S+H_{\rm PM})t]$, where $H_S + H_{\rm PM} = H_S + \sum_k H_{\rm PM}^k$ is the Hamiltonian in the system+pseudomode space. Explicitly,

$$\begin{aligned} \langle B_k^\dagger(t_2)B_k(t_1)\rangle &= \frac{1}{\pi}\int_{-\infty}^{\infty} d\omega J_k(\omega)n_k(\omega)e^{-i\omega(t_1-t_2)} \\ &= 2\Gamma_k n_k\delta(t_2-t_1) \\ \langle B_k(t_2)B_k^\dagger(t_1)\rangle &= \frac{1}{\pi}\int_{-\infty}^{\infty} d\omega J_k(\omega)[1+n_k(\omega)]e^{-i\omega(t_1-t_2)} \\ &= 2\Gamma_k[1+n_k]\delta(t_2-t_1), \end{aligned} \tag{B23}$$

where $2n_k(\omega)+1 = \coth\beta_k(\omega)\omega/2$ and, importantly, we used the condition in Eq. (B6) to obtain $2n_k(\omega)+1 = \coth\beta_k\Omega_k/2$, effectively implying

$$n_k(\omega) \mapsto n_k(\Omega_k) \equiv n_k. \tag{B24}$$

Using Eq. (B23) into Eq. (B20), we get

$$\begin{aligned} F_t[\cdot] = -\Big\{ &\sum_k (1+n_k)\Gamma_k[a_k^\dagger(t)a_k(t)[\cdot] + [\cdot]a_k^\dagger(t)a_k(t) \\ &-2a_k(t)[\cdot]a_k^\dagger(t)]t \\ &+ \sum_k n_k\Gamma_k[a_k(t)a_k^\dagger(t)[\cdot] + [\cdot]a_k(t)a_k^\dagger(t) \\ &-2a_k^\dagger(t)[\cdot]a_k(t)]t\Big\}, \end{aligned} \tag{B25}$$

where we used $\int_0^t dt'\delta(t-t') = 1/2$ (see Eq. 5.3.12 in Ref. [2]). Going back to the Shrödinger picture, using Eq. (B19), and taking a time derivative, we get

$$\dot{\rho}_{\text{S-PM}} = L_{\text{S-PM}}[\rho_{\text{S-PM}}], \tag{B26}$$

where

$$L_{\text{S-PM}}[\cdot] = -i[H_S+H_{\rm PM},\cdot] + \sum_{k=0}^{N_{\rm PM}} D_k[\cdot], \tag{B27}$$

and

$$\begin{aligned} D_k[\cdot] = &(n_k+1)\Gamma_k(2a_k[\cdot]a_k^\dagger - a_k^\dagger a_k[\cdot] - [\cdot]a_k^\dagger a_k) \\ &+n_k\Gamma_k(2a_k^\dagger[\cdot]a_k - a_k a_k^\dagger[\cdot] - [\cdot]a_k a_k^\dagger), \end{aligned} \tag{B28}$$

This is Eq. (A1) in the main text.

c. Correlations for the dissipative pseudomodes

As a consistency check, we now show that the correlation function computed in Eq. (B18) can, equivalently, also be computed using the Lindblad model developed in the previous section. Specifically, we want to show that

$$C'_{\rm PM}(t) = C_{\rm PM}(t), \tag{B29}$$

where $C'_{\rm PM}(t) = {\rm Tr}_{\rm PM}[X_{\rm PM}(t)X_{\rm PM}(0)]$, with $X_{\rm PM}(t) = \exp\{L^\dagger_{PM}[\cdot]t\}X_{\rm PM}$, where

$$L^\dagger_{\rm PM} = i[H_S + H_{\rm PM}, \cdot] + \sum_k D^\dagger_k[\cdot], \tag{B30}$$

with

$$\begin{aligned} D^\dagger_k[\cdot] = (n_k+1)\Gamma_k(2a^\dagger_k[\cdot]a_k - [\cdot]a^\dagger_k a_k - a^\dagger_k a_k[\cdot]) \\ +n_k\Gamma_k(2a_k[\cdot]a^\dagger_k - [\cdot]a_k a^\dagger_k - a_k a^\dagger_k[\cdot]). \end{aligned} \tag{B31}$$

We then have

$$\begin{aligned} L^\dagger_{\rm PM}[a_k] &= i[\Omega_k a^\dagger_k a_k, a_k] + D^\dagger_k[a_k] = -i\Omega_k a_k - \Gamma_k a_k \\ L^\dagger_{\rm PM}[a^\dagger_k] &= i[\Omega_k a^\dagger_k a_k, a^\dagger_k] + D^\dagger_k[a^\dagger_k] = i\Omega_k a_k - \Gamma_k a_k, \end{aligned} \tag{B32}$$

so that

$$\begin{aligned} C'_{\rm PM}(t) &= \sum_{k=0}^{N_{\rm PM}} \frac{\lambda_k^2}{2\Omega_k}\langle(a_k e^{-i\Omega_k} + a^\dagger_k e^{-i\Omega_k})(a_k + a^\dagger_k)\rangle e^{-\Gamma_k t} \\ &= \sum_{k=0}^{N_{\rm PM}} \frac{\lambda_k^2}{2\Omega_k}[n_k e^{i\Omega_k t} + (1+n_k)e^{-i\Omega_k t}]e^{-\Gamma_k t}, \end{aligned} \tag{B33}$$

which implies Eq. (B29).

d. Proof of Eq. (B11)

Here we prove that

$$[H_B, F_0] = 0, \tag{B34}$$

where

$$\begin{aligned} F_0 &= \sum_k \beta_k \Omega_k a^\dagger_k a_k + \sum_{k,\alpha} \beta_{k,\alpha}\omega_{k,\alpha} b^\dagger_{k,\alpha} b_{k,\alpha} \\ H_B &= \sum_k \Bigg[\Omega_k a^\dagger_k a_k + i\sum_\alpha \frac{g_{k,\alpha}}{\sqrt{2\omega_\alpha}}(b^\dagger_{k\alpha} a_k - a^\dagger_k b_{k\alpha}) \\ &\quad + \sum_\alpha \omega_{k\alpha} b^\dagger_{k,\alpha} b_{k,\alpha} \Bigg]. \end{aligned} \tag{B35}$$

In fact, we have

$$\begin{aligned} [H_B, F_0] &= i\sum_{k,\alpha} \frac{g_{k,\alpha}}{\sqrt{2\omega_\alpha}}[(b^\dagger_{k\alpha} a_k - a^\dagger_k b_{k\alpha}), F^{\rm eq}] \\ &= i\sum_{k,\alpha} \frac{g_{k,\alpha}}{\sqrt{2\omega_\alpha}}(b^\dagger_{k\alpha} a_k + a^\dagger_k b_{k\alpha}) \\ &\quad \times (\beta_k\Omega_k - \beta_{k,\alpha}\omega_{k,\alpha}) = 0, \end{aligned} \tag{B36}$$

where, in the last step, we used Eq. (B6).

2. A hybrid pseudomode model

As shown in Ref. [95], it is possible replace some of the quantum degrees of freedom present in the fully deterministic pseudomode model presented in the previous section with a classical stochastic colored noise $\xi(t)$ which is stationary, Gaussian, and with zero mean. In fact, the addition of a driving term $\xi(t)\hat{s}$ in the Hamiltonian in Eq. (B2) effectively adds, after averaging over the noise, a term

$$C_{\rm class}(t) = \mathbb{E}[\xi(t_2)\xi(t_1)], \tag{B37}$$

where $t_2 - t_1 = t$ and which accounts for the statistics of the field. In turn, the dynamics of this hybrid model can be explicitly written by adding the stochastic noise in Eq. (B26) to write the Lindblad operator as

$$L_{\text{S-PM}} = L_S + \sum_{k=1}^{N_{\rm PM}} L^k_{\text{S-PM}}[\cdot] - i[\xi(t)\hat{s}, \cdot]. \tag{B38}$$

While we refer to Ref. [95] for more details, here we note that the addition of noise in the model corresponds to a decomposition of the effects of the original environment into a classical and a quantum part, i.e.,

$$C_E(t) = C_Q(t) + C_{\rm class}(t), \tag{B39}$$

in which the second term is symmetric under time reversal (so that it can be modeled using classical resources) while the first term is more general and requires ancillary quantum degrees of freedom. Interestingly, this decomposition is *not* unique, allowing for further possibility of optimization in the model. For example, it is possible to chose the classical contribution $C_{\rm class}(t)$ [hence the field $\xi(t)$] in such a way that all the pseudomodes modeling $C_Q(t)$ are, initially, at zero temperature. This is the choice which is used throughout this article.

3. Underdamped Brownian spectral density

In this section, we describe the explicit form of the pseudomode model for the spectral density $J_B(t)$ in Eq. (50). At zero temperature, the deterministic pseudomode mode can be defined using a single resonant mode at $N_{\rm mats}$ zero-frequency Matsubara modes. This follows from the decomposition

$$C^B(t;\beta=\infty) = C_{\rm res}(t) + M(t), \tag{B40}$$

in terms of the resonant and Matsubara contributions,

$$\begin{aligned} C_{\rm res}(t) &= \frac{\lambda^2}{2\Omega}\exp[-i\Omega t - \Gamma|t|] \\ M(t) &= -\frac{\lambda^2\gamma}{\pi}\int_0^\infty \frac{dx\, x e^{-x|t|}}{[(\Omega+i\Gamma)^2 + x^2][(\Omega - i\Gamma)^2 + x^2]}. \end{aligned} \tag{B41}$$

It is possible to model these terms by introducing a resonant and $N_{\rm Mats}$ Matsubara harmonic modes $a_{\rm res}$, a_k ($k = 1, \ldots, N_{\rm Mats}$) and define a pseudomode model through the Lindblad operator

$$L^B_{\rm PM} = L_{\rm res} + L_{\rm Mats}, \tag{B42}$$

where

$$L_{\rm res}[\cdot] = -i[H_{\rm res}, \cdot] + \Gamma_{\rm res}[2a_{\rm res}\cdot a^\dagger_{\rm res} - a^\dagger_{\rm res}a_{\rm res}\cdot - \cdot a^\dagger_{\rm res}a_{\rm res}],$$

with

$$H_{\rm res} = \Omega_{\rm res}a^\dagger_{\rm res}a_{\rm res} + \lambda_{\rm res}(a_{\rm res} + a^\dagger_{\rm res})\hat{s}. \tag{B43}$$

These parameters are explicitly given by

$$\begin{aligned} \lambda_{\rm res} &= \lambda^2/2\Omega \\ \Omega_{\rm res} &= \Omega = \sqrt{\omega_0^2 - \Gamma_{\rm res}^2} \\ \Gamma_{\rm res} &= \Gamma = \gamma/2. \end{aligned} \tag{B44}$$

The remaining contribution to the Lindbladian can be written as

$$L_{\rm Mats} = \sum_{k=1}^{N_{\rm Mats}} L^k_{\rm Mats}, \tag{B45}$$

in terms of

$$L^k_{\rm Mats}[\cdot] = -i\big[H^k_{\rm Mats}, \cdot\big] + \Gamma^k_{\rm Mats}[2a_k \cdot a_k^\dagger - a_k^\dagger a_k \cdot - \cdot a_k^\dagger a_k],$$

with

$$H^k_{\rm Mats} = \Omega_k a_k^\dagger a_k + \lambda_k (a_k + a_k^\dagger)\hat{s}. \tag{B46}$$

These parameters can be estimated by fitting the corresponding correlation,

$$C_{\rm Mats}(t) = \sum_{k=1}^{N_{\rm Mats}} \frac{\lambda_k^2}{2\Omega_k}[n_k e^{i\Omega_k t} + (1+n_k)e^{-i\Omega_k t}]e^{-\Gamma_k t}, \tag{B47}$$

to $M(t)$; see Ref. [90]. However, because of the absence of oscillatory behavior in $M(t)$, it is possible to directly impose $\Omega_k = 0$, $k = 1, \ldots, N_{\rm Mats}$.

It is interesting to note that, in general, the number of Matsubara modes needed to reproduce the effects of $M(t)$ depends on the simulation time. In fact, we note that the domain of integration in the integral in Eq. (B41) is effectively restricted to values $x \ll 1/t$ by the presence of the exponential [165]. Therefore,

$$M(t) \overset{t\gg 1/\Omega, 1/\Gamma}{\simeq} -\frac{\lambda^2\gamma}{\pi}\frac{\partial}{\partial t}\int_0^\infty \frac{e^{-x|t|}}{\omega_0^4} = -\frac{\alpha}{\pi}\frac{1}{t^2}, \tag{B48}$$

where

$$\alpha = \lambda^2\gamma/\omega_0^2. \tag{B49}$$

This shows that $M(t)$ is characterized by an asymptotic ($\sim 1/t^2$) polynomial decay which contrasts with the exponential decay present in the Matsubara correlation; see Eq. (B47).

At finite temperatures, the decomposition of the correlation becomes

$$C^B(t;\beta) = C^B_{\rm res}(t;\beta) + M(t;\beta), \tag{B50}$$

where

$$\begin{aligned} C^B_{\rm res}(t;\beta) = {} & \frac{\lambda^2}{4\Omega}\coth[\beta(\Omega + i\Gamma)/2]e^{i\Omega|t|}e^{-\Gamma|t|} \\ & -\frac{\lambda^2}{4\Omega}\coth[\beta(-\Omega + i\Gamma)/2]e^{-i\Omega|t|}e^{-\Gamma|t|} \\ & -\frac{\lambda^2}{4\Omega}(-e^{-i\Omega t} + e^{i\Omega t})e^{-\Gamma|t|} \end{aligned}$$

$$M(t;\beta) = \frac{2i}{\beta}\sum_{k>0} J^B\big(\omega_k^M\big)\exp\big[-\big|\omega_k^M\big||t|\big], \tag{B51}$$

in terms of $\omega_k^M = 2\pi k i/\beta$ ($k = 1, \ldots, \infty$). In order to reproduce it, we can introduce three "resonant" modes $a_{j;\rm res}$, $j = 1, 2, 3$ alongside $N_{\rm mats}$ "Matsubara" modes a_k, $k = 1, \ldots, N_{\rm mats}$ characterized by the Lindblad operator

$$L^\beta_{\rm PM} = L^\beta_{\rm res} + L^\beta_{\rm Mats}. \tag{B52}$$

The Matsubara contribution is formally the same as in the zero-temperature case, but its parameters are defined to fit $M(t;\beta)$ instead of its zero-temperature limit in Eq. (B41). However, the resonant part has to be updated and defined by

$$L^\beta_{\rm res}[\cdot] = -i\big[H^\beta_{\rm res}, \cdot\big] + D^\beta_{\rm res}[\cdot], \tag{B53}$$

where

$$\begin{aligned} H^\beta_{\rm res} &= \sum_{j=1}^{3}\lambda^j_{\rm res}\big[a^j_{\rm res} + \big(a^j_{\rm res}\big)^\dagger\big]\hat{s} + \Omega^j_{\rm res}\big(a^j_{\rm res}\big)^\dagger a^j_{\rm res} \\ D^\beta_{\rm res}[\rho] &= \sum_{j=1}^{N_{\rm mats}}\Gamma_j[(n_j+1)(2a_j\rho a_j^\dagger - a_j^\dagger a_j\rho - \rho a_j^\dagger a_j) \\ &\quad + n_j(2a_j^\dagger\rho a_j - a_j a_j^\dagger\rho - \rho a_j a_j^\dagger)], \end{aligned} \tag{B54}$$

as a function of the parameters

$$\begin{aligned} &\lambda_1 = \sqrt{\frac{\lambda^2}{2\Omega}} \quad \lambda_2 = \sqrt{\frac{I_B\lambda^2}{4\Omega}} \quad \lambda_3 = \sqrt{\frac{-I_B\lambda^2}{4\Omega}} \\ &\Omega_1 = \Omega \quad \Omega_2 = 0 \quad \Omega_3 = 0 \\ &\Gamma_1 = \Gamma \quad \Gamma_2 = \Gamma - i\Omega \quad \Gamma_3 = \Gamma + i\Omega \\ &n_1 = \frac{R_B - 1}{2} \quad n_2 = 0 n_3 = 0, \end{aligned} \tag{B55}$$

characterizing the resonant modes through the definitions

$$\begin{aligned} R_B &= {\rm Re}\{\coth[\beta(\Omega + i\Gamma)/2)\} \\ I_B &= {\rm Im}\{\coth[\beta(\Omega + i\Gamma)/2)\}. \end{aligned} \tag{B56}$$

We note that other choices which only use two resonant modes initially prepared with complex-temperature values are possible [166].

The hybrid pseudomode model relies on writing the correlation function of the bath in the following alternative form:

$$C^B(t;\beta) = C^B_{\rm class}(t;\beta) + C^B_Q(t), \tag{B57}$$

where

$$\begin{aligned} C^B_{\rm class}(t;\beta) = {} & \frac{\lambda^2}{4\Omega}\coth[\beta(\Omega + i\Gamma)/2]e^{i\Omega|t| - \Gamma|t|} \\ & -\frac{\lambda^2}{4\Omega}\coth[\beta(-\Omega + i\Gamma)/2]e^{-i\Omega|t| - \Gamma|t|} \\ & -\frac{\lambda^2}{4\Omega}(e^{-i\Omega t} + e^{i\Omega t})e^{-\Gamma|t|} \\ & +\frac{2i}{\beta}\sum_{k>0} J^B\big(\omega_k^M\big)\exp\big[-\big|\omega_k^M\big||t|\big] \end{aligned}$$

$$C^B_Q(t;\beta) = \frac{\lambda^2}{2\Omega}\exp[-i\Omega t - \Gamma|t|], \tag{B58}$$

Since the "classical" contribution $C^B_{\rm class}(t)$ is symmetric under time reversal, it can be reproduced by a single classical stochastic process $\xi^B(t)$ with autocorrelation function

$$\mathbb{E}[\xi^B(t_2)\xi^B(t_1)] = C^B_{\rm class}(t_2 - t_1). \tag{B59}$$

The remaining "quantum" contribution can be reproduced with a single "resonant" pseudomode characterized by the same Lindblad $L_{\rm res}$ as the one defined in the zero-temperature case.

Despite the presence of a series dependent on the Matsubara frequencies, the spectrum $S[\omega]$ can be computed in a closed form. In fact, we can write

$$\begin{aligned} S[\omega] &= \int_{-\infty}^{\infty} dt\ C(t)e^{-i\omega t} \\ &= \int_0^{\infty} \frac{d\bar{\omega}}{2\pi} J(\bar{\omega}) \int_{-\infty}^{\infty} dt \{[\coth(\beta\bar{\omega}/2) - 1]e^{i(\bar{\omega}-\omega)t} \\ &\quad + [\coth(\beta\bar{\omega}/2) + 1]e^{-i(\bar{\omega}+\omega)t}\} \\ &= \theta(\omega)J(\omega)[\coth(\beta\omega/2) - 1] \\ &\quad + \theta(-\omega)J(-\omega)[\coth(-\beta\omega/2) + 1], \end{aligned} \tag{B60}$$

and

$$S[\omega] = S_Q[\omega] + S_{\text{class}}[\omega], \tag{B61}$$

in terms of the Fourier transforms of the quantum and classical contributions to the correlation

$$S_{Q/\text{class}}[\omega] = \int_{-\infty}^{\infty} dt\ C_{Q/\text{class}}(t)e^{-i\omega t}. \tag{B62}$$

Assuming continuity and $J(0) = 0$, the zero-frequency limit becomes

$$S[0] = \lim_{\omega\to 0^+} J(\omega)\coth(\beta\omega/2) = \frac{2}{\beta}J^*(0), \tag{B63}$$

where $J^*(\omega) \equiv J(\omega)/\omega$ which we assume to be defined at $\omega = 0$ by continuity. For the Brownian spectral density above, we have

$$S_Q^B[\omega] = \frac{\lambda^2\Gamma}{\Omega}\frac{1}{(\Omega+\omega)^2 + \Gamma^2}, \tag{B64}$$

which allows us to write the classical spectrum in a closed form as

$$S_{\text{class}}^B = S^B[\omega] - S_Q^B[\omega], \tag{B65}$$

where

$$\begin{aligned} S^B[\omega] &= \theta(\omega)J^B(\omega)[\coth(\beta\omega/2) - 1] \\ &\quad + \theta(-\omega)J^B(-\omega)[\coth(-\beta\omega/2) + 1]. \end{aligned} \tag{B66}$$

We can further write the zero-frequency limit in the following explicit form:

$$S^B[0] = \frac{2}{\beta}\frac{\gamma\lambda^2}{\omega_0^4}. \tag{B67}$$

We now present an intuitive estimation for the temperature above which this spectrum is positive. To do this, we note that, for low temperatures, the classical spectrum is negative (due to the fact that the classical correlation is dominated by the Matsubara contribution) and peaked at zero frequency while, at high temperature, the spectrum becomes positive over all frequencies. As a consequence of this consideration, there must be a crossover temperature β^* such that $S_{\text{class}}[0] = 0$. Using the results above, this temperature can be computed explicitly. In fact, we have

$$S_{\text{class}}^B[0] = S^B[0] - S_Q^B[0] = \frac{4\Gamma\lambda^2}{\beta\omega_0^4} = \frac{\lambda^2\Gamma}{\Omega\omega_0^2}. \tag{B68}$$

By imposing $S_{\text{class}}^B[0] = 0$, the value β^* can be written as

$$\beta^*\omega_0 = 2\sqrt{4 - (\gamma/\omega_0)^2}. \tag{B69}$$

APPENDIX C: ERROR ANALYSIS

In this section, we present an analytical analysis of the estimation error of the polynomial extrapolation algorithm presented in Sec. IV B. To start, we briefly review the main setting of the extrapolation protocol presented in the main article.

1. General setting

Following Sec. IV B, we define $f(\Lambda)$ as the analytical continuation, in the parameter $\Lambda \in \mathbb{C}$, of the expectation value of the system variable $\hat{O}_S$ at time t. We note that, in this Appendix, all time dependencies are omitted to simplify the notation. Explicitly, the above definition amounts to the requirement that

$$f(\Lambda) \equiv \langle\hat{O}_S\rangle(\Lambda), \tag{C1}$$

within the restricted domain $\Lambda \in [-1, 1]$, which parametrizes the physical ensemble where $\hat{O}_S$ is measured. Despite this complete functional information not being practically available, we can assume to have access to $N + 1$ experimental values,

$$f_n^{\text{exp}} \equiv \langle\hat{O}_S\rangle(\Lambda_n) + \epsilon_n \equiv f_n^{\text{true}} + \epsilon_n, \tag{C2}$$

in the set $\Lambda_n \in [-1, 1]$, $n = 0, \ldots, N$. Here we further defined $f_n^{\text{true}} \equiv \langle\hat{O}_S\rangle(\Lambda_n)$ as the "true" value of the observable affected by noise through unbiased Gaussian random variables ϵ_n with zero mean and variance σ_{exp}^2. We will provide a more detailed analysis on these errors in Appendix D. The data in the variables f_n^{exp} can be used to introduce an order M polynomial $p_M^{\text{exp}}(\Lambda)$ which minimizes the least-squares distance,

$$d^2 = \sum_{n=0}^{N} \left|p_M^{\text{exp}}(\Lambda_n) - f_n^{\text{exp}}\right|^2. \tag{C3}$$

In other words, $p_M^{\text{exp}}(\Lambda)$ constitutes our best estimate for the analytical function $f(\Lambda)$ using the discrete set of available data f_n^{exp}. As explained in Sec. IV B, we are ultimately interested in reconstructing the expectation $\langle\hat{O}_S\rangle^{\text{reconstructed}}$ corresponding to an analytical continuation at a specific unphysical value denoted by $\Lambda_c \in \mathbb{C}$, i.e.,

$$\langle\hat{O}_S\rangle^{\text{reconstructed}} \equiv p_M^{\text{exp}}(\Lambda_c). \tag{C4}$$

In the following, we further limit the analysis to the case $N \geqslant M$, so that the number of data points available is bigger than the order of the extrapolating polynomial.

The goal of the following section is to provide an estimate for the extrapolation error of the quantity in Eq. (C4), i.e.,

$$\begin{aligned} \text{Err} &= \mathbb{E}_{\text{exp}}[|\langle\hat{O}_S\rangle(\Lambda_c) - \langle\hat{O}_S\rangle^{\text{reconstructed}}|] \\ &\equiv \mathbb{E}_{\text{exp}}\left[\left|f(\Lambda_c) - p_M^{\text{exp}}(\Lambda_c)\right|\right]. \end{aligned} \tag{C5}$$

where $\langle\hat{O}_S\rangle(\Lambda_c)$ is the "true" analytically continued value which we ultimately want to compute. Importantly, the

average $\mathbb{E}_{\text{exp}}$ takes into account the uncertainties on the experimental data encoded in the random variables ϵ_n.

To analytically approach the estimation of this error, in the next section we follow Ref. [161] and take advantage of an explicit extrapolation form, expressed in terms of Chebyshev polynomials.

2. Chebyshev polynomials

This subsection reviews the definitions and properties of the Chebyshev polynomials of first kind, adapting Refs. [167–169].

The Chebyshev polynomials of first kind are defined as

$$T_m(x) = \cos n\theta, \tag{C6}$$

for $m \geqslant 0$ and for $x \in [-1, 1]$, such that $x = \cos\theta$, which immediately implies the bound

$$|T_m(x)| \leqslant 1 \quad \text{for} \quad x \in [-1, 1]. \tag{C7}$$

While not immediately apparent from the definition, these functions satisfy the recurrence relation

$$T_m(x) = 2xT_{m-1}(x) - T_{m-1}(x), \tag{C8}$$

which, together with the initial conditions $T_0(x) = 1$ and $T_1(x) = x$ imply that each $T_m(x)$ is a polynomial of order m. It is further possible to analytically continue these polynomials and to write them as

$$T_m(z) = [(z + \sqrt{z^2 - 1})^m + (z - \sqrt{z^2 - 1})^m]/2, \tag{C9}$$

where $z \in \mathbb{C}$. Given a parameter $\rho > 0$, it is possible to define the so-called Bernstein ellipse

$$E_\rho = \{z \in \mathbb{C} : z = (w + w^{-1})/2, w \in \mathbb{C}, |w| = \rho > 1\}, \tag{C10}$$

such that

$$|T_m(z \in \Gamma_\rho)| = |(\rho^m e^{im\theta} + \rho^{-m} e^{-im\theta})|/2. \tag{C11}$$

Given a point $z \in \mathbb{C}$, it is useful to define, at least implicitly, the parameter ρ_z such that $z \in \Gamma_{\rho_z}$. In other words, the Bernstein ellipse with parameter $\rho_z > 1$ passes through the point z when

$$\frac{\text{Re}^2[z]}{\left(\rho_z + \rho_z^{-1}\right)^2} + \frac{\text{Im}^2[z]}{\left(\rho_z - \rho_z^{-1}\right)^2} = 1, \tag{C12}$$

is satisfied.

In the following, we will denote by $\tilde{E}_\rho$ the open Bernstein ellipse, i.e., the region of the complex plane inside E_ρ (i.e., the one containing the origin). This constitutes a rather interesting identity because it implies that, on the Bernstein ellipse E_ρ, the Chebyshev polynomials satisfy the bounds

$$[\rho^m - \rho^{-m}]/2 \leqslant |T_m(z \in \Gamma_\rho)| \leqslant [\rho^m + \rho^{-m}]/2, \tag{C13}$$

and, since $\rho > 1$, the cleaner, but less strict one,

$$|T_m(z \in \Gamma_\rho)| \leqslant \rho^m. \tag{C14}$$

The Chebyshev polynomials $T(x)$ are a basis for functions in the interval $[-1, 1]$. This means that every function $g(x)$ can be written [167], in this interval, in terms of the Chebyshev series,

$$g(x) = \sum_{m=0}^{\infty} g_m T_m(x) = \sum_{m=0}^{\infty} g_m \left(z_\theta^m + z_\theta^{-m}\right)/2 \equiv G(z_\theta). \tag{C15}$$

where $g_m \in \mathbb{C}$ and where we used Eq. (C6) to define the function $G(z)$ on the unit circle $z_\theta = \exp[i\theta]$, $\theta \in [0, 2\pi]$. It is further possible to follow an elegant geometric construction [167] to show that an analytical continuation of $g(x)$ in $\tilde{E}_\rho$ corresponds to analytically continue $G(z)$ inside the annulus $\rho^{-1} \leqslant |z| \leqslant \rho$. Intuitively, this is a consequence of the fact that $G(z)$ can be interpreted as the pull-back of $g(x)$ on the unit circle by the Joukoasky map $J(z) = (z + z^{-1})/2$, $z \in \mathbb{C}$ (which projects the unit circle onto the real axis, i.e., $J(z) = \text{Re}[z]$ for $|z| = 1$). In other words, $F(z) = g(x)$. In turn, this allows us to take advantage of the Laurent series in Eq. (C15) to write [167]

$$\frac{g_m}{2} = \frac{1}{2\pi i} \int_{|z|=\rho} dz\, z^{-1+m} G(z), \tag{C16}$$

where the factor $1/2$ should not appear on the left-hand side for $m = 0$. By further assuming $|g(z)| \leqslant Q_\rho$ for $x \in \tilde{E}_\rho$ the expression above implies

$$|g_0| \leqslant Q_\rho, \quad \text{and} \quad |g_m| \leqslant 2Q_\rho \rho^{-m} \quad \text{for} \quad m \geqslant 1, \tag{C17}$$

see Theorem 8.1 in Ref. [167]. We can now use these bounds to analyze the error made by truncating the Chebyshev series in Eq. (C15). To do this, we can define $g_M(x)$ as the truncated series,

$$g_M(x) = \sum_{m=0}^{M} g_m T_m(x). \tag{C18}$$

Using Eq. (C7) and (C17), the error made by this truncation can be quantified as

$$\begin{aligned} \sup_{x\in[-1,1]} |g(x) - g_M(x)| &= \sup_{x\in[-1,1]} \left| \sum_{m=M+1}^{\infty} g_m T_m(x) \right| \\ &\leqslant 2Q_\rho \sum_{m=M+1}^{\infty} \rho^{-m} = 2Q_\rho \frac{\rho^{-M}}{\rho - 1}. \end{aligned} \tag{C19}$$

We note that this bound is valid for all parameters $\rho > 1$ defining an open Bernstein ellipse $\tilde{E}_\rho$ inside which $g(x)$ admits an analytical continuation.

In the following subsection, we show how to use these results in order to provide an estimate for the error made in a polynomial extrapolation.

3. Error analysis using Chebyshev polynomials

In this subsection, we adapt the results elegantly presented in Ref. [161] to analyze in more detail the expression for the extrapolation error in Eq. (C5) which averages the difference between the "true" extrapolation value $f(\Lambda_c) = \langle \hat{O}_S \rangle(\Lambda_c)$ and its M-order polynomial estimate $p_M^{\text{exp}}(\Lambda_c)$. Assuming that the function $f(\Lambda)$ admits analytical continuation, we can

always write it in terms of a Chebyshev series as

$$f(z) = \sum_{m=0}^{\infty} a_m T_m(z), \tag{C20}$$

with $a_m \in \mathbb{C}$. Similarly, the polynomial $p_M^{\text{exp}}(z)$ can be written as a truncated series

$$p_M(z) = \sum_{m=0}^{M} c_m T_m(z), \tag{C21}$$

whose coefficients c_n solve the least-squares optimization defined by the distance in Eq. (C3). Explicitly, we can write $c_m \equiv \vec{c}_m$, where

$$\vec{c} = (T^\dagger T)^{-1} T^\dagger (\vec{f} + \vec{\epsilon}) \tag{C22}$$

is written in terms of the vector $\vec{\epsilon} = (\epsilon_0, \cdots, \epsilon_N)^T$ and

$$\vec{f} = \begin{pmatrix} f_0 \\ \vdots \\ f_N \end{pmatrix} = \begin{bmatrix} f(\Lambda_0) \\ \vdots \\ f(\Lambda_N) \end{bmatrix} \equiv \begin{pmatrix} \langle \hat{O} \rangle_{\Lambda_0} \\ \vdots \\ \langle \hat{O} \rangle_{\Lambda_N} \end{pmatrix}, \tag{C23}$$

and

$$T = \begin{bmatrix} T_0(\lambda_0) & \cdots & T_M(\Lambda_0) \\ \vdots & & \vdots \\ T_0(\Lambda_N) & \cdots & T_M(\Lambda_N) \end{bmatrix}. \tag{C24}$$

In order to introduce some of this definitions to analyze the full series in Eq. (C20), we can decompose it as

$$f(z) = f_M(z) + \sum_{m=M+1}^{\infty} a_m T_m(z) \tag{C25}$$

in terms of the truncated series

$$f^M(z) \equiv \sum_{m=0}^{M} a_m T_m(z). \tag{C26}$$

In this way, the coefficients a_m $(m = 0, \ldots, M)$ can be written explicitly as $a_m \equiv \vec{a}_m$, where

$$\vec{a} = (T^\dagger T)^{-1} T^\dagger \vec{f}^M. \tag{C27}$$

Here we introduced the vector

$$\vec{f}^M = \begin{bmatrix} f^M(\Lambda_0) \\ \vdots \\ f^M(\Lambda_N) \end{bmatrix}, \tag{C28}$$

which, as can be noted by comparison, is not equivalent to the one in Eq. (C23) since it relies on the truncated series rather than the "true" value. With this notation, we have

$$\begin{aligned} \text{Err} &= \mathbb{E}_{\text{exp}}\left[\left|\sum_{m=0}^{\infty} a_m T_m(z) - \sum_{m=0}^{M} c_m T_m(z)\right|\right] \\ &\leqslant \mathbb{E}_{\text{exp}}\left[\left|\sum_{m=0}^{M} (\vec{a}_m - \vec{c}_m) T_m(z)\right|\right] + \left|\sum_{m=M+1}^{\infty} a_m T_m(z)\right| \\ &\leqslant ||(T^\dagger T)^{-1} T^\dagger||_\infty ||(\vec{f}_M - \vec{f})||_\infty \sum_{m=0}^{M} |T_m(z)| \\ &\quad + \sum_{m=M+1}^{\infty} |a_m|\, |T_m(z)| \\ &\quad + \mathbb{E}_{\text{exp}}[||(T^\dagger T)^{-1} T^\dagger \vec{\epsilon}||_\infty] \sum_{m=0}^{M} |T_m(z)| \\ &\equiv \text{Err}_1 + \text{Err}_2, \end{aligned} \tag{C29}$$

where we introduced the infinity norm and used Eq. (G8), see Appendix G 1, and defined

$$\begin{aligned} \text{Err}_1 &= ||(T^\dagger T)^{-1} T^\dagger||_\infty ||(\vec{f}_M - \vec{f})||_\infty \sum_{m=0}^{M} |T_m(z)| \\ &\quad + \sum_{m=M+1}^{\infty} |a_m|\, |T_m(z)| \\ \text{Err}_2 &= \mathbb{E}_{\text{exp}}[||(T^\dagger T)^{-1} T^\dagger \vec{\epsilon}||_\infty] \sum_{m=0}^{M} |T_m(z)|. \end{aligned} \tag{C30}$$

Our goal is now to compute the quantities in the expressions above. To begin, using Eq. (G6), we have

$$||(T^\dagger T)^{-1} T^\dagger||_\infty \leqslant \sqrt{N+1}\, ||(T^\dagger T)^{-1} T^\dagger||_2. \tag{C31}$$

Now, since T is a $(N+1) \times (M+1)$ matrix, we can write it, in singular value decomposition, as

$$T = V_{(N+1)\times(N+1)} \Sigma_{(N+1)\times(M+1)} U_{(M+1)\times(M+1)}, \tag{C32}$$

where U and V are unitary and Σ has nonzero elements only on the diagonal. Omitting the size of the matrices we have

$$(T^\dagger T)^{-1} T^\dagger = U^{-1} (\Sigma^\dagger \Sigma)^{-1} \Sigma V^{-1}. \tag{C33}$$

Since $(\Sigma^\dagger \Sigma)^{-1} \Sigma$ has nonzero elements only on the diagonal, this constitutes a singular value decomposition for $(T^\dagger T)^{-1} T^\dagger$. Moreover, the diagonal elements of $(\Sigma^\dagger \Sigma)^{-1} \Sigma$ are the inverse of the diagonal elements of Σ. Using Eq. (G9), this implies

$$||(T^\dagger T)^{-1} T^\dagger||_2 = \frac{1}{\min(\sigma_T)}. \tag{C34}$$

Using this result into Eq. (C31), we obtain

$$||(T^\dagger T)^{-1} T^\dagger||_\infty \leqslant \frac{\sqrt{N+1}}{\min(\sigma_T)}, \tag{C35}$$

where σ_T are the singular values of the matrix T. In order to compute $||\vec{f} - \vec{f}_M||_\infty$, we note that all evaluations of $f(z)$ and $f_M(z)$ inside its expression are within the interval $[-1, 1]$. This implies that we can use Eq. (C19) to deduce that

$$||\vec{f} - \vec{f}_M||_\infty \leqslant 2 Q_\rho \frac{\rho^{-M}}{\rho - 1}. \tag{C36}$$

The remaining two terms can be immediately bounded using Eq. (C14), Eq. (C17), and Eq. (C12) as

$$\sum_{m=0}^{M}|T_m(z)| \leqslant \sum_{m=0}^{M}\rho_z^m = \frac{1-\rho_z^{M+1}}{1-\rho_z}$$
$$\sum_{m=M+1}^{\infty}|a_m|\,|T_m(z)| \leqslant 2Q_\rho \sum_{m=M+1}^{\infty}\left(\frac{\rho_z}{\rho}\right)^m = 2Q_\rho\frac{(\rho_z/\rho)^{M+1}}{(1-\rho_z/\rho)}. \tag{C37}$$

Using Eqs. (C35), (C36), and (C37) into the first line of Eq. (C30), we get

$$\mathrm{Err}_1 = 2Q_\rho\left[\frac{\sqrt{N+1}}{\min(\sigma_T)}\frac{\rho^{-M}\left(1-\rho_z^{M+1}\right)}{(\rho-1)(1-\rho_z)} + \frac{(\rho_z/\rho)^{M+1}}{(1-\rho_z/\rho)}\right]. \tag{C38}$$

Note that a more conservative bound can be found in place of the first bound in Eq. (C37) as

$$\textstyle\sum_{m=0}^{M}|T_m(z)| \leqslant \sum_{m=0}^{M}\rho_z^m \leqslant (M+1)\rho_z^M, \tag{C39}$$

which would result in the less tight bound,

$$\mathrm{Err}_1 = 2Q_\rho\left(\frac{\rho_z}{\rho}\right)^M\left[\frac{(M+1)\sqrt{N+1}}{\min(\sigma_T)} + \frac{(\rho_z/\rho)}{(1-\rho_z/\rho)}\right], \tag{C40}$$

instead of Eq. (C38), see Ref. [161], Theorem 6. Reference [161] further proves a lower bound for $\min(\sigma_T)$ in the case of equispaced points $\Lambda_r = -1 + 2r/N$, $r = 0,\ldots,N$ and the oversampling condition $\sqrt{N} \geqslant 2M$. Using Eq. (20) of Ref. [161] into the second equation of Theorem 4 of Ref. [161], the bound reads

$$\min(\sigma_T)^2 \geqslant \frac{1}{25}\left(\frac{N-M^2/2}{2M+1} - \frac{27\sqrt{N}}{32\pi}\right), \tag{C41}$$

which can be inserted in Eq. (C40). The tightness of this bound can be further relaxed (using the second equation of Theorem 3 into the second equation of Theorem 4 of Ref. [161]) to

$$\min(\sigma_T)^2 \geqslant \left[\frac{2N}{125(2M+1)}\right]. \tag{C42}$$

We now compute

$$\mathrm{Err}_2 = \mathbb{E}_{\exp}\left[\left|\sum_{m=0}^{M}[(T^\dagger T)^{-1}T^\dagger\vec{\epsilon}]_m T_m(z)\right|\right]. \tag{C43}$$

First, we give a tight estimation of this term which can be used for numerical analysis. To do this, we just note that

$$\begin{aligned}\mathrm{Err}_2^2 &= \mathbb{E}_{\exp}^2\left[\left|\sum_{m=0}^{M}[(T^\dagger T)^{-1}T^\dagger\vec{\epsilon}]_m T_m(z)\right|\right]\\ &\leqslant \mathbb{E}_{\exp}^2\left[\left|\sum_{j=0}^{N}\epsilon_j\sum_{m=0}^{M}[(T^\dagger T)^{-1}T^\dagger]_{mj}T_m(z)\right|\right]\\ &\leqslant \mathbb{E}_{\exp}\left[\left|\sum_{j=0}^{N}\epsilon_j\sum_{m=0}^{M}[(T^\dagger T)^{-1}T^\dagger]_{mj}T_m(z)\right|^2\right]\\ &\leqslant \mathbb{E}_{\exp}\left[\sum_{j=0}^{N}\epsilon_j^2\sum_{m=0}^{M}|[(T^\dagger T)^{-1}T^\dagger]_{mj}|^2|T_m(z)|^2\right]\\ &\leqslant \sigma^2\sum_{j=0}^{N}\sum_{m=0}^{M}|[(T^\dagger T)^{-1}T^\dagger]_{mj}|^2|T_m(z)|^2,\end{aligned} \tag{C44}$$

which leads to

$$\mathrm{Err}_2^2 \leqslant \sigma_{\exp}^2\sum_{j=0}^{N}\sum_{m=0}^{M}|[(T^\dagger T)^{-1}T^\dagger]_{mj}|^2|T_m(z)|^2. \tag{C45}$$

This relatively tight bound can now be directly numerically evaluated. However, we now go back to Eq. (C43), i.e.,

$$\mathrm{Err}_2 \leqslant \mathbb{E}_{\exp}[||(T^\dagger T)^{-1}T^\dagger\vec{\epsilon}||_\infty]\sum_{m=0}^{M}|T_m(z)|, \tag{C46}$$

with the intention to find an analytical bound. To make progress, we follow Ref. [161], as done throughout the whole section. It is possible to define a projector $P = T(T^\dagger T)^{-1}T^\dagger$ onto the range of T which has the property

$$(T^\dagger T)^{-1}T^\dagger P = (T^\dagger T)^{-1}T^\dagger. \tag{C47}$$

This means that we can write

$$\begin{aligned}\mathbb{E}_{\exp}[\|(T^\dagger T)^{-1}T^\dagger\vec{\epsilon}\|_2]^2 &= \mathbb{E}_{\exp}[\|(T^\dagger T)^{-1}T^\dagger P\vec{\epsilon}\|_2]^2\\ &\leqslant K^2\cdot\mathbb{E}_{\exp}[\|P\vec{\epsilon}\|_2]^2\\ &\leqslant K^2\cdot\mathbb{E}_{\exp}\left[\|P\vec{\epsilon}\|_2^2\right],\end{aligned} \tag{C48}$$

where, in the second step, we used Eq. (G8), and where we defined

$$K^2 = [\|(T^\dagger T)^{-1}T^\dagger\|_2]^2. \tag{C49}$$

We also used $\mathbb{E}_{\exp}[X]^2 \leqslant \mathbb{E}_{\exp}[X^2]$ for a generic random variable X (special case of Jensen's inequality), in the last step. Now, since P projects onto the range R_T of T, we can write

$$\begin{aligned}\mathbb{E}_{\exp}[\|P\vec{\epsilon}\|_2]^2 &= \mathbb{E}_{\exp}\left[\left\|\sum_{\vec{v}\in R_T}|\vec{v}\rangle\langle\vec{v}|\vec{\epsilon}\right\|_2\right]\\ &= \mathbb{E}_{\exp}\left[\left\|\sum_{\vec{v},\vec{v}'\in R_T}\langle\vec{\epsilon}|\vec{v}'\rangle\langle\vec{v}'||\vec{v}\rangle\langle\vec{v}|\vec{\epsilon}\right\|_2\right]\\ &= \mathbb{E}_{\exp}\left[\left\|\sum_{\vec{v}\in R_T}|\langle\vec{\epsilon}|\vec{v}\rangle|^2\right\|\right]\\ &= \mathbb{E}_{\exp}\left[\left\|\sum_{\vec{v}\in R_T}\sum_{j=0}^{N}|\epsilon^j\vec{v}^j|^2\right\|\right]\end{aligned}$$

$$= \sigma_{\text{exp}}^2 \mathbb{E}_{\text{exp}} \left[\left\| \sum_{\vec{v} \in R_T} \sum_{j=0}^{N} |\vec{v}^j|^2 \right\| \right]$$
$$= \sigma_{\text{exp}}^2 \mathbb{E}_{\text{exp}} \left[\left\| \sum_{\vec{v} \in R_T} 1 \right\| \right]$$
$$= (M+1)\sigma_{\text{exp}}^2, \tag{C50}$$

where $\vec{v} \in R_T$ are orthonormal vectors and where we used a notation borrowed from quantum mechanics to indicate vectors and their duals as kets and bras, respectively. Note that, in the last step, we assumed that $M < N$, i.e., that the number of measurements is bigger than the degree of the interpolating polynomial, as it is the regime relevant for us. In that case, since T is a $(N+1) \times (M+1)$ matrix, its rank cannot be bigger than $(M+1)$, justifying the last step.

Using Eq. (C50) into Eq. (C48), we obtain

$$\mathbb{E}_{\text{exp}}[\|(T^\dagger T)^{-1} T^\dagger \vec{\epsilon}\|_2] \leqslant \sigma_{\text{exp}} \sqrt{M+1} \|(T^\dagger T)^{-1} T^\dagger\|_2. \tag{C51}$$

Now, using Eqs. (C31), (C51), and (C34), we obtain

$$\mathbb{E}_{\text{exp}}[\|(T^\dagger T)^{-1} T^\dagger \vec{\epsilon}\|_\infty] \leqslant \sqrt{N+1} E[\|(T^\dagger T)^{-1} T^\dagger \vec{\epsilon}\|_2]$$
$$\leqslant \sigma_{\text{exp}} \frac{\sqrt{N+1}\sqrt{M+1}}{\min(\sigma_T)}. \tag{C52}$$

Now, using Eq. (C14), Eq. (C52), and the first of Eq. (C37) into Eq. (C46), we get

$$\text{Err}_2 \leqslant \sigma_{\text{exp}} \frac{\sqrt{N+1}\sqrt{M+1}}{\min(\sigma_T)} \frac{1-\rho_z^{M+1}}{1-\rho_z}. \tag{C53}$$

Note that, using the bound in Eq. (C39) instead of the one in Eq. (C37) results in the cleaner but less tight bound

$$\text{Err}_2 \leqslant \sigma_{\text{exp}} \frac{\sqrt{N+1}(M+1)^{3/2}}{\min(\sigma_T)} \rho_z^M, \tag{C54}$$

which can be compared to the expression in Ref. [161], Corollary 3.

In summary, we followed Ref. [161] to derive an upper bound for the error made when extrapolating the value $f(z)$ of a function f at a point $z \in \mathbb{C}$ using Chebyshev polynomials (and given a set of noisy data in the interval $[-1, 1]$). This bound explicitly reads

$$\text{Err} \leqslant \text{Err}_1 + \text{Err}_2, \tag{C55}$$

in which Err_1 represents the bias due to the finite order of the extrapolating polynomial and Err_2 represents the effects of uncertainties on the available data. An upper bound for these contributions can be found in Eq. (C40) and Eq. (C54). In particular, Eq. (C40) shows that the bound on the "bias" contribution depends on the properties of the function $f(z)$ over the complex plane (i.e., it is not limited to the extrapolating value) and, as expected, it converges to zero, exponentially in the order of the extrapolating polynomial. This feature is compensated for by the fact that the expression for the "stability" contribution in Eq. (C54) ultimately requires a precision in the estimation of the initial data which scales exponentially in the polynomial order.

We now more clearly specify these results using the notation for the actual analytical continuation procedure outlined in the main text, which we now briefly summarize.

a. Summary of the analytical continuation protocol

The analytical continuation protocol defined in this article focuses on the expectation value $\langle \hat{O}_S \rangle(t, \Lambda)$ of a system observable $\hat{O}_S$ at time t and as a function of a single parameter $\Lambda \in \mathbb{C}$. As shown in Sec. IV, it is possible to define a physical ensemble which allows us to measure the value for the expectation above when $\Lambda \in D_{\text{phys}} = [-1, 1]$. Our ultimate goal is to analytically continue this physical information to estimate $\langle \hat{O}_S \rangle(t, \Lambda_c)$ for a value outside of the physical domain, i.e., for $\Lambda_c = -1 + 2i \notin D_{\text{phys}}$. To achieve this, we simply consider N_{cont} values $\Lambda_n \in D_{\text{phys}}$ and extrapolate the values for the corresponding expectations $\langle \hat{O}_S \rangle(t, \Lambda_n)$ to Λ_c.

We now further present a summary for the error analysis analyzed in this section.

b. Summary of the error analysis

Here we reinterpret the results of this section for the specific notation used in the main part of the article. We do this by writing Eq. (C55) as

$$\text{Err}_{\text{cont}} \leqslant \text{Err}_{\text{bias}} + \text{Err}_{\text{stability}}. \tag{C56}$$

The first contribution to this expression explicitly reads

$$\text{Err}_{\text{bias}} = \inf_{r>1} 2Q_r r^{-M} \left[\sqrt{\frac{5^3 (N_{\text{cont}}+1)(M+1)^3}{N_{\text{cont}}}} + \frac{1}{(r-1)} \right]$$
$$\simeq \inf_{r>1} 2Q_r r^{-M} \left[5^{3/2} (M+1)^{3/2} + \frac{1}{(r-1)} \right], \tag{C57}$$

where we used Eq. (C42) and further bounded the resulting expression. In the last step, we assumed $N_{\text{cont}} \gg 1$, corresponding to tuning the parameters of the experimental setup over a large number of values. Here Q_r represents a bound for $|\langle \hat{O}_S \rangle(t, \Lambda)|$ when Λ is evaluated on a Bernstein ellipse with parameter $r\rho_c$, where ρ_c characterizes the Bernstein ellipse passing through the analytical continuation value Λ_c. Explicitly, we can write

$$Q_r = \sup_{\theta \in [0, 2\pi]} \left| \langle O_S \rangle \left(t, \frac{\rho e^{i\theta} + \rho^{-1} e^{-i\theta}}{2} \right) \right|, \tag{C58}$$

for $\rho = r\rho_c$. Using $\Lambda_c = -1 + 2i$, the explicit expression for the parameter ρ_c can be found by solving Eq. (C12), which leads to $\rho_c \simeq 2.5$.

The second contribution to Eq. (C56) reads

$$\text{Err}_{\text{stability}} \leqslant \sigma_{\text{exp}} \sqrt{\frac{N_{\text{cont}}+1}{N_{\text{cont}}}} 5^{3/2} (M+1)^2 \rho_c^M$$
$$\simeq \sigma_{\text{exp}} 5^{3/2} (M+1)^2 \rho_c^M, \tag{C59}$$

where, as before, we used Eq. (C42), further bounded the resulting expression, and then considered the limit $N_{\text{cont}} \gg 1$. We note that the simplicity of these expressions comes at the price of rather loose bounds. However, the intermediate expressions presented in this section could allow us, in principle, to compute tighter, but less transparent, bounds.

To complete the analytical treatment presented in this section, it is necessary to analyze in more detail both the variance $\sigma^2_{\rm exp}$ quantifying experimental errors (done in Appendix D), and the term Q_r bounding the observable of interest in the complex plane (done in Appendix E).

For the sake of completeness, here we are going to directly use the results derived in Appendixes D and E to give our final estimate for the analytical continuation error in Eq. (C56). First, using Eq. (E15), we find that a bound for the quantity on the right hand-side of Eq. (C58) can be written as

$$\frac{|\langle O_S\rangle(t,\Lambda)|}{\|O_S\|_\infty} \leqslant \exp\left[2\|\hat{s}\|_\infty \int_0^t du \int_{-u}^{u} d\tau \left|C^{\rm unph}_{\rm PM}(t;\Lambda)\right|\right]. \tag{C60}$$

Here we further considered the fact that the extrapolation is done over the open system made by the original (physical) environment and the pseudomode model whose correlation is given in Eq. (B18). We further defined $C^{\rm unph}_{\rm PM}(t;\Lambda)$ as

$$C^{\rm unph}_{\rm PM}(t;\Lambda) = C_{\rm PM}(t;\Lambda) - C_{\rm phys,PM}(t;\Lambda), \tag{C61}$$

where $C_{\rm phys,PM}(t;\Lambda)$ is a physical correlation which minimizes Eq. (C60). We note that any choice which does not minimize such an expression (such as $C_{{\rm phys}(t;\Lambda),{\rm PM}} \to 0$) is also valid while leading to a less-strict bound. In other words, it is always possible to simplify the previous expression by simply substituting $C^{\rm unph}_{\rm PM}(t;\Lambda) \to C_{\rm PM}(t;\Lambda)$.

In parallel, a bound for the variance in Eq. (C59) can be written, using Eq. (D6), as

$$\frac{\sigma^2_{\rm exp}}{\|\hat{O}_S\|^2_\infty} \leqslant \frac{1}{N_{\rm exp}} + \frac{G^2_{\rm class}(t)}{\sqrt{\pi}N_{\rm stoch}}, \tag{C62}$$

where $G_{\rm class}(t)$ is a quantity bounding the stochastic contribution to the error in case a stochastic field is used in the model, and it is explicitly given in Eq. (F14). When the completely deterministic pseudomode model is used, then $G_{\rm class}(t) \to 0$. As a consequence of the law of large numbers, we note that the variance is inversely proportional to the number $N_{\rm exp}$ of independent measurements for the observable $\hat{O}_S$ and the number $N_{\rm stoch}$ of independent samples for the stochastic field.

This concludes the overview on the analysis of the error ${\rm Err}_{\rm cont}$ in Eq. (C56) made when analytically continuing the expectation values for an observable $\hat{O}_S$ as

$$\langle \hat{O}_S\rangle(t;\Lambda_{\rm c}) = p_M(t;\Lambda_{\rm c}) \pm {\rm Err}_{\rm cont}, \tag{C63}$$

where we used Eq. (41) and where the error estimate is given by Eq. (C56).

As promised, in the next two sections, we are going to derive a bound for the experimental variance $\sigma^2_{\rm exp}$, and the quantity Q_r which are required to obtain the results above.

APPENDIX D: EXPERIMENTAL VARIANCE

In this section, we analyze the variance $\sigma^2_{\rm exp}$ appearing in the estimated error for the analytical continuation procedure given in Eq. (C59). While, from an operative point of view, such a variance can always be computed after the measurements, our goal is, here, to provide an *a priori* upper bound. To do this, we can start by analyzing the meaning of the noise appearing in Eq. (C2). Since such expression contains expectation values taken over the system state, one might be tempted to consider the variances,

$$\langle \hat{O}^2_S\rangle(\Lambda_n) - \langle \hat{O}_S\rangle^2(\Lambda_n). \tag{D1}$$

However, this would imply the possibility of completely tracing out the degrees of freedom of the pseudomode model (which, in this case, is physical since, by construction, $\Lambda_n \in D_{\rm phys}$). Unfortunately, whenever the stochastic version of this model is used, a full average over the statistics of the drive $\xi(t)$ introduced in Eq. (A11) is, in general, not possible. To consider this extra source of uncertainty, we can consider

$$\sigma^2_{n,\rm exp} = \langle \hat{O}^2_S\rangle_{S\text{-PM-}\xi}(\Lambda_n) - \langle \hat{O}_S\rangle^2_{S\text{-PM-}\xi}(\Lambda_n), \tag{D2}$$

whose trace is made over the system, pseudomode, and classical degrees of freedom, i.e., $\langle\cdot\rangle_{S\text{-PM-}\xi} = {\rm Tr}_S{\rm Tr}_{\rm PM}\mathbb{E}_\xi[\cdot]$. This expression is conceptually much more interesting than the bare one in Eq. (D1) as, for example, it encodes the fact that the statistics distributed accordingly to the quantum density matrix further depends on Gaussian random variables. In order to properly account for the compound nature of this distribution, we can resort to the law of total variance to write

$$\begin{aligned}\sigma^2_{n,\rm exp} &= \mathbb{E}_\xi {\rm Var}_{S\text{-PM}}[\hat{O}] + {\rm Var}_\xi {\rm Tr}_{S\text{-PM}}[\hat{O}] \\ &= \mathbb{E}_\xi[\langle \hat{O}^2\rangle_{S\text{-PM}} - \langle \hat{O}\rangle^2_{S\text{-PM}}] + {\rm Var}_\xi[\langle \hat{O}\rangle_{S\text{-PM}}],\end{aligned} \tag{D3}$$

in terms of the sum of the variance of $\hat{O}$ in the Hilbert space and the variance over the classical noise. Here we omitted extra dependencies and labels to simplify the notation, and also defined ${\rm Var}_\xi[f(\xi)] = \mathbb{E}_\xi[f^2(\xi) - \mathbb{E}^2_\xi[f(\xi)]]$ for a generic function f of ξ. We can now analyze each term in Eq. (D3) separately. For the first contribution, we can write

$$\mathbb{E}_\xi\left[\langle \hat{O}^2\rangle_{S\text{-PM}} - \langle \hat{O}\rangle^2_{S\text{-PM}}\right] \leqslant \mathbb{E}_\xi[\langle \hat{O}^2\rangle_{S\text{-PM}}] \leqslant \|\hat{O}\|^2_\infty. \tag{D4}$$

Using the law of large numbers, this variance can always be reduced by a factor $N_{\rm exp}$ by considering $N_{\rm exp}$ independent and identically distributed measurements. Estimating an upper bound for the second contribution in Eq. (D3) is a little more complicated. However, this problem has already been analyzed in Ref. [95], whose proof used the ideas previously presented in Ref. [87]. For consistency, in Appendix F, we provide a generalized version for such a proof. Mainly, these derivation show how to bound the variance in terms of a function $G_{\rm class}(t)$ which depends on the "classical" correlation function modeled by $\xi(t)$ and is explicitly given in Eq. (F14).

Overall, using these results, we can write a bound for the variances in Eq. (D2) as

$$\sigma_{n,\rm exp} \leqslant \sigma_{\rm exp}, \tag{D5}$$

where

$$\sigma^2_{\rm exp} \leqslant \frac{\|\hat{O}\|^2_\infty}{N_{\rm exp}} + \frac{\|\hat{O}\|^2_\infty}{\sqrt{\pi}N_{\rm stoch}} G^2_{\rm class}(t). \tag{D6}$$

Here the integers $N_{\rm exp}$ and $N_{\rm stoch}$ simply characterize the number of independent sampling over the measurement of the observable $\hat{O}$ and the field $\xi(t)$. In other words, the full average ${\rm Tr}_S{\rm Tr}_{\rm PM}\mathbb{E}_\xi[\cdot]$ is meant to be computed $N_{\rm exp}N_{\rm stoch}$ times, i.e., for each of the $N_{\rm stoch}$ independent copies of the noise ξ and $N_{\rm exp}$ independent measurements on the underlying quantum system. This concludes the analysis of the terms in Eq. (D3).

In summary, we provided an estimate for an upper bound on the errors on the data, given in Eq. (39), required to define the extrapolating polynomial needed to perform the analytical continuation of the model parameters. In fact, this noise propagates through the extrapolation procedure as described in Appendix C 3 and ultimately contribute to the analytical continuation error as described in Eq. (C59).

In the next section, we analyze a bound on $|\langle \hat{O}_S(t,\Lambda)\rangle|$, in terms of the expectation value over the whole complex plane.

APPENDIX E: A BOUND ON ANALYTICALLY CONTINUED EXPECTATION VALUES

The goal of this section is to analyze the behavior of the function representing the analytical continuation of the expectation value $\langle \hat{O}_S\rangle(t,\Lambda)$ of a system observable $\hat{O}_S$ at time t and in terms of the complex parameter Λ. To do this, we are going to closely follow, and adapt, the analysis given in Refs. [87,95].

We start by defining a decomposition of the correlation function characterizing the effects of an environment on the system in terms of a physical and an unphysical contribution. Specifically, we define a contribution to the correlation as physical when its spectrum is real and positive; see Ref. [90]. This ensures that the corresponding bosonic environment has a real and positive spectral density defined for all frequencies. In turn, this ensures that the interaction between this environment and the system leads to a unitary dynamics. With this definition, any correlation can be decomposed as

$$C(t;\Lambda) = C_{\rm phys}(t;\Lambda) + C_{\rm unph}(t;\Lambda), \tag{E1}$$

where $C_{\rm phys}(t;\Lambda)$ is physical. We further point out that the analytical continuation is operated over the open system made by the original one and the pseudomode model whose parameters are a function of Λ, i.e., the left hand-side of Eq. (E1) reads, explicitly, as in Eq. (B18). In the following, unless explicitly required, we will omit the label Λ so we do not overburden the notation. Thanks to these definitions, we can now interpret the effects of the environment having correlation $C(t)$ as those originating from a composite environment composed by two independent baths U and P having correlations $C_{\rm unph}(t)$ and $C_{\rm phys}(t)$, respectively. We note that this is an adaptation of the ideas presented in Refs. [87,95], where an analogous decomposition is used to estimate the effect of modeling errors. We can further denote the space S' composed of the system and the "physical" environment by $S' \equiv S + P$. Given a system observable $\hat{O}_S$ (and omitting, from now on, the label S when it would overburden the notation), we consider the quantity

$$\Delta O_S(t) = |O_{\rm full}(t) - O_{\rm phys}(t)|, \tag{E2}$$

where $O_{\rm phys}(t)$ is the expectation of $\hat{O}_S$ in the absence of the environment U, i.e.,

$$O_{\rm phys}(t) = {\rm Tr}_{S'}[\hat{O}_S(t)\rho(0)], \tag{E3}$$

where $\rho(0)$ is the initial density matrix in the space S' and where $\hat{O}_S(t)$ evolves with the free dynamics in S'. On the other hand, $O_{\rm full}(t)$ denotes the expectation value in the full space $T \equiv S + P + U = S' + U$. We can now trace out the effects of the environment U to write

$$\Delta O_S(t) = \left|{\rm Tr}_{S'}\hat{O}_S(t)\mathcal{T}e^{\mathcal{F}_{\rm unph}(t)}\rho(0) - {\rm Tr}_{S'}\hat{O}_S(t)\rho(0)\right|, \tag{E4}$$

where $\mathcal{F}_{\rm unph}(t)$ is the influence superoperator dependent on the correlation $C_{\rm unph}(t)$ which explicitly reads

$$\mathcal{F}_{\rm unph}(t) = \int_0^t dt'' \int_0^{t''} dt' \sum_{j=1}^{4} C_j(t'',t')\hat{\hat{s}}_j, \tag{E5}$$

where $C_j(t'',t') = C_{\rm unph}(t''-t')(\delta_{j1}+\delta_{j2}) - C_{\rm unph}(t'-t'')(\delta_{j3}+\delta_{j4})$, and where

$$\begin{aligned}
\hat{\hat{s}}_1(t'',t')[\cdot] &= -\mathcal{S}_2(t'')\mathcal{S}_1(t')[\cdot] = \hat{s}(t')[\cdot]\hat{s}(t'')\\
\hat{\hat{s}}_2(t'',t')[\cdot] &= -\mathcal{S}_2(t')\mathcal{S}_2(t'')[\cdot] = -[\cdot]\hat{s}(t'')\hat{s}(t')\\
\hat{\hat{s}}_3(t'',t')[\cdot] &= \mathcal{S}_1(t')\mathcal{S}_1(t'')[\cdot] = \hat{s}(t')\hat{s}(t'')[\cdot]\\
\hat{\hat{s}}_4(t'',t')[\cdot] &= \mathcal{S}_1(t'')\mathcal{S}_2(t')[\cdot] = -\hat{s}(t'')[\cdot]\hat{s}(t'),
\end{aligned} \tag{E6}$$

in terms of the system coupling operator $\hat{s}$ and where $\mathcal{S}_1(t)[\cdot] = \hat{s}(t)\cdot$, $\mathcal{S}_2(t)[\cdot] = -\cdot\,\hat{s}(t)$. It is worth noting that the time-ordering operator acts on the superoperators $\mathcal{S}$. With these definitions, we can write

$$\begin{aligned}
\Delta O_S(t) &= \left|\sum_{n=1}^{\infty}\frac{1}{n!}{\rm Tr}_{S'}\hat{O}_S(t)\mathcal{T}\mathcal{F}_{\rm unph}^n\rho(0)\right| \leqslant \sum_{n=1}^{\infty}\frac{1}{n!}|{\rm Tr}_{S'}\hat{O}_S(t)\mathcal{T}\mathcal{F}_{\rm unph}^n\rho(0)|\\
&\leqslant \sum_{n=1}^{\infty}\frac{1}{n!}\sum_{j_1,\cdots j_n}\left(\prod_{k=1}^{n}\int_0^t dt_k''\int_0^{t_k''}dt_k'\right)|{\rm Tr}_{S'}\hat{O}_S(t)C_{j_n}(t_n'',t_n')\cdots C_{j_1}(t_1'',t_1')\mathcal{T}\hat{\hat{s}}_{j_n}(t_n'',t_n')\cdots\hat{\hat{s}}_{j_1}(t_1'',t_1')\rho(0)|\\
&= \sum_{n=1}^{\infty}\frac{1}{n!}\sum_{j_1,\cdots j_n}\left(\prod_{k=1}^{n}\int_0^t dt_k''\int_0^{t_k''}dt_k'\right)|C_{j_n}(t_n'',t_n')|\cdots|C_{j_1}(t_1'',t_1')\|{\rm Tr}_{S'}\hat{O}_S(t)\mathcal{T}\hat{\hat{s}}_{j_n}(t_n'',t_n')\cdots\hat{\hat{s}}_{j_1}(t_1'',t_1')\rho(0)|.
\end{aligned} \tag{E7}$$

To proceed, we use the fact that, for bounded operators A and B, it is possible to write ${\rm Tr}[AB] \leqslant \|A\|_\infty\|B\|_1$; see Ref. [170]. This expression can also be considered a special case of the Hölder inequality. Furthermore, since in our case the operators have a unitary evolution, the requirement on the boundness translates to the same assumption for the observable $\hat{O}$ and the coupling operator $\hat{s}$, despite S' being a continuum. We then obtain

$$\Delta O_S(t) \leqslant \sum_{n=1}^{\infty}\frac{1}{n!}\sum_{j_1,\cdots j_n}\left(\prod_{k=1}^{n}\int_0^t dt_k''\int_0^{t_k''}dt_k'\right)|C_{j_n}(t_n'',t_n')|\cdots|C_{j_1}(t_1'',t_1')|\,\|\hat{O}_S\|_\infty\,\|\mathcal{T}\hat{\hat{s}}_{j_n}(t_n'',t_n')\cdots\hat{\hat{s}}_{j_1}(t_1'',t_1')\rho(0)\|_1, \tag{E8}$$

where we further used the unitarity of the norm. An upper bound for the last term in the previous expression can be computed by iteratively using the Hölder inequality $\|AB\|_1 \leqslant \|A\|_\infty \|B\|_1$. In fact, we can explicitly write the operators $\hat{\hat{s}}$ in terms of the superoperators $\mathcal{S}$ which define them and which are time ordered. The resulting expression will then ultimately contain a sequence of $2n$ operators $\hat{s}(\tau)$ (for some $\tau \in [0, t]$) acting either on the left or the right of $\rho(0)$. We can then use the Hölder inequality $2n$ times to write everything in terms of a product of quantities $\|\hat{s}(\tau)\|_\infty$ and $\|\rho(0)\|_1$. By further using the unitarity of the norm, all time dependencies drop, leading to

$$\begin{aligned}\Delta O_S(t) &\leqslant \sum_{n=1}^{\infty} \frac{1}{n!} \sum_{j_1,\cdots j_n} \left(\prod_{k=1}^{n} \int_0^t dt_k'' \int_0^{t_k''} dt_k'\right) |C_{j_n}(t_n'', t_n')| \cdots |C_{j_1}(t_1'', t_1')| \, \|\hat{O}_S\|_\infty \, \|\hat{s}\|_\infty^{2n} \\ &= \sum_{n=1}^{\infty} \frac{\|\hat{O}_S\|_\infty \, \|\hat{s}\|_\infty^{2n}}{n!} \sum_{j_1,\cdots j_n} \left(\prod_{k=1}^{n} \int_0^t dt_k'' \int_0^{t_k''} dt_k'\right) |C_{j_n}(t_n'', t_n')| \cdots |C_{j_1}(t_1'', t_1')|, \end{aligned} \tag{E9}$$

where we used $\|\rho(0)\|_1 = 1$. We also have that

$$\sum_j |C_j(t'', t'')| = 2[|C_{\text{unph}}(t'' - t')| + |C_{\text{unph}}(t' - t'')|], \tag{E10}$$

which leads to

$$\frac{\Delta O_S(t)}{\|\hat{O}_S\|_\infty} \leqslant \exp\left[2\|\hat{s}\|_\infty \int_0^t du \int_{-u}^{u} d\tau |C_{\text{unph}}(\tau)|\right] - 1. \tag{E11}$$

This expression can now be used to bound the quantity $|\langle O_S(t, \Lambda)\rangle|$ on the complex plane using

$$\begin{aligned}|\langle O_S(t, \Lambda)\rangle| &= |O_{\text{full}}(t) + O_{\text{phys}}(t) - O_{\text{phys}}(t)| \\ &\leqslant |O_{\text{phys}}(t)| + \Delta O_S(t). \end{aligned} \tag{E12}$$

We can further use the fact that

$$|O_{\text{phys}}(t)| = |\text{Tr}[O(t)\rho(0)]| \leqslant \|O\|_\infty \|\rho(0)\|_1 = \|O\|_\infty, \tag{E13}$$

where the dynamics is in the $S + P$ space. Using this equation together with Eq. (E11) and Eq. (E12), we finally arrive at

$$\frac{|\langle O_S\rangle(t, \Lambda)|}{\|O_S\|_\infty} \leqslant \exp\left[2\|\hat{s}\|_\infty \int_0^t du \int_{-u}^{u} d\tau |C_{\text{unph}}(\tau; \Lambda)|\right], \tag{E14}$$

whose dependence on the parameter Λ is fully encoded in the unphysical part of the correlation function.

The expression in Eq. (E14) can now be explicitly computed after writing the correlation of the model which we need to analytically continue and decompose it into its physical and unphysical contributions using Eq. (E1). This further allows us to write an optimization version of the previous expression. To do this, we start by defining $\mathcal{D}_{\text{ph}}$ as the domain of functions with positive spectrum so that $C_{\text{ph}}(t) \in \mathcal{D}_{\text{ph}}$. We can then use Eq. (E1) in Eq. (E14) and then interpret the resulting expression as an optimization over any domain $\mathcal{D}$ contained in $\mathcal{D}_{\text{ph}}$, i.e.,

$$\begin{aligned}\frac{|\langle O_S\rangle(t, \Lambda)|}{\|O_S\|_\infty} \leqslant \inf_{\tilde{C}_{\text{ph}} \in \mathcal{D} \subset \mathcal{D}_{\text{ph}}} \exp\Bigg[&2\|\hat{s}\|_\infty \int_0^t du \\ &\times \int_{-u}^{u} d\tau |C(\tau; \Lambda) - \tilde{C}_{\text{ph}}(\tau; \Lambda)|\Bigg], \end{aligned} \tag{E15}$$

since the infimum over a subset is necessarily at least as big as the infimum over the whole space. The convenience of this expression is in the fact that it can be used to generate less strict, but analytically more transparent, upper bounds by choosing an ansatz for $\mathcal{D} \in \mathcal{D}_{\text{ph}}$. This expression can also be used in Eq. (C58) to compute Q_r, thereby concluding this general analysis. However, in order to provide an example, in the next section, we are going to evaluate this equation for a specific case.

1. An explicit example

The goal of this section is to explicitly evaluate the bound in Eq. (E15) for a specific analytical continuation procedure. To do this, we can follow the pseudomode model and assume the original correlation to be well approximated by a sum of decaying exponentials with complex, Λ-dependent coefficients $C^\Lambda(t) = \sum_{j\in J} \lambda_j^2(\Lambda) \exp[-i\Omega_j(\Lambda)t - \Gamma_j(\Lambda)|t|]$ such that $\lambda_j^\Lambda, \Omega_j^\Lambda, \Gamma_j^\Lambda \in \mathbb{C}$ for a set J listing the labels j. In this case, we can choose the optimization domain $\mathcal{D}$ as the one consisting of all functions which can be written as a positive linear combination of exponentials with real frequency and positive decay rate, i.e., such that $\lambda_j^2(\Lambda) > 0$, $\Omega_j(\Lambda) \in \mathbb{R}$, and $\Gamma_j(\Lambda) > 0$. We note that this might correspond to an assumption stronger than needed, since it considers physicality for each individual parameter instead of the overall series. In this case, the observable bound can then be written explicitly as

$$\begin{aligned}&\frac{|\langle O_S\rangle(t, \Lambda)|}{\|O_S\|_\infty} \\ &\leqslant \exp\Bigg[2\|\hat{s}\|_\infty \int_0^t du \int_{-u}^{u} d\tau \\ &\quad\times \left|\sum_{j'\in J'\subset J} \lambda_{j'}^2(\Lambda) \exp[-i\Omega_{j'}(\Lambda)t - \Gamma_{j'}(\Lambda)|t|]\right|\Bigg], \end{aligned} \tag{E16}$$

where the sum is over all $j' \in J' \subset J$ such that at least one of the coefficients $\lambda_{j'}^2(\Lambda)$, $\Omega_{j'}(\Lambda)$, and $\Gamma_{j'}(\Lambda)$ does not satisfy the constraints above.

A notable instance of this example is the case in which the original correlation is decomposed as a linear combination of decaying exponentials with physical frequencies and physical

decay rates, i.e., such that all unphysicalities are restricted to having a complex coupling between the pseudomodes and the system. We note that this includes the examples presented in the main article (for example, the presence of a stochastic drive corresponds to expanding the symmetric part of the correlation in terms of nondecaying exponentials with real frequencies). For clarity, we now further restrict to the case where only one of such unphysical exponential is present and such that the coefficient $\lambda(\Lambda)$, corresponding to the coupling between the pseudomode and the system, is unphysical. In this case, we simply have

$$\frac{|\langle O_S\rangle(t,\Lambda)|}{\|O_S\|_\infty} \leqslant \exp\left[\frac{4\lambda^2_{\rm unph}(\Lambda)\|\hat{s}\|_\infty}{\Gamma^2}(-1+e^{-\Gamma t}+\Gamma t)\right], \tag{E17}$$

in terms of the unphysical coefficient $\lambda^2_{\rm unph}(\Lambda) \equiv \lambda^2(\Lambda) - {\rm Re}[\lambda^2(\Lambda)]\theta({\rm Re}[\lambda^2(\Lambda)])$ corresponding to the fact that, depending on the value of Λ, the parameter $\lambda^2(\Lambda)$ can be either unphysical [so that $\lambda^2_{\rm unph}(\Lambda) \to \lambda^2(\Lambda)$] or physical [so that $\lambda^2_{\rm unph}(\Lambda) \to 0$].

We can now use these results to compute an explicit bound for the quantity Q_r in Eq. (C58). To do this, we further assume the coupling to take the form given in Eq. (32), i.e., $\lambda(\Lambda) = \bar{\lambda}(1+\Lambda)/2$ in terms of a physical frequency scale $\bar{\lambda}$. This case was analyzed in Sec. IV and it is defined in order to allow an analytical continuation of the coupling to an imaginary value to model a contribution to the correlation which is negative at zero time. In other words, the choice above implies that $\lambda(\Lambda_c) = i\bar{\lambda}$. Now, in order to use Eq. (E17) to compute Q_r in Eq. (C58), we need to evaluate $\lambda_{\rm unph}(\Lambda)$ on the Bernstein ellipse with parameter $\rho = r\rho_c$. We can then parametrize this function by ρ and an angle φ specifying the position on the ellipse to write

$$\begin{aligned} A(\rho,\varphi) &\equiv \left|\lambda^2_{\rm unph}(\rho e^{i\varphi}/2 + \rho^{-1}e^{-i\varphi}/2)\right| \\ &\leqslant \bar{\lambda}^2\frac{|4(\rho+\rho^{-1})\cos\varphi + (\rho^2+\rho^{-2})\cos 2\varphi|}{16} \\ &\quad + \bar{\lambda}^2\frac{|4(\rho-\rho^{-1})\sin\varphi + (\rho^2-\rho^{-2})\sin 2\varphi|}{16} \\ &\leqslant \bar{\lambda}^2\frac{3}{4}\frac{4\rho+\rho^2}{4} \leqslant \frac{3\rho_c}{4}\bar{\lambda}^2\left(\frac{\rho}{\rho_c}+1\right)^2 \\ &= \frac{3\rho_c}{4}\bar{\lambda}^2(r+1)^2, \end{aligned} \tag{E18}$$

where ρ_c is the parameter for the Bernstein ellipse passing through the point $\Lambda_c = -1+2i$, which can be evaluated solving Eq. (C12) and which satisfies $\rho_c^2/4 \leqslant 2$. We further made use of the inequality

$$|\alpha+\beta-\theta(\alpha+\beta)(\alpha+\beta)| \leqslant \beta, \tag{E19}$$

when $\alpha > 0$, and also the rather conservative bounds $\rho + \rho^{-1} < 2\rho$ and $\rho - \rho^{-1} < \rho$ since $\rho > 1$. We can now use this result in Eq. (E17) to finally obtain

$$Q_r \leqslant \|O(t)\|_\infty \exp\left[6\bar{\lambda}^2\|\hat{s}\|_\infty(r+1)^2\rho_c\frac{e^{-t\Gamma}-1+t\Gamma}{\Gamma^2}\right]. \tag{E20}$$

It is perhaps more elegant to express these results in terms of the total relative error,

$$\epsilon = {\rm Err}/\|\hat{O}\|_\infty, \tag{E21}$$

as

$$\epsilon = \epsilon_{\rm bias} + \epsilon_{\rm stability}, \tag{E22}$$

where, using the notation in Eq. (C56),

$$\epsilon_{\rm bias} = {\rm Err}_{\rm bias}/\|\hat{O}\|_\infty\,,\ \epsilon_{\rm stability} = {\rm Err}_{\rm stability}/\|\hat{O}\|_\infty\,. \tag{E23}$$

The "bias" and "stability" contribution to the relative error above can be written, more explicitly, using Eq. (E20) in Eq. (C57) and Eq. (D6) in Eq. (C59), to find

$$\begin{aligned} \epsilon_{\rm stability} &\leqslant \sqrt{\frac{1}{N_{\rm exp}} + \frac{G^2_{\rm class}(t)}{\sqrt{\pi}N_{\rm stoch}}}\,5^{3/2}(M+1)^2\rho_c^M \\ \epsilon_{\rm bias} &\leqslant \inf_{r>1}\frac{2e^{6\alpha_{\rm compl}(r+1)^2\rho_c}}{r^M}\left[5^{3/2}(M+1)^{3/2} + \frac{1}{r-1}\right], \end{aligned} \tag{E24}$$

in terms of the "complexity" parameter,

$$\alpha_{\rm compl} = \bar{\lambda}^2\|\hat{s}\|_\infty\frac{e^{-t\Gamma}-1+t\Gamma}{\Gamma^2} \leqslant t\bar{\lambda}^2\|\hat{s}\|_\infty/\Gamma, \tag{E25}$$

which encodes the information about the physical quantities involved, i.e., the time t, the pseudomode decay rate Γ, the overall strength $\bar{\lambda}$ of the pseudomode-system interaction, and the norm of the system interaction operator $\hat{s}$. Because of its adimensionality and its critical influence on the scaling of the error, it can be used to intuitively characterize the "complexity" of the extrapolating the effects of the environment on the system.

As a final note, we mention that the parameters in the expression for $\alpha_{\rm compl}$ should, through the pseudomode mapping, be expressed in terms of the parameter characterizing the original open quantum system. This could ultimately allow us to further analyze how the complexity of the task scales in terms of physical parameters such as the system size.

APPENDIX F: STOCHASTIC ERROR

In this subsection, we consider a stochastic version of the pseudomode model and adapt the proofs in Refs. [87,95] to estimate the stochastic error

$$\Delta_{\rm stoch}O(t) = \mathbb{E}[|\langle O^\xi(t;N_{\rm stoch})\rangle - \mathbb{E}[\langle O^\xi(t;N_{\rm stoch})\rangle]|]. \tag{F1}$$

Using Jensen inequality, this error satisfies

$$\Delta_{\rm stoch}O(t) \leqslant \sqrt{{\rm Var}_\xi[O^\xi(t;N_{\rm stoch})]}, \tag{F2}$$

i.e., it can be bounded by the square root of the variance of the random variable $\langle O^\xi(t;N_{\rm stoch})\rangle$, defined as

$${\rm Var}_\xi[O^\xi(t)] = \mathbb{E}[\langle O^\xi(t)\rangle^2] - \mathbb{E}^2[\langle O^\xi(t)\rangle], \tag{F3}$$

in which we omitted the dependency on $N_{\rm stoch}$ for clarity.

In order to analyze this variance in more detail, it is useful to distinguish among three different effects: the ones

originating from the stochastic field, the ones from physical environments, and the ones from unphysical ones. In fact, before tracing them out, physical environments produce unitary dynamics, whose effects are more easily bounded. This is not true for unphysical environments which, for this reason, require more care. Furthermore, the full dependence of the expectation value on the noise has to be carried over the calculation.

After these intuitive considerations, we proceed by defining S' as the system plus all physical environments. The effects of unphysical environments are, instead, encoded in the corresponding influence superoperator $\mathcal{F}(t,\hat{s},C_{\text{unphys}}(t))$, dependent on the correlation $C_{\text{unphys}}(t)$. For clarity, in the following we will omit the dependence of this superoperator on its arguments and replace it with $\mathcal{F}_{\text{unphys}}$ instead. In this setting, we can write

$$\begin{aligned}\langle\hat{O}^{\xi}(t;N_{\text{stoch}})\rangle &= \frac{1}{N_{\text{stoch}}}\sum_{j=1}^{N_{\text{stoch}}}\text{Tr}_{S'}\left[\hat{O}(t)\mathcal{T}e^{-i\int_0^t d\tau\xi^j(\tau)\hat{s}^{\times}(\tau)}e^{\mathcal{F}(t,\hat{s},C_{\text{unphys}}(t))}\rho_S(0)\right]\\ &= \frac{1}{N_{\text{stoch}}}\sum_{j=1}^{N_{\text{stoch}}}\sum_{n=0}^{\infty}\frac{(-i)^n}{n!}\int_0^t dt_1\cdots\int_0^t dt_n\xi^j(t_1)\cdots\xi^j(t_n)\text{Tr}_{S'}[\hat{O}(t)\mathcal{T}s^{\times}(t_1)\cdots s^{\times}(t_n)e^{\mathcal{F}_{\text{unphys}}}\rho_{S'}(0)],\end{aligned}\tag{F4}$$

and the corresponding version for its square as

$$\begin{aligned}\langle\hat{O}^{\xi}(t;N_{\text{stoch}})\rangle^2 &= \sum_{n,m}\frac{(-i)^{n+m}}{n!\,m!}\int_0^t dt_1\cdots\int_0^t dt_n\int_0^t d\tau_1\cdots\int_0^t d\tau_m\frac{1}{N_{\text{stoch}}^2}\sum_{j,k}\xi^j(t_1)\cdots\xi^j(t_n)\xi^k(\tau_1)\cdots\xi^k(\tau_m)\\ &\times\text{Tr}_{S'}[\hat{O}(t)\mathcal{T}s^{\times}(t_1)\cdots s^{\times}(t_n)e^{\mathcal{F}_{\text{unphys}}}\rho_{S'}(0)]\text{Tr}_{S'}[\hat{O}(t)\mathcal{T}s^{\times}(\tau_1)\cdots s^{\times}(\tau_m)e^{\mathcal{F}_{\text{unphys}}}\rho_{S'}(0)].\end{aligned}\tag{F5}$$

Using these expression, a bound for the stochastic error can be written as

$$\begin{aligned}\Delta^2_{\text{stoch}}O(t) &\leqslant \mathbb{E}[\langle O^{\xi}(t;N_{\text{stoch}})\rangle^2]-\mathbb{E}^2[\langle O^{\xi}(t)\rangle]\\ &= \sum_{n,m}\frac{(-i)^{n+m}}{n!\,m!}\int_0^t dt_1\cdots\int_0^t dt_n\int_0^t d\tau_1\cdots\int_0^t d\tau_m\\ &\times\frac{1}{N_{\text{stoch}}^2}\sum_{j,k}\{\mathbb{E}[\xi^j(t_1)\cdots\xi^j(t_n)\xi^k(\tau_1)\cdots\xi^k(\tau_n)]-\mathbb{E}[\xi^j(t_1)\cdots\xi^j(t_n)]\mathbb{E}[\xi^k(\tau_1)\cdots\xi^k(\tau_n)]\}\\ &\times\text{Tr}_{S'}[\hat{O}(t)\mathcal{T}s^{\times}(t_1)\cdots s^{\times}(t_n)e^{\mathcal{F}_{\text{unphys}}}\rho_{S'}(0)]\text{Tr}_{S'}[\hat{O}(t)\mathcal{T}s^{\times}(\tau_1)\cdots s^{\times}(\tau_m)e^{\mathcal{F}_{\text{unphys}}}\rho_{S'}(0)].\end{aligned}\tag{F6}$$

We can now note that the contractions which do not mix the indexes j and k will simply reproduce, and simplify with, the product of the expectation. The nontrivial part for the expression above is in fact the one containing at least one contraction between the indexes j and k. Since ξ^j and ξ^k are independent for $j\neq 0$, such a contraction will impose a δ_{jk}. This is simply a manifestation of the law of large number which leads to

$$\begin{aligned}\Delta^2_{\text{stoch}}O(t) &\leqslant \frac{1}{N_{\text{stoch}}}\sum_{n,m}\frac{(-i)^{n+m}}{n!\,m!}\int_0^t dt_1\cdots\int_0^t dt_n\int_0^t d\tau_1\cdots\int_0^t d\tau_m\tilde{\mathbb{E}}[\xi(t_1)\cdots\xi(t_n)\xi(\tau_1)\cdots\xi(\tau_n)]\\ &\times\text{Tr}_{S'}[\hat{O}(t)\mathcal{T}s^{\times}(t_1)\cdots s^{\times}(t_n)e^{\mathcal{F}_{\text{unphys}}}\rho_{S'}(0)]\text{Tr}_{S'}[\hat{O}(t)\mathcal{T}s^{\times}(\tau_1)\cdots s^{\times}(\tau_m)e^{\mathcal{F}_{\text{unphys}}}\rho_{S'}(0)],\end{aligned}\tag{F7}$$

where we used the symbol $\tilde{\mathbb{E}}$ to signify the constraint that at least one of the contractions is between the fields indexed by the times t and τ. We now are going to adopt rather drastic bounds. The first consists in taking the absolute value and then write

$$\begin{aligned}\left|\Delta^2_{\text{stoch}}O(t)\right| &\leqslant \frac{1}{N_{\text{stoch}}}\sum_{n,m}\frac{1}{n!\,m!}\int_0^t dt_1\cdots\int_0^t dt_n\int_0^t d\tau_1\cdots\int_0^t d\tau_m|\tilde{\mathbb{E}}[\xi(t_1)\cdots\xi(t_n)\xi(\tau_1)\cdots\xi(\tau_n)]|\\ &\times|\text{Tr}_{S'}[\hat{O}(t)\mathcal{T}s^{\times}(t_1)\cdots s^{\times}(t_n)e^{\mathcal{F}_{\text{unphys}}}\rho_{S'}(0)]||\text{Tr}_{S'}[\hat{O}(t)\mathcal{T}s^{\times}(\tau_1)\cdots s^{\times}(\tau_m)e^{\mathcal{F}_{\text{unphys}}}\rho_{S'}(0)]|.\end{aligned}\tag{F8}$$

We can now take some time to analyze different terms in Eq. (F8). For example, using the upper bound in Eq. (F23) proven in Appendix F 1, we can write

$$|\text{Tr}_{S'}[\hat{O}(t)\mathcal{T}s^{\times}(t_1)\cdots s^{\times}(t_n)e^{\mathcal{F}_{\text{unphys}}}\rho_{S'}(0)]|\leqslant||\hat{O}||_{\infty}||2\hat{s}||_{\infty}^n\exp\left[2||\hat{s}||_{\infty}\int_0^t du\int_{-u}^{u}d\tau|C_{\text{unphys}}(\tau)|\right].\tag{F9}$$

We now consider the term

$$|\tilde{\mathbb{E}}[\xi(t_1)\cdots\xi(t_n)\xi(\tau_1)\cdots\xi(\tau_m)]|,\tag{F10}$$

which can always be expressed as the product of $(n+m)/2$ correlations C_{class} (when $n+m$ is even, otherwise it is zero) thanks to Wick's theorem. For simplicity, we will further loose the bound by overcounting all the possible contractions

$(n+m-1)!! - (n-1)!!(m-1)!!$, i.e., not imposing the constraint defined by the symbol $\tilde{\mathbb{E}}$. In this context, we can further note that

$$(n+m-1)!! \leqslant \frac{2^{(n+m)/2}}{\sqrt{\pi}}\sqrt{\Gamma(n+1)\Gamma(m+1)}. \tag{F11}$$

Using these considerations, together with Eq. (F9) and Eq. (F11), into Eq. (F8), we then obtain

$$\begin{aligned}\left|\Delta^2_{\text{stoch}}O(t)\right| \leqslant \frac{||\hat{O}||^2_\infty e^{4||\hat{s}||_\infty \int_0^t du \int_{-u}^u d\tau |C_{\text{unphys}}(\tau)|}}{N_{\text{stoch}}} \widetilde{\sum_{n,m}} \frac{1}{n!\,m!}\left[\frac{2^{(n+m)/2}}{\sqrt{\pi}}\sqrt{\Gamma(n+1)\Gamma(m+1)} - (n-1)!!(m-1)!!\right] \\ \times\left[\int_0^t dt_1 \int_0^t dt_2 |C_{\text{class}}(t_2,t_1)|\right]^{(n+m)/2} ||2\hat{s}||^n_\infty ||2\hat{s}||^m_\infty,\end{aligned} \tag{F12}$$

where $\widetilde{\sum}_{n,m}$ indicates that we should only sum terms such that $n+m$ is even. We can obtain a more readable, but considerably less tight, bound by replacing this sum with an unconstrained one and neglecting the negative term to write

$$\begin{aligned}\left|\Delta^2_{\text{stoch}}O(t)\right| &\leqslant \frac{||\hat{O}||^2_\infty e^{4||\hat{s}||_\infty \int_0^t du \int_{-u}^u d\tau |C_{\text{unphys}}(\tau)|}}{\sqrt{\pi}N_{\text{stoch}}} \sum_{n,m} \frac{||2\hat{s}||^{n+m}_\infty 2^{(n+m)/2}}{\sqrt{n!}\sqrt{m!}}\left[\int_0^t dt_1 \int_0^t dt_2 |C_{\text{class}}(t_2,t_1)|\right]^{(n+m)/2} \\ &= \frac{||\hat{O}||^2_\infty e^{4||\hat{s}||_\infty \int_0^t du \int_{-u}^u d\tau |C_{\text{unphys}}(\tau)|}}{\sqrt{\pi}N_{\text{stoch}}} G^2_{\text{class}}(t),\end{aligned} \tag{F13}$$

where we defined

$$\begin{aligned}G_{\text{class}}(t) &\equiv \sum_n \frac{2^n||\hat{s}||^n_\infty}{\sqrt{n!}}\left[2\int_0^t dt_1 \int_0^t dt_2 |C_{\text{class}}(t_2,t_1)|\right]^{n/2} \\ &= \sum_n \frac{2^n||\hat{s}||^n_\infty}{\sqrt{n!}}\left[2\int_0^t du \int_{-u}^u dt |C_{\text{class}}(t)|\right]^{n/2}.\end{aligned} \tag{F14}$$

It is interesting to note that the stochastic error depends not only on the classical part of the correlation [which in turn defines the stochastic drive $\xi(t)$] but also on the unphysical part of the correlation of the model. In other words, the task of averaging over a stochastic-driven pseudomode model can become more difficult whenever its complementary quantum part has unphysical parameters. In fact, this corresponds to the intuition that a stochastic unphysical dynamics is more difficult to average out than a physical one because it can explore larger, nonphysically constrained spaces.

1. An upper bound

This technical subsection (following the general gist of Appendix E), explicitly derives the upper bound used in Eq. (F9) for the term

$$A_m = |\text{Tr}_{S'}[\hat{O}_S(t)\mathcal{T}s^\times(t_1)\cdots s^\times(t_m)e^{\mathcal{F}_{\text{unphys}}}\rho_{S'}(0)]|. \tag{F15}$$

Here $\mathcal{F}_{\text{unph}}(t)$ is the influence superoperator dependent on the correlation $C_{\text{unph}}(t)$, which explicitly reads

$$\mathcal{F}_{\text{unph}}(t) = \int_0^t dt'' \int_0^{t''} dt' \sum_{j=1}^4 C_j(t'',t')\hat{\hat{s}}_j, \tag{F16}$$

where $C_j(t'',t') = C_{\text{unph}}(t''-t')(\delta_{j1}+\delta_{j2}) - C_{\text{unph}}(t'-t'')(\delta_{j3}+\delta_{j4})$ and where

$$\begin{aligned}\hat{\hat{s}}_1(t'',t')[\cdot] &= -\mathcal{S}_2(t'')\mathcal{S}_1(t')[\cdot] = s(t')[\cdot]s(t'') \\ \hat{\hat{s}}_2(t'',t')[\cdot] &= -\mathcal{S}_2(t')\mathcal{S}_2(t'')[\cdot] = -[\cdot]s(t'')s(t') \\ \hat{\hat{s}}_3(t'',t')[\cdot] &= \mathcal{S}_1(t')\mathcal{S}_1(t'')[\cdot] = s(t')s(t'')[\cdot] \\ \hat{\hat{s}}_4(t'',t')[\cdot] &= \mathcal{S}_1(t'')\mathcal{S}_2(t')[\cdot] = -s(t'')[\cdot]s(t'),\end{aligned} \tag{F17}$$

with $\mathcal{S}_1(t)[\cdot] = s(t)\cdot$, $\mathcal{S}_2(t)[\cdot] = -\cdot s(t)$. It is worth noting that the time-ordering operator acts on the superoperators $\mathcal{S}$. With these definitions, we can write

$$\begin{aligned}A_m &= \left|\sum_{n=0}^\infty \frac{1}{n!}\text{Tr}_{S'}\hat{O}_S(t)\mathcal{T}s^\times(t_1)\cdots s^\times(t_m)\mathcal{F}^n_{\text{unph}}\rho(0)\right| \\ &\leqslant \sum_{n=0}^\infty \frac{1}{n!}|\text{Tr}_{S'}\hat{O}_S(t)\mathcal{T}s^\times(t_1)\cdots s^\times(t_m)\mathcal{F}^n_{\text{unph}}\rho(0)|,\end{aligned} \tag{F18}$$

by the triangle inequality. We can proceed as

$$\begin{aligned}A_m &\leqslant \sum_{n=0}^\infty \frac{1}{n!}\sum_{j_1,\cdots j_n}\left(\prod_{k=1}^n \int_0^t dt''_k \int_0^{t''_k} dt'_k\right)\left|\text{Tr}_{S'}\hat{O}_S(t)C_{j_n}(t''_n,t'_n)\cdots C_{j_1}(t''_1,t'_1)\mathcal{T}\{[s^\times(t_1)\cdots s^\times(t_m)]\hat{\hat{s}}_{j_n}(t''_n,t'_n)\cdots\hat{\hat{s}}_{j_1}(t''_1,t'_1)\rho(0)\}\right| \\ &= \sum_{n=1}^\infty \frac{1}{n!}\sum_{j_1,\cdots j_n}\left(\prod_{k=1}^n \int_0^t dt''_k \int_0^{t''_k} dt'_k\right)\left|C_{j_n}(t''_n,t'_n)\right|\cdots\left|C_{j_1}(t''_1,t'_1)\right|\left|\text{Tr}_{S'}\hat{O}_S(t)\mathcal{T}\{[s^\times(t_1)\cdots s^\times(t_m)]\hat{\hat{s}}_{j_n}(t''_n,t'_n)\cdots\hat{\hat{s}}_{j_1}(t''_1,t'_1)\rho(0)\}\right|.\end{aligned} \tag{F19}$$

Repeating the considerations done in Appendix E, we can now use the fact that, for bounded operators A and B, $|\mathrm{Tr}[AB]| \leqslant ||A||_\infty ||B||_1$, see Ref. [170] and which can also be considered as a special case of the Hölder inequality. In this case, since the operators evolve unitarily within a physical dynamics, this results in assuming the boundness for the observable O and the coupling operator s despite S' being a very large space. We then obtain

$$A_m \leqslant \sum_{n=0}^{\infty} \frac{1}{n!} \sum_{j_1,\cdots j_n} \left(\prod_{k=1}^{n} \int_0^t dt_k'' \int_0^{t_k''} dt_k' \right) \left| C_{j_n}(t_n'', t_n') \right| \cdots \left| C_{j_1}(t_1'', t_1') \right| \, ||\hat{O}_S||_\infty ||\mathcal{T}[s^\times(t_1) \cdots s^\times(t_m)] \hat{\hat{s}}_{j_n}(t_n'', t_n') \cdots \hat{\hat{s}}_{j_1}(t_1'', t_1') \rho(0)||_1, \tag{F20}$$

where we further used the fact the unitarity of the norm. An upper bound for the last term in the previous expression can be computed by iteratively using the Hölder inequality $||AB||_1 \leqslant ||A||_\infty ||B||_1$. In fact, we can explicitly write the operators $\hat{\hat{s}}$ in terms of the superoperators $\mathcal{S}$ which define them. These superoperators will then be ordered by time-ordering operator. We can then write the superoperators $\hat{\hat{s}}$ in terms of operators $s(\tau)$ (for some $\tau \in [0, t]$) acting either on the left or the right of $\rho(0)$. We can then use the Hölder inequality $2n$ times to write everything in terms of a product of quantities $||s(\tau)||_\infty$ and $||\rho(0)||_1$. By further using the unitarity of the norm, such a product is going to be a time-independent bound leading to

$$\begin{aligned} A_m &\leqslant ||2s||_\infty^m \sum_{n=0}^{\infty} \frac{1}{n!} \sum_{j_1,\cdots j_n} \left(\prod_{k=1}^{n} \int_0^t dt_k'' \int_0^{t_k''} dt_k' \right) \left| C_{j_n}(t_n'', t_n') \right| \cdots \left| C_{j_1}(t_1'', t_1') \right| \, ||\hat{O}_S||_\infty \, ||s||_\infty^{2n} \\ &= ||2s||_\infty^m \sum_{n=0}^{\infty} \frac{||\hat{O}_S||_\infty \, ||s||_\infty^{2n}}{n!} \sum_{j_1,\cdots j_n} \left(\prod_{k=1}^{n} \int_0^t dt_k'' \int_0^{t_k''} dt_k' \right) \left| C_{j_n}(t_n'', t_n') \right| \cdots \left| C_{j_1}(t_1'', t_1') \right|, \end{aligned} \tag{F21}$$

where we used $||\rho(0)||_1 = 1$. We also have that

$$\sum_j |C_j(t'', t'')| = 2[|C_{\mathrm{unph}}(t'' - t')| + |C_{\mathrm{unph}}(t' - t'')|], \tag{F22}$$

which leads to

$$\begin{aligned} A_m &\leqslant ||2s||_\infty^m ||\hat{O}_S(t)||_\infty \\ &\quad \times \exp\left[2||s||_\infty \int_0^t du \int_{-u}^{u} d\tau |C_{\mathrm{unph}}(\tau)| \right], \end{aligned} \tag{F23}$$

which is the expression used in Eq. (F9).

APPENDIX G: USEFUL DEFINITIONS AND IDENTITIES

Here we present identities which are used in other sections.

1. Definitions and identities on norms

The vector space $\mathbb{C}^n$ can be endowed with norms such that

$$||\vec{v}||_n = \left(\sum_i |v_i|^n \right)^{1/n} \qquad ||\vec{v}||_\infty = \max(|v_i|), \tag{G1}$$

where $\vec{v} \in \mathbb{C}^n$. All the norms above are equivalent for a finite-dimensional vector space. We consider, specifically, the following properties:

$$||\vec{v}||_1 = \sqrt{\left(\sum_i |v_i| \right)^2} \leqslant \sqrt{n \sum_i v_i^2} = \sqrt{n} \, ||\vec{v}||_2, \tag{G2}$$

where to derive the second step, we used the Holder inequality

$$|x^T y| \leqslant ||x||_p ||y||_q, \tag{G3}$$

for $1/p + 1/q = 1$ (the case $p = q = 2$ being the Cauchy-Schwartz inequality). We have

$$\begin{aligned} \left(\sum_{i=1}^{n} x_i \right)^2 &= \left(\sum_{i=1}^{n} 1 \cdot x_i \right)^2 = |x^T \vec{1}|^2 \\ &\leqslant ||x||_2^2 ||\vec{1}||_2^2 = n^2 \sum_{i=1}^{n} x_i^2, \end{aligned} \tag{G4}$$

where $\vec{1}$ is a reference vector whose entries are all ones. We note that this identity has been used in Eq. (G2). We also have

$$||\vec{v}||_\infty = \max |v_i| \leqslant \sum_i |v|_i = ||\vec{v}||_1, \tag{G5}$$

which, together with Eq. (G2) implies

$$||\vec{v}||_\infty \leqslant \sqrt{n} ||\vec{v}||_2. \tag{G6}$$

The definitions above regarding the vector spaces $\mathbb{C}^n$ can be used to define induced norms in the vector space of operators $A : \mathbb{C}^q \to \mathbb{C}^p$ as

$$||A||_n = \sup_{\vec{x} \neq 0} \frac{||A\vec{x}||_n}{||\vec{x}||_n} = \sup_{||\vec{x}||_n = 1} ||A\vec{x}||_n. \tag{G7}$$

Note that it is possible to extend the previous definition to $n \to \infty$. Note that, when $||\vec{x}||_n \neq 0$, the previous definition implies

$$||A||_n ||\vec{x}||_n \geqslant ||A\vec{x}||_n. \tag{G8}$$

It is interesting to explicitly compute $||A||_2$. To do this, we notice that A can be represented by a $p \times q$ matrix A_{pq} which, using singular value decomposition, can be written as $A_{p\times q} = V_{p\times p} \Sigma_{p\times q} U_{q\times q}$ in terms of unitary matrices V and U and an

upper diagonal Σ. We have

$$\begin{aligned}||A||_2 &= \sup_{||\vec{x}||_2=1} ||A\vec{x}||_2 = \sup_{||\vec{x}||_2=1} ||V\Sigma(U\vec{x})||_2 \\ &= \sup_{||\vec{x}'||_2=1} ||V\Sigma\vec{x}'||_2 = (\max\sigma_A) \sup_{||\vec{x}'||_2=1} ||V\vec{x}'||_2 \\ &= \max\sigma_A, \end{aligned} \tag{G9}$$

where σ_A are the singular values of the matrix A (square root of the eigenvalues of $A^\dagger A$).

Note that other choices of norms for operators are possible such as the Shatten norms,

$$||A||_n^S = [\mathrm{tr}(|A|^n)]^{1/n}, \tag{G10}$$

where $|A| = \sqrt{A^\dagger A}$. For future reference, we also write here the following identities:

$$\sum_{n=0}^{A} r^n = \frac{1-r^{A+1}}{1-r}, \quad \sum_{n=A}^{\infty} r^n = \frac{r^A}{1-r}, \tag{G11}$$

with $|r| < 1$ for the second identity to hold.

2. Least squares

We want to define the best estimate for a vector $\vec{c} \in \mathbb{C}^q$ such that its image under a linear mapping $T : \mathbb{C}^q \mapsto \mathbb{C}^p$ is as close as possible to a given vector $\vec{f} \in \mathbb{C}^p$ under the $||\cdot||_2$ norm. Equivalently, we want to find the vector $\vec{c}$ which minimizes the function

$$L = ||T\vec{c} - \vec{f}||_2^2. \tag{G12}$$

We have

$$\begin{aligned} L &= (T\vec{c} - \vec{f})^\dagger (T\vec{c} - \vec{f}) \\ &= \sum_{i,j,k} (T_{ij}^* c_j^* - f_i^*)(T_{ik}c_k - f_i), \end{aligned} \tag{G13}$$

which allows us to write

$$\begin{aligned} \partial_{c_\alpha} L &= \sum_{i,j} (T_{ij}^* c_j^* - f_i^*) T_{i\alpha} \\ \partial_{c_\alpha^*} L &= \sum_{i,k} T_{i\alpha}^* (T_{ik}c_k - f_i). \end{aligned} \tag{G14}$$

The equations $\partial_{c_\alpha} L = 0$ and $\partial_{c_\alpha^*} L = 0$ are equivalent and lead to

$$T^\dagger T\vec{c} = T^\dagger \vec{f}. \tag{G15}$$

When $T^\dagger T$ is invertible, this leads to

$$\vec{c} = (T^\dagger T)^{-1} T^\dagger \vec{f}, \tag{G16}$$

which is the explicit expression for the vector $\vec{c}$ minimizing the least-squares distance L in Eq. (G12).

[1] H.-P. Breuer and F. Petruccione, *The Theory of Open Quantum Systems* (Oxford University Press, Oxford, 2002).

[2] C. Gardiner and P. Zoller, *Quantum Noise: A Handbook of Markovian and Non-Markovian Quantum Stochastic Methods with Applications to Quantum Optics* (Springer Science, New York, 2004).

[3] T. Holstein, Studies of polaron motion: Part I. The molecular-crystal model, Ann. Phys. **8**, 325 (1959).

[4] T. Holstein, Studies of polaron motion: Part II. The "small" polaron, Ann. Phys. **8**, 343 (1959).

[5] B. Jackson and R. Silbey, On the calculation of transfer rates between impurity states in solids, J. Chem. Phys. **78**, 4193 (1983).

[6] R. Silbey and R. A. Harris, Variational calculation of the dynamics of a two level system interacting with a bath, J. Chem. Phys. **80**, 2615 (1984).

[7] R. A. Harris and R. Silbey, Variational calculation of the tunneling system interacting with a heat bath. II. Dynamics of an asymmetric tunneling system, J. Chem. Phys. **83**, 1069 (1985).

[8] U. Weiss, *Quantum Transport Theory* (World Scientific, Singapore, 2008).

[9] S. Jang, Y.-C. Cheng, D. R. Reichman, and J. D. Eaves, Theory of coherent resonance energy transfer, J. Chem. Phys. **129**, 101104 (2008).

[10] S. Jang, Theory of coherent resonance energy transfer for coherent initial condition, J. Chem. Phys. **131**, 164101 (2009).

[11] A. Nazir, Correlation-dependent coherent to incoherent transitions in resonant energy transfer dynamics, Phys. Rev. Lett. **103**, 146404 (2009).

[12] D. P. S. McCutcheon and A. Nazir, On the calculation of transfer rates between impurity states in solids, New J. Phys. **12**, 113042 (2010).

[13] S. Jang, Theory of multichromophoric coherent resonance energy transfer: A polaronic quantum master equation approach, J. Chem. Phys. **135**, 034105 (2011).

[14] D. P. S. McCutcheon and A. Nazir, Coherent and incoherent dynamics in excitonic energy transfer: Correlated fluctuations and off-resonance effects, Phys. Rev. B **83**, 165101 (2011).

[15] A. Kolli, A. Nazir, and A. Olaya-Castro, Electronic excitation dynamics in multichromophoric systems described via a polaron-representation master equation, J. Chem. Phys. **135**, 034105 (2011).

[16] F. A. Pollock, D. P. S. McCutcheon, E. M. Lovett, B. W. Gauger, and A. Nazir, A multi-site variational master equation approach to dissipative energy transfer, New J. Phys. **15**, 075018 (2013).

[17] F. Pollock, Energy transport in open quantum systems, Ph.D. thesis, Oxford University, UK, 2014.

[18] D. Xu and J. Cao, Non-canonical distribution and non-equilibrium transport beyond weak system-bath coupling regime: A polaron transformation approach, Front. Phys. **11**, 110308 (2016).

[19] A. W. Chin, A. Rivas, S. F. Huelga, and M. B. Plenio, Exact mapping between system-reservoir quantum models and semi-infinite discrete chains using orthogonal polynomials, J. Math. Phys. **51**, 092109 (2010).

[20] J. Prior, A. W. Chin, S. F. Huelga, and M. B. Plenio, Efficient simulation of strong system-environment interactions, Phys. Rev. Lett. **105**, 050404 (2010).

[21] M. P. Woods, R. Groux, A. W. Chin, S. F. Huelga, and M. B. Plenio, Mappings of open quantum systems onto chain representations and Markovian embeddings, J. Math. Phys. **55**, 032101 (2014).

[22] A. Nüßeler, I. Dhand, S. F. Huelga, and M. B. Plenio, Efficient simulation of open quantum systems coupled to a Fermionic bath, Phys. Rev. B **101**, 155134 (2020).

[23] M. Brenes, J. J. Mendoza-Arenas, A. Purkayastha, M. T. Mitchison, S. R. Clark, and J. Goold, Tensor-network method to simulate strongly interacting quantum thermal machines, Phys. Rev. X **10**, 031040 (2020).

[24] A. D. Somoza, O. Marty, J. Lim, S. F. Huelga, and M. B. Plenio, Dissipation-assisted matrix product factorization, Phys. Rev. Lett. **123**, 100502 (2019).

[25] F. Mascherpa, A. Smirne, A. D. Somoza, P. Fernández-Acebal, S. Donadi, D. Tamascelli, S. F. Huelga, and M. B. Plenio, Optimized auxiliary oscillators for the simulation of general open quantum systems, Phys. Rev. A **101**, 052108 (2020).

[26] M. Cirio, N. Lambert, P. Liang, P.-C. Kuo, Y.-N. Chen, P. Menczel, K. Funo, and F. Nori, Pseudofermion method for the exact description of fermionic environments: From single-molecule electronics to the Kondo resonance, Phys. Rev. Res. **5**, 033011 (2023).

[27] M. Lotem, A. Weichselbaum, J. von Delft, and M. Goldstein, Renormalized lindblad driving: A numerically exact nonequilibrium quantum impurity solver, Phys. Rev. Res. **2**, 043052 (2020).

[28] A. Garg, J. N. Onuchic, and V. Ambegaokar, Effect of friction on electron transfer in biomolecules, J. Chem. Phys. **83**, 4491 (1985).

[29] R. Martinazzo, B. Vacchini, K. H. Hughes, and I. Burghardt, Communication: Universal Markovian reduction of Brownian particle dynamics, J. Chem. Phys. **134**, 011101 (2011).

[30] J. Iles-Smith, N. Lambert, and A. Nazir, Environmental dynamics, correlations, and the emergence of noncanonical equilibrium states in open quantum systems, Phys. Rev. A **90**, 032114 (2014).

[31] P. Strasberg, G. Schaller, T. L. Schmidt, and M. Esposito, Fermionic reaction coordinates and their application to an autonomous Maxwell demon in the strong-coupling regime, Phys. Rev. B **97**, 205405 (2018).

[32] M. Wertnik, A. Chin, F. Nori, and N. Lambert, Optimizing co-operative multi-environment dynamics in a dark-state-enhanced photosynthetic heat engine, J. Chem. Phys. **149**, 084112 (2018).

[33] S. Nakajima, On quantum theory of transport phenomena: Steady diffusion, Prog. Theor. Phys. **20**, 948 (1958).

[34] R. Zwanzig, Ensemble method in the theory of irreversibility, J. Chem. Phys. **33**, 1338 (1960).

[35] L. Diósi and W. T. Strunz, The non-Markovian stochastic Schrödinger equation for open systems, Phys. Lett. A **235**, 569 (1997).

[36] L. Diósi, Exact semiclassical wave equation for stochastic quantum optics, Quant. Semiclass. Opt. **8**, 309 (1996).

[37] L. Diósi, N. Gisin, and W. T. Strunz, Non-Markovian quantum state diffusion, Phys. Rev. A **58**, 1699 (1998).

[38] W. T. Strunz, L. Diósi, and N. Gisin, Open system dynamics with non-Markovian quantum trajectories, Phys. Rev. Lett. **82**, 1801 (1999).

[39] R. Feynman and F. Vernon Jr., The theory of a general quantum system interacting with a linear dissipative system, Ann. Phys. **24**, 118 (1963).

[40] A. Caldeira and A. Leggett, Path integral approach to quantum Brownian motion, Physica A **121**, 587 (1983).

[41] A. Caldeira and A. Leggett, Quantum tunnelling in a dissipative system, Ann. Phys. **149**, 374 (1983).

[42] P. Hedegård and A. O. Caldeira, Quantum dynamics of a particle in a Fermionic environment, Phys. Scr. **35**, 609 (1987).

[43] L. Bönig, K. Schönhammer, and W. Zwerger, Influence-functional theory for a heavy particle in a Fermi gas, Phys. Rev. B **46**, 855 (1992).

[44] M. W. Y. Tu and W.-M. Zhang, Non-Markovian decoherence theory for a double-dot charge qubit, Phys. Rev. B **78**, 235311 (2008).

[45] J. Jin, M. W. Y. Tu, W.-M. Zhang, and Y. Yan, Non-equilibrium quantum theory for nanodevices based on the Feynman-Vernon influence functional, New J. Phys. **12**, 083013 (2010).

[46] W.-M. Zhang, P.-Y. Lo, H.-N. Xiong, Matisse Wei-Yuan Tu, and F. Nori, General non-Markovian dynamics of open quantum systems, Phys. Rev. Lett. **109**, 170402 (2012).

[47] H.-N. Xiong, P.-Y. Lo, W.-M. Zhang, D. H. Feng, and F. Nori, Non-Markovian complexity in the quantum-to-classical transition, Sci. Rep. **5**, 13353 (2015).

[48] J. Ma, Z. Sun, X. Wang, and F. Nori, Entanglement dynamics of two qubits in a common bath, Phys. Rev. A **85**, 062323 (2012).

[49] E. Aurell, R. Kawai, and K. Goyal, An operator derivation of the Feynman–Vernon theory, with applications to the generating function of bath energy changes and to an-harmonic baths, J. Phys. A: Math. Theor. **53**, 275303 (2020).

[50] J. Ma (private communication).

[51] M. Cirio, P.-C. Kuo, Y.-N. Chen, F. Nori, and N. Lambert, Canonical derivation of the Fermionic influence superoperator, Phys. Rev. B **105**, 035121 (2022).

[52] J. T. Stockburger and C. H. Mak, Stochastic Liouvillian algorithm to simulate dissipative quantum dynamics with arbitrary precision, J. Chem. Phys. **110**, 4983 (1999).

[53] J. T. Stockburger and H. Grabert, Non-Markovian quantum state diffusion, Chem. Phys. **268**, 249 (2001).

[54] J. T. Stockburger and H. Grabert, Exact *c*-number representation of non-Markovian quantum dissipation, Phys. Rev. Lett. **88**, 170407 (2002).

[55] J. Shao, Decoupling quantum dissipation interaction via stochastic fields, J. Chem. Phys. **120**, 5053 (2004).

[56] J. T. Stockburger, Simulating spin-Boson dynamics with stochastic Liouville-von Neumann equations, Chem. Phys. **296**, 159 (2004).

[57] W. Koch, F. Großmann, J. T. Stockburger, and J. Ankerhold, Non-Markovian dissipative semiclassical dynamics, Phys. Rev. Lett. **100**, 230402 (2008).

[58] J. T. Stockburger, Exact propagation of open quantum systems in a system-reservoir context, Europhys. Lett. **115**, 40010 (2016).

[59] L. Han, V. Chernyak, Y.-A. Yan, X. Zheng, and Y. J. Yan, Stochastic representation of non-Markovian fermionic quantum dissipation, Phys. Rev. Lett. **123**, 050601 (2019).

[60] L. Han, A. Ullah, Y.-A. Yan, X. Zheng, Y. Yan, and V. Chernyak, Stochastic equation of motion approach to

fermionic dissipative dynamics. I. Formalism, J. Chem. Phys. **152**, 204105 (2020).
[61] A. Ullah, L. Han, Y.-A. Yan, X. Zheng, Y. Yan, and V. Chernyak, Stochastic equation of motion approach to fermionic dissipative dynamics. II. Numerical implementation, J. Chem. Phys. **152**, 204106 (2020).
[62] D. Matos, M. A. Lane, I. J. Ford, and L. Kantorovich, Efficient choice of colored noise in the stochastic dynamics of open quantum systems, Phys. Rev. E **102**, 062134 (2020).
[63] Y.-A. Yan, X. Zheng, and J. Shao, Piecewise ensemble averaging stochastic Liouville equations for simulating non-Markovian quantum dynamics, New J. Phys. **24**, 103012 (2022).
[64] Y. Tanimura and R. Kubo, Time evolution of a quantum system in contact with a nearly Gaussian-Markoffian noise bath, J. Phys. Soc. Jpn. **58**, 101 (1989).
[65] Y. Tanimura, Nonperturbative expansion method for a quantum system coupled to a harmonic-oscillator bath, Phys. Rev. A **41**, 6676 (1990).
[66] Y.-A. Yan, F. Yang, Y. Liu, and J. Shao, Hierarchical approach based on stochastic decoupling to dissipative systems, Chem. Phys. Lett. **395**, 216 (2004).
[67] A. Ishizaki and Y. Tanimura, Quantum dynamics of system strongly coupled to low-temperature colored noise bath: Reduced hierarchy equations approach, J. Phys. Soc. Jpn. **74**, 3131 (2005).
[68] Y. Tanimura, Stochastic Liouville, Langevin, Fokker-Planck, and master equation approaches to quantum dissipative systems, J. Phys. Soc. Jpn. **75**, 082001 (2006).
[69] A. Ishizaki and G. R. Fleming, Unified treatment of quantum coherent and incoherent hopping dynamics in electronic energy transfer: Reduced hierarchy equation approach, J. Chem. Phys. **130**, 234111 (2009).
[70] A. G. Dijkstra and Y. Tanimura, Non-Markovian entanglement dynamics in the presence of system-bath coherence, Phys. Rev. Lett. **104**, 250401 (2010).
[71] A. G. Dijkstra and Y. Tanimura, System bath correlations and the nonlinear response of qubits, J. Phys. Soc. Jpn. **81**, 063301 (2012).
[72] J. M. Moix and J. Cao, A hybrid stochastic hierarchy equations of motion approach to treat the low temperature dynamics of non-Markovian open quantum systems, J. Chem. Phys. **139**, 134106 (2013).
[73] Y. Tanimura, Reduced hierarchical equations of motion in real and imaginary time: Correlated initial states and thermodynamic quantities, J. Chem. Phys. **141**, 044114 (2014).
[74] J. Shao and Y.-A. Yan, Stochastic description of quantum Brownian dynamics, Front. Phys. **11**, 110309 (2016).
[75] C. Y. Hsieh and J. Cao, A unified stochastic formulation of dissipative quantum dynamics. I. Generalized hierarchical equations., J. Chem. Phys. **148**, 014103 (2018).
[76] C. Y. Hsieh and J. Cao, A unified stochastic formulation of dissipative quantum dynamics. II. Beyond linear response of spin baths., J. Chem. Phys. **148**, 014104 (2018).
[77] N. Lambert, T. Raheja, S. Cross, P. Menczel, S. Ahmed, A. Pitchford, D. Burgarth, and F. Nori, Qutip-bofin: A bosonic and fermionic numerical hierarchical-equations-of-motion library with applications in light-harvesting, quantum control, and single-molecule electronics, Phys. Rev. Res. **5**, 013181 (2023).
[78] Y. Tanimura, Numerically "exact" approach to open quantum dynamics: The hierarchical equations of motion (HEOM), J. Chem. Phys. **153**, 020901 (2020).
[79] K. Nakamura and Y. Tanimura, Optical response of laser-driven charge-transfer complex described by Holstein-Hubbard model coupled to heat baths: Hierarchical equations of motion approach, J. Chem. Phys. **155**, 064106 (2021).
[80] A. Imamoglu, Stochastic wave-function approach to non-Markovian systems, Phys. Rev. A **50**, 3650 (1994).
[81] B. M. Garraway, Nonperturbative decay of an atomic system in a cavity, Phys. Rev. A **55**, 2290 (1997).
[82] E. Arrigoni, M. Knap, and W. von der Linden, Nonequilibrium dynamical mean-field theory: An auxiliary quantum master equation approach, Phys. Rev. Lett. **110**, 086403 (2013).
[83] A. Dorda, M. Nuss, W. von der Linden, and E. Arrigoni, Auxiliary master equation approach to nonequilibrium correlated impurities, Phys. Rev. B **89**, 165105 (2014).
[84] I. Titvinidze, A. Dorda, W. von der Linden, and E. Arrigoni, Transport through a correlated interface: Auxiliary master equation approach, Phys. Rev. B **92**, 245125 (2015).
[85] F. Schwarz, M. Goldstein, A. Dorda, E. Arrigoni, A. Weichselbaum, and J. von Delft, Lindblad-driven discretized leads for nonequilibrium steady-state transport in quantum impurity models: Recovering the continuum limit, Phys. Rev. B **94**, 155142 (2016).
[86] A. Dorda, M. Sorantin, W. von der Linden, and E. Arrigoni, Optimized auxiliary representation of non-Markovian impurity problems by a Lindblad equation, New J. Phys. **19**, 063005 (2017).
[87] F. Mascherpa, A. Smirne, S. F. Huelga, and M. B. Plenio, Open systems with error bounds: Spin-boson model with spectral density variations, Phys. Rev. Lett. **118**, 100401 (2017).
[88] A. Lemmer, C. Cormick, D. Tamascelli, T. Schaetz, S. F. Huelga, and M. B. Plenio, A trapped-ion simulator for spin-Boson models with structured environments, New J. Phys. **20**, 073002 (2018).
[89] D. Tamascelli, A. Smirne, S. F. Huelga, and M. B. Plenio, Nonperturbative treatment of non-Markovian dynamics of open quantum systems, Phys. Rev. Lett. **120**, 030402 (2018).
[90] N. Lambert, S. Ahmed, M. Cirio, and F. Nori, Modelling the ultra-strongly coupled spin-Boson model with unphysical modes, Nat. Commun. **10**, 3721 (2019).
[91] D. Tamascelli, A. Smirne, J. Lim, S. F. Huelga, and M. B. Plenio, Efficient simulation of finite-temperature open quantum systems, Phys. Rev. Lett. **123**, 090402 (2019).
[92] F. Chen, G. Cohen, and M. Galperin, Auxiliary master equation for nonequilibrium dual-Fermion approach, Phys. Rev. Lett. **122**, 186803 (2019).
[93] F. Chen, E. Arrigoni, and M. Galperin, Markovian treatment of non-Markovian dynamics of open Fermionic systems, New J. Phys. **21**, 123035 (2019).
[94] G. Pleasance, B. M. Garraway, and F. Petruccione, Generalized theory of pseudomodes for exact descriptions of non-Markovian quantum processes, Phys. Rev. Res. **2**, 043058 (2020).
[95] S. Luo, N. Lambert, P. Liang, and M. Cirio, Quantum-classical decomposition of Gaussian quantum environments: A stochastic pseudomode model, PRX Quant. **4**, 030316 (2023).
[96] H.-B. Chen, N. Lambert, Y.-C. Cheng, Y.-N. Chen, and F. Nori, Using non-Markovian measures to evaluate

quantum master equations for photosynthesis, Sci. Rep. **5**, 12753 (2015).

[97] A. Fruchtman, N. Lambert, and E. Gauger, When do perturbative approaches accurately capture the dynamics of complex quantum systems? Sci. Rep. **6**, 28204 (2016).

[98] A. Blais, J. Gambetta, A. Wallraff, D. I. Schuster, S. M. Girvin, M. H. Devoret, and R. J. Schoelkopf, Quantum-information processing with circuit quantum electrodynamics, Phys. Rev. A **75**, 032329 (2007).

[99] I. Buluta and F. Nori, Quantum simulators, Science **326**, 108 (2009).

[100] D. L. Underwood, W. E. Shanks, J. Koch, and A. A. Houck, Low-disorder microwave cavity lattices for quantum simulation with photons, Phys. Rev. A **86**, 023837 (2012).

[101] J. Raftery, D. Sadri, S. Schmidt, H. E. Türeci, and A. A. Houck, Observation of a dissipation-induced classical to quantum transition, Phys. Rev. X **4**, 031043 (2014).

[102] I. M. Georgescu, S. Ashhab, and F. Nori, Quantum simulation, Rev. Mod. Phys. **86**, 153 (2014).

[103] S. Hacohen-Gourgy, V. V. Ramasesh, C. De Grandi, I. Siddiqi, and S. M. Girvin, Cooling and autonomous feedback in a Bose-Hubbard chain with attractive interactions, Phys. Rev. Lett. **115**, 240501 (2015).

[104] M. Dalmonte, S. I. Mirzaei, P. R. Muppalla, D. Marcos, P. Zoller, and G. Kirchmair, Realizing dipolar spin models with arrays of superconducting qubits, Phys. Rev. B **92**, 174507 (2015).

[105] P. Roushan, C. Neill, A. Megrant, Y. Chen, R. Babbush, R. Barends, B. Campbell, Z. Chen, B. Chiaro, A. Dunsworth, A. Fowler, E. Jeffrey, J. Kelly, E. Lucero, J. Mutus, P. J. J. O'Malley, M. Neeley, C. Quintana, D. Sank, A. Vainsencher *et al.*, Chiral ground-state currents of interacting photons in a synthetic magnetic field, Nat. Phys. **13**, 146 (2017).

[106] M. Fitzpatrick, N. M. Sundaresan, A. C. Y. Li, J. Koch, and A. A. Houck, Observation of a dissipative phase transition in a one-dimensional circuit QED lattice, Phys. Rev. X **7**, 011016 (2017).

[107] R. Cleve and C. Wang, Efficient quantum algorithms for simulating Lindblad evolution, in *44th International Colloquium on Automata, Languages, and Programming (ICALP 2017)*, Leibniz International Proceedings in Informatics (LIPIcs) Vol. 80, edited by I. Chatzigiannakis, P. Indyk, F. Kuhn, and A. Muscholl (Schloss Dagstuhl–Leibniz-Zentrum für Informatik, Dagstuhl, Germany, 2017), pp. 17:1–17:14.

[108] H.-Y. Su and Y. Li, Quantum algorithm for the simulation of open-system dynamics and thermalization, Phys. Rev. A **101**, 012328 (2020).

[109] M. Raghunandan, F. Wolf, C. Ospelkaus, P. O. Schmidt, and H. Weimer, Initialization of quantum simulators by sympathetic cooling, Sci. Adv. **6**, eaaw9268 (2020).

[110] R. Trivedi, D. Malz, and J. I. Cirac, Convergence guarantees for discrete mode approximations to non-Markovian quantum baths, Phys. Rev. Lett. **127**, 250404 (2021).

[111] R. Trivedi, Description and complexity of non-Markovian open quantum dynamics, arXiv:2204.06936 [quant-ph].

[112] N. Lambert, M. Cirio, J. dong Lin, P. Menczel, P. Liang, and F. Nori, Fixing detailed balance in ancilla-based dissipative state engineering, arXiv:2310.12539 [quant-ph].

[113] Z. Ding, C.-F. Chen, and L. Lin, Single-ancilla ground state preparation via Lindbladians, arXiv:2308.15676 [quant-ph].

[114] F. Gallina, M. Bruschi, and B. Fresch, From stochastic Hamiltonian to quantum simulation: Exploring memory effects in exciton dynamics, arXiv:2404.06264 [quant-ph].

[115] Y. Li and S. C. Benjamin, Efficient variational quantum simulator incorporating active error minimization, Phys. Rev. X **7**, 021050 (2017).

[116] K. Temme, S. Bravyi, and J. M. Gambetta, Error mitigation for short-depth quantum circuits, Phys. Rev. Lett. **119**, 180509 (2017).

[117] S. Endo, S. C. Benjamin, and Y. Li, Practical quantum error mitigation for near-future applications, Phys. Rev. X **8**, 031027 (2018).

[118] S. Endo, Q. Zhao, Y. Li, S. Benjamin, and X. Yuan, Mitigating algorithmic errors in a Hamiltonian simulation, Phys. Rev. A **99**, 012334 (2019).

[119] T. Giurgica-Tiron, Y. Hindy, R. LaRose, A. Mari, and W. J. Zeng, Digital zero noise extrapolation for quantum error mitigation, in *2020 IEEE International Conference on Quantum Computing and Engineering (QCE)* (IEEE, Los Alamitos, CA, 2020), pp. 306–316.

[120] H. Hakoshima, Y. Matsuzaki, and S. Endo, Relationship between costs for quantum error mitigation and non-Markovian measures, Phys. Rev. A **103**, 012611 (2021).

[121] J. Vovrosh, K. E. Khosla, S. Greenaway, C. Self, M. S. Kim, and J. Knolle, Simple mitigation of global depolarizing errors in quantum simulations, Phys. Rev. E **104**, 035309 (2021).

[122] C. Zhenyu, Multi-exponential error extrapolation and combining error mitigation techniques for NISQ applications, npj Quant. Inf. **7**, 80 (2021).

[123] A. Strikis, D. Qin, Y. Chen, S. C. Benjamin, and Y. Li, Learning-based quantum error mitigation, PRX Quant. **2**, 040330 (2021).

[124] Z. Cai, R. Babbush, S. C. Benjamin, S. Endo, W. J. Huggins, Y. Li, J. R. McClean, and T. E. O'Brien, Quantum error mitigation, Rev. Mod. Phys. **95**, 045005 (2022).

[125] A. Wang, J. Zhang, and Y. Li, Error-mitigated deep-circuit quantum simulation of open systems: Steady state and relaxation rate problems, Phys. Rev. Res. **4**, 043140 (2022).

[126] Y. Kim, C. J. Wood, T. J. Yoder, S. T. Merkel, J. M. Gambetta, K. Temme, and A. Kandala, Scalable error mitigation for noisy quantum circuits produces competitive expectation values, Nat. Phys. **19**, 752 (2023).

[127] D. Qin, Y. Chen, and Y. Li, Error statistics and scalability of quantum error mitigation formulas, npj Quant. Inf. **9**, 35 (2023).

[128] J. D. Guimarães, J. Lim, M. I. Vasilevskiy, S. F. Huelga, and M. B. Plenio, Noise-assisted digital quantum simulation of open systems using partial probabilistic error cancellation, PRX Quant. **4**, 040329 (2023).

[129] S. Iblisdir, M. Cirio, O. Boada, and G. K. Brennen, Low depth quantum circuits for Ising models, Ann. Phys. **340**, 205 (2014).

[130] C. M. Bender and S. Boettcher, Real spectra in non-Hermitian Hamiltonians having PT symmetry, Phys. Rev. Lett. **80**, 5243 (1998).

[131] C.-Y. Ju, A. Miranowicz, Y.-N. Chen, G.-Y. Chen, and F. Nori, Emergent parallel transports and curvatures in non-Hermitian quantum mechanics, Quantum **8**, 1277 (2024).
[132] R. N. Silver, D. S. Sivia, and J. E. Gubernatis, Maximum-entropy method for analytic continuation of quantum Monte Carlo data, Phys. Rev. B **41**, 2380 (1990).
[133] J. E. Gubernatis, M. Jarrell, R. N. Silver, and D. S. Sivia, Quantum Monte Carlo simulations and maximum entropy: Dynamics from imaginary-time data, Phys. Rev. B **44**, 6011 (1991).
[134] M. Jarrell and J. Gubernatis, Bayesian inference and the analytic continuation of imaginary-time quantum Monte Carlo data, Phys. Rep. **269**, 133 (1996).
[135] A. W. Sandvik, Stochastic method for analytic continuation of quantum Monte Carlo data, Phys. Rev. B **57**, 10287 (1998).
[136] K. S. D. Beach, R. J. Gooding, and F. Marsiglio, Reliable Padé analytical continuation method based on a high-accuracy symbolic computation algorithm, Phys. Rev. B **61**, 5147 (2000).
[137] K. Vafayi and O. Gunnarsson, Analytical continuation of spectral data from imaginary time axis to real frequency axis using statistical sampling, Phys. Rev. B **76**, 035115 (2007).
[138] S. Fuchs, T. Pruschke, and M. Jarrell, Analytic continuation of quantum Monte Carlo data by stochastic analytical inference, Phys. Rev. E **81**, 056701 (2010).
[139] O. Gunnarsson, M. W. Haverkort, and G. Sangiovanni, Analytical continuation of imaginary axis data for optical conductivity, Phys. Rev. B **82**, 165125 (2010).
[140] D. Bergeron and A.-M. S. Tremblay, Algorithms for optimized maximum entropy and diagnostic tools for analytic continuation, Phys. Rev. E **94**, 023303 (2016).
[141] O. Goulko, A. S. Mishchenko, L. Pollet, N. Prokof'ev, and B. Svistunov, Numerical analytic continuation: Answers to well-posed questions, Phys. Rev. B **95**, 014102 (2017).
[142] J. Otsuki, M. Ohzeki, H. Shinaoka, and K. Yoshimi, Sparse modeling approach to analytical continuation of imaginary-time quantum Monte Carlo data, Phys. Rev. E **95**, 061302(R) (2017).
[143] L.-F. Arsenault, R. Neuberg, L. A. Hannah, and A. J. Millis, Projected regression method for solving Fredholm integral equations arising in the analytic continuation problem of quantum physics, Inverse Probl. **33**, 115007 (2017).
[144] R. Levy, J. LeBlanc, and E. Gull, Implementation of the maximum entropy method for analytic continuation, Comput. Phys. Commun. **215**, 149 (2017).
[145] H. Yoon, J.-H. Sim, and M. J. Han, Analytic continuation via domain knowledge free machine learning, Phys. Rev. B **98**, 245101 (2018).
[146] I. Krivenko and M. Harland, TRIQS/SOM: Implementation of the stochastic optimization method for analytic continuation, Comput. Phys. Commun. **239**, 166 (2019).
[147] R. Fournier, L. Wang, O. V. Yazyev, and Q. S. Wu, Artificial neural network approach to the analytic continuation problem, Phys. Rev. Lett. **124**, 056401 (2020).
[148] H. Shao and A. W. Sandvik, Progress on stochastic analytic continuation of quantum Monte Carlo data, Phys. Rep. **1003**, 1 (2023).
[149] J. Kaufmann and K. Held, ana_cont: Python package for analytic continuation, Comput. Phys. Commun. **282**, 108519 (2023).
[150] L. Huang, ACFlow: An open source toolkit for analytic continuation of quantum Monte Carlo data, Comput. Phys. Commun. **292**, 108863 (2023).
[151] C. N. Self, S. Iblisdir, G. K. Brennen, and K. Meichanetzidis, Estimating the Jones polynomial for Ising anyons on noisy quantum computers, arXiv:2210.11127 [quant-ph].
[152] P. Bridgman, *The Logic of Modern Physics* (The Macmillan Company, New York, 1927).
[153] J. R. Johansson, P. D. Nation, and F. Nori, QuTiP: An open-source Python framework for the dynamics of open quantum systems, Comput. Phys. Commun. **183**, 1760 (2012).
[154] J. R. Johansson, P. D. Nation, and F. Nori, QuTiP 2: A Python framework for the dynamics of open quantum systems, Comput. Phys. Commun. **184**, 1234 (2013).
[155] N. Shammah, S. Ahmed, N. Lambert, S. De Liberato, and F. Nori, Open quantum systems with local and collective incoherent processes: Efficient numerical simulations using permutational invariance, Phys. Rev. A **98**, 063815 (2018).
[156] B. Li, S. Ahmed, S. Saraogi, N. Lambert, F. Nori, A. Pitchford, and N. Shammah, Pulse-level noisy quantum circuits with QuTiP, Quantum **6**, 630 (2022).
[157] A. Ishizaki and G. R. Fleming, Theoretical examination of quantum coherence in a photosynthetic system at physiological temperature, Proc. Natl. Acad. Sci. USA **106**, 17255 (2009).
[158] A. Ishizaki and G. R. Fleming, Quantum coherence in photosynthetic light harvesting, Annu. Rev. Condens. Matter Phys. **3**, 333 (2012).
[159] N. Lambert, Y.-N. Chen, Y.-C. Cheng, C.-M. Li, G.-Y. Chen, and F. Nori, Quantum biology, Nat. Phys. **9**, 10 (2013).
[160] J. Iles-Smith, A. G. Dijkstra, N. Lambert, and A. Nazir, Energy transfer in structured and unstructured environments: Master equations beyond the Born-Markov approximations, J. Chem. Phys. **144**, 044110 (2016).
[161] L. Demanet and A. Townsend, Stable extrapolation of analytic function, Found. Comput. Math. **19**, 297 (2019).
[162] S. Aaronson, Shadow tomography of quantum states, in *Proceedings of the 50th Annual ACM SIGACT Symposium on Theory of Computing* (ACM, New York, 2018), p. 325.
[163] S. Aaronson and G. N. Rothblum, Gentle measurement of quantum states and differential privacy, in *Proceedings of the 51st Annual ACM SIGACT Symposium on Theory of Computing* (ACM, New York, 2019), p. 322.
[164] H.-Y. Huang, R. Kueng, and J. Preskill, Predicting many properties of a quantum system from very few measurements, Nat. Phys. **16**, 1050 (2020).
[165] D. Loss (private communication).
[166] P. Menczel, K. Funo, M. Cirio, N. Lambert, and F. Nori, Non-Hermitian pseudomodes for strongly coupled open quantum systems: Unravelings, correlations and thermodynamics, arXiv:2401.11830.
[167] L. N. Trefethen, *Approximation Theory and Approximation Practice* (Society for Industrial and Applied Mathematics, Philadelphia, PA, 2013).
[168] J. Mason and D. Handscomb, *Chebyshev Polynomials* (Chapman & Hall/CRC, London, 2002).
[169] R. Pachón, Algorithms for polynomial and rational approximation, Ph.D. thesis, University of Oxford, 2010.
[170] F. Kittaneh, Inequalities for the schatten P-norm, Glasg. Math. J. **26**, 141 (1985).